RESUM - Català

Aquest projecte consisteix en la recerca de maneres alternatives per millorar la eficiència dels motors de gasolina. Per tal d'aconseguir aquest objectiu, el projecte es focalitza en el sistema d'encesa, ja que s'ha vist que el sistema d'encesa actual només ofereix control de el moment en que la combustió comença, però no ofereix cap tipus de control mentre el combustible crema. Per tant, l'objectiu es trobar un mètode d'ignició alternatiu que ofereixi la capacitat de controlar com crema el combustible. Obtenint aquesta funció, la eficiència de l'encesa en el motor incrementarà, fent que el motor sigui més eficient i, a la mateixa vegada, produir menys contaminats.

Per aconseguir l'objectiu d'aquest projecte, s'ha considerat la utilització del denominat efecte Descàrrega Corona en la bugia. Assumint aquesta tecnologia, s'ha fet una recerca amplia de les tecnologies disponibles actualment per substituir l'actual sistema d'ignició per guspira. Dins la recerca s'ha investigat com es genera l'encesa en cada tecnologia, prenent especial atenció a l'encesa per descàrrega corona. Després de la recerca, el projecta entra en detall en l'estudi de l'efecte corona, posant exemples d'actuals investigacions i de mètodes per mesurar i visualitzar l'efecte corona, finalitzant amb la proposta d'una modificació de l'actual sistema d'encesa per implementar l'efecte corona.

SUMMARY - English

This project consists in the research of a way on improving the efficiency of gasoline engines. To achieve this goal the project will be focused in the ignition system, because the actual system only gives control on the moment the burn starts, but not to what happens while the fuel is burning, so the objective is look for a way of ignition that is completely capable of controlling the burnt in the combustion chamber. By achieving this goal, the efficiency of the burnt in the engine would be increased, and also the emissions would be more stable.

In order to achieve the objective of the project, the Corona Discharge effect has been considered in order to apply it as an alternative spark plug for the engine. By having assumed this technology as the one chosen to improve the ignition, in order to achieve this project's goals a wide research of the actual state of art of corona discharge and how to control it has been done. The project will look at all the actual research completed regarding alternative ignition systems, investigating how the spark is generated in each of them and how they are controlled. After all the research, an investigation is made in the Corona Discharge generation, finalizing with an ignition system modification to allow the implementation of this effect in conventional engines.

CONTENTS

GLOSSARY

- **CD** → *Corona Discharge*
- **MTE** → *Machine and Thermal Engines Department*
- **ETSEIB** → *School of Industrial Engineering of Barcelona*
- **PRC** → *Piston, rod and crank system*
- **TDC** → *Top dead centre*
- **BDC** → *Bottom dead centre*
- **CC** → *Combustion chamber*
- **ICE** → *Internal Combustion Engine*
- **HV** → *High Voltage*
- **CB** → *Contact Breaker*
- **SCR** → *Silicon Controlled Rectifier*
- **MEP** → *Mean Effective Pressure*
- **PDE** → *Pulse Detonation Engine*
- **DDT** → *Deflagration-to-Detonation Transition*
- **SST** → *Second Positive System*
- **FNS** → *First Negative System*
- **DS** → *Dielectric Strength*
- **NYAG** → *Neodymium Yttrium Aluminium Garnet laser*
- **ECU** → *Electric Control Unit*
- **RF** → *Radio Frequency*
- **IC** → *Integrated Circuit*

PREFACE

This Final Career Thesis, with title "*Study of an ignition system for gasoline engines consisting in the corona discharge effect*" has been realised as part of the research done in the Machine and Thermal Engines Department of the School of Industrial Engineering of Barcelona. Also, the subject of the project is intended to complete the formation of the author in the Automotive Diploma specialisation related to the Industrial Engineering degree.

The development of this thesis has been done by own research and in collaboration with the department previously named. The principal coordinator of the project is Jesús Andrés Àlvarez Florez from the School of Industrial Engineering of Barcelona.

- **Project origin**

Every year new emissions regulations are made and the amount of restrictions in the vehicle emissions are always growing narrower. In order to develop a commercial vehicle that meets the regulations, automotive engineers have to find new technologies able to decrease the amount of contaminants in the exhaust gases, making the engine more efficient.

This project pretends to be a study of a possible future option for car manufacturers in order to achieve that goal and meet future regulations by implementing new ideas in the ignition of the fuel.

- **Motivation**

The author of this project has been specialising in automotive engineering, doing the intensification related to the Diploma in Automotive during his Superior degree, so this project was a very interesting option for him as it involves a subject which is already being under research by car manufacturers and can help the automotive world. Also, the subject of this project is a way to a cleaner future in automotive industry and a possible way to increase the efficiency of the gasoline engines.

- **Previous requirements**

In order to carry out the project, a deep research in how ignition works had to be done, as well as the investigation in how to generate and maintain the CD effect. To understand this investigation, knowledge in electricity is fundamental, as well as electronic control. Also, knowledge in how gasoline engines work and how the full ignition-burnt process work is important to understand the improvements this system adds to actual engines.

INTRODUCTION

A big problem for commercial vehicles is the emissions they generate. The levels of contaminants in their gasses are a big variable to considerate when developing a new engine for a car. Every new emissions regulation that comes in is stricter than the previous one, so the research in new technologies which produce less contaminants is getting more important than ever.

The intention of this project is to provide a deep understanding of a new technology capable of reducing the amount of these contaminants, so that vehicles which now don't have a good rate of emissions are capable of meeting the regulations in the future. To achieve this, the project focuses on the gasoline engines, concretely on the ignition system.

Currently, the ignition doesn't give control in how the burn of the fuel develops in the combustion chamber, the only parameter able to control is the moment this ignition starts. Once it starts, the way it develops on the combustion chamber depends on lots of variables which, in certain moments of the cycle, might generate improperly combustion, generating problems with the effectiveness of the engine, the contaminants, and being possible to cause damage in the engine elements.

Objective

The principal objective of this project is to provide an introduction to an alternative ignition system that provides a better efficiency in the combustion, generating less contaminants and ensuring the combustion is done correctly. In order to achieve this end, an alternative way of ignition is proposed, an ignition consisting in the CD effect which maintains this effect while all the combustion is completed. To do this, the ignition system will have to be reengineered so that the CD generation is implemented successfully.

This project will focus in the research of information regarding the CD, looking at the different patents that have been released and at current prototypes that have already been manufactured. As a conclusion, a circuit will be proposed for the generation of the CD effect.

Project Scope

This project contains a first study in the actual ignition system and its disadvantages and why it should be replaced, as well as a study of the CD effect, explaining how it is produced and which advantages has compared to the actual ignition system. After this first study, the project focuses in the patents and research documents that have been released until now.

After all the investigation, an analysis in the improvements will be done to prove the advantages that the new system has over the currently one, proposing a modification in the ignition system to implement successfully the new ignition technology.

This project doesn't include the physical design of the system, as well as the material selection and manufacturing process. The project only includes the research done and the theoretical design of the system (elements needed, power needed, special requirements …).

At the end of this project, the reader will have a deep dive in how the CD is generated and how it should be implemented in a gasoline engine. This document is meant to be used as an estate of art of the CD ignition system.

1. INTRODUCTION TO GASOLINE ENGINES

In order to understand the ignition of a gasoline engine and why the system which this project refers to could improve its performance, first it's needed to have a brief look on how a gasoline engine works. This first chapter is not relevant to understand the subject of this project, however it has been added to help the reader to understand better the next points that the project will go through in case the reader doesn't have previous knowledge in internal combustion engines. If the reader of this document already has knowledge related to gasoline engines direct to Chapter 2.

A gasoline engine is an endothermic engine consisting in the piston, rod, and crank (PRC) system appeared on the ending years of the XIX century as a way of being able to move light vehicles without the need of animals. This supposed a big change in the era of the vehicles, until then all vehicles had to be powered by the help of animals and, in the case of trains, steam engines. This discovery, made by Nicolaus Otto has been the base of all the actual gasoline engines. Through all the years, this first engine created by Otto has been able to evolve thanks to the continuous progress in science and technology, achieving levels of performance previously unreachable.

Before describing the stages of gasoline engines, it is needed to know some references used when talking about engines.

1.1. Engine elements and terms

As described before, a gasoline engine consists in the PRC system, consisting in the piston, which moves in a straight direction with an alternate sense, the connecting rod, which moves both linear and rotary ways, and the crankshaft, which transforms the linear movement of the piston into rotary movement. The connection between the crankshaft and the piston is done by the connecting rod and can be seen in *Figure 1.1*.

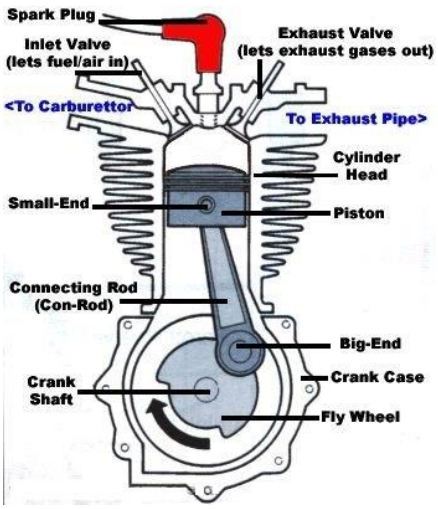

Figure 1.1. *Elements of a gasoline engine refrigerated by air*

Having a look at the previous figure, other elements that are part of a gasoline engine can be noticed, as the exhaust and intake valves, the cylinder head (which in the case of a currently car engine is refrigerated by oil, having some differences with the picture shown above), the crank case, which contains the lubrication oil, and spark plug, which is the one that ignites the mixture of gasoline and air.

Some of the terms and elements that don't appear on the figure but are very important when studying the performance of an engine are the camshaft (responsible of the opening and closing of the valves), top dead centre or TDC and bottom dead centre or BDC (positions when the piston is at its highest and lowest position respectively), and the combustion chamber, which is the chamber that remains of the cylinder chamber when the piston is at its TDC.

1.2. Four strokes cycle

Currently, all automotive engines work in a four stroke system. These four strokes are:

- **Intake:** The admission valve opens while the piston is at the TDC and lets the mixture enter the cylinder chamber, filling it until the piston reaches the BDC and the valve closes.
- **Compression:** Following the previous stroke, the piston continues with his move upwards, compressing all the mixture that is in the cylinder chamber until the piston gets at the TDC.
- **Power:** After the spark plug creates an ignition, the force of this ignition pushes the piston down, transferring the force to the crankshaft to transform it to rotatory force.
- **Exhaust:** When the piston reaches the BDC, the exhaust valve opens and lets the gases generated in the combustion go out of the chamber. The movement of the piston

upwards helps pushing these gases out. When the piston reaches the TDC, the exhaust valve closes and the whole cycle starts again.

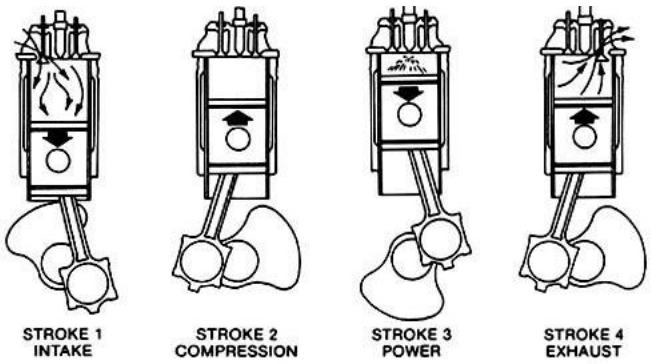

Figure 1.2. *Four strokes in a gasoline engine*

The engines currently used in vehicles can be Otto engines (commonly known as gasoline engines) or Diesel engines. The only difference between their strokes is the power one. In Otto engines the power is given by the spark plug, which, as its name says, generates a spark in order to ignite the compressed mixture. In Diesel the ignition is produced by the high pressure and temperature that is in the combustion chamber when the fuel is injected. So, on the admission of a Diesel, only air enters the chamber, and the mixture is done while the ignition occurs.

This project is only focused in the Otto engines, so it isn't going deeper into how Diesel engines work. In *Figure 1.3* and *Figure 1.4.* The theoretical and real Otto cycles are compared in a P-V diagram, where the numbers refer to:

5-1 → Intake stroke

1-2 → Compression stroke

2-3 → Instant ignition

3-4 → Expansion stroke

4-1-5 → Exhaust stroke

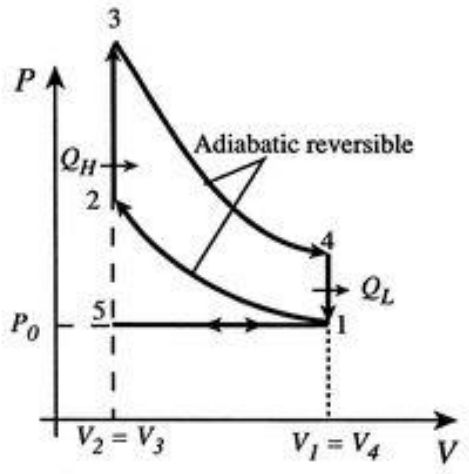

Figure 1.3. *Theoretical Otto P-V diagram*

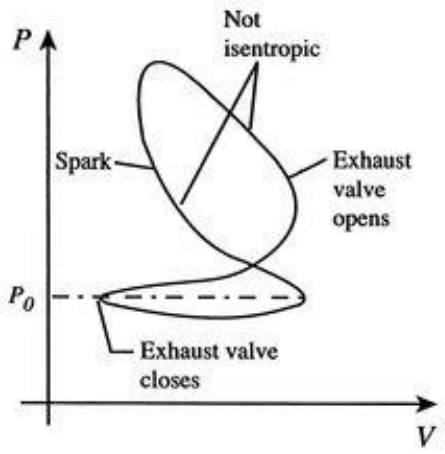

Figure 1.4. *Real Otto P-V diagram*

In these figures, the area inside the cycle 1-2-3-4 is the positive work of the cycle, while the one in 1-5-1 is the negative work generated when opening the valves.

The object studied in this project is the one that produces the instant ignition of the mixture, which is currently the spark plug. The usage of a plug consisting in the CD effect pretends to improve the efficiency of the ignition by making it more instant and, by this way, increasing the work generated by the engine.

1.3. Gasoline combustion

As this project consists in the design of an ignition system, there is no need to know if the intake is with direct or indirect injection. The important thing to study now is the heat input to ignite the mixture.

In order to assure that all of the gasoline is burnt on the process, it's needed to have a minimum quantity of air. Besides, too much air isn't good for the combustion because the power of the combustion itself is decreased and in continuous state operation some of the elements, like valves or the plug itself, might be damaged. So, the engine needs to work at a stoichiometric rate. These stoichiometric relation air/fuel is of 14.7, so, in order to burn 1 gram of gasoline, it will be needed 14.7 grams of air.

The combustion not only depends in the relation air/fuel, the type of ignition or where the ignition is generated also determines the effectiveness of the combustion. The type of chamber and its advantages are:

- **Wedge:** Concentrates the mixture around the plug and has an easy distribution, but the flame progress is relatively slow.

- **Hemispherical:** A compact chamber, so the flame doesn't have to progress a long distance (faster combustion), but it is complex.
- **Carved in piston:** It's simple, compact and has a great turbulence (better combustion)

In *Figure 1.5.* the schematic representation of these chambers is shown.

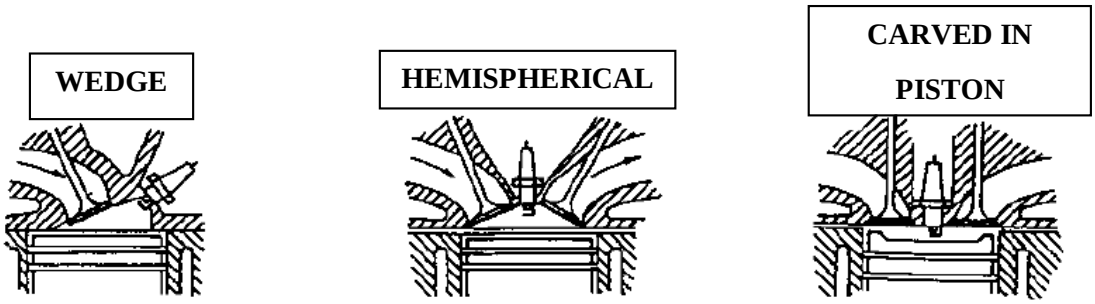

Figure 1.5. *Different type of CC*

As well, the turbulence of the mixture when ignited will determine how fast the combustion is done, and as seen in *Figure 1.4.* the faster this ignition is, more effective work will be obtained. There are three types of turbulence applied to gasoline engines, these are:

- **Swirl:** The mixture spins around the symmetry axis of the piston.
- **Squish:** The air is confined between the piston and the cylinder head as shown in *Figure 1.6.*
- **Tumble:** The mixture enters in a vertical vortex way.

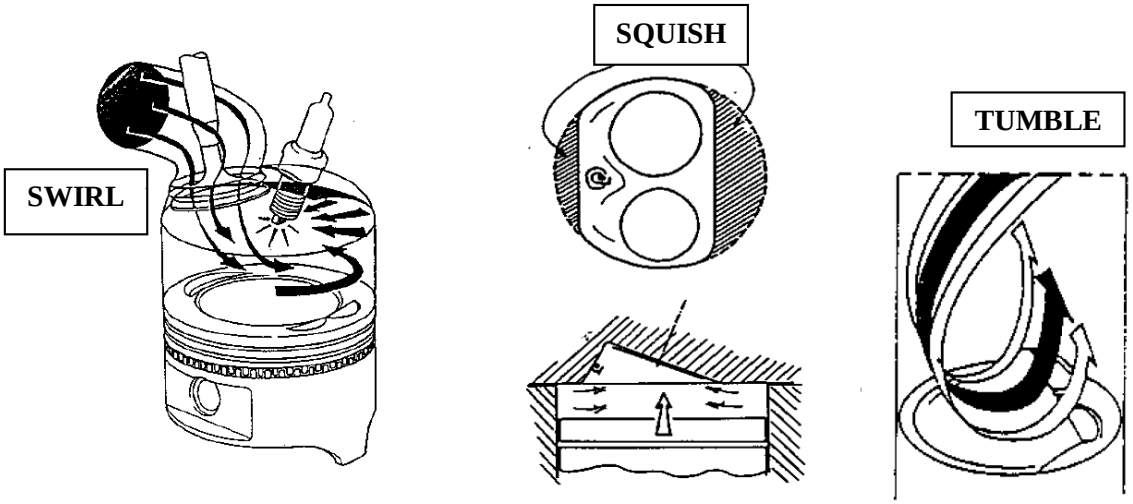

Figure 1.6. *Mixture turbulence*

Concluding, the essential criteria to consider on gasoline combustion is the relation air/fuel (stoichiometric relation), CC type, turbulence of the mixture. Some criteria not named but very important in the combustion are the rotatory speed and the advance of the ignition. Both of these criteria are explained in point 2.1. because they are closely related to the spark plug.

For this project it isn't considered a variation of the actual chamber form or point of ignition in priori, as well as a way of giving more turbulence to the mixture. It is considered that this would be another project in order to study how the design proposed in this project could be improved by adjusting some of the chamber parameters.

2. STATE OF ART

In this chapter the actual state of the ignition system in gasoline engines is described, taking interest in the way it is produced and how it's controlled, as well as an explanation of the actual investigations about CD and how to apply it to engines. As part of the investigation, some examples of actual developers are exposed.

In order to understand how the ignition system works, a differentiation between control of the ignition and development of the ignition is done. The control of the ignition system includes the electrical design, analysing the values of power (P), voltage (V) and intensity (I) over time. The development of the ignition includes the development of the spark plug, looking into the different phases in the production of the spark and how the burn in the engine proceeds.

The chapter is divided in two sections, a first one talking about the ignition system used in gasoline engines at the moment and a second one talking about the alternative ignition systems explaining which are the advantages observed for the moment in the actual investigations in the plugs consisting in CD effect in front of the common and alternative ignition spark plugs.

2.1. Common ignition system

The ignition system is currently done by using a spark plug, shown in *Figure 2.1*. It's been the system used since the beginning of the ICE, a HV spark that ignites the fuel, but there have been different ways of achieving this spark, different electric configurations. Nowadays electronic ignition systems are the used in new vehicles, but conventional systems can still be seen in the old ones.

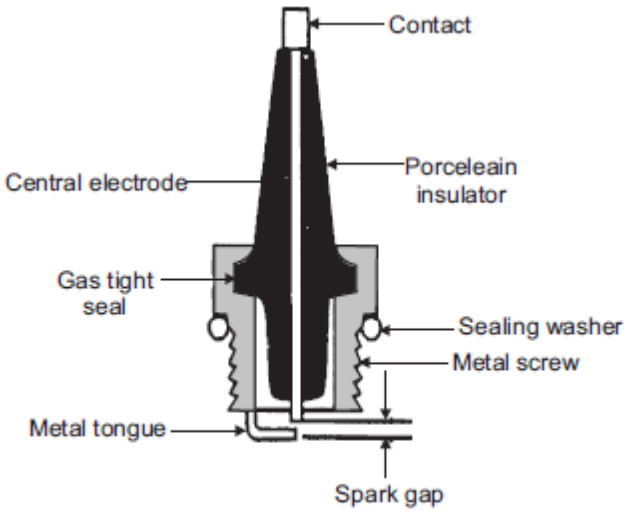

Figure 2.1. *Spark plug*

There are two conventional configurations used to create the HV spark:

- Battery or Coil Ignition System
- Magneto Ignition System

Some of the advantages that the Electronic Ignition Systems show in front of the conventional systems are:

- No moving parts – so no maintenance
- No arcing (CB points absent)
- Spark plug's life considerably increased (~50%), making them useful for about 60.000 km without any problem
- Better combustion. About 90-95% of air/fuel mixture is burnt compared with 70-75% with conventional ignition system
- More power output
- More fuel efficiency

The most used Electronic ignition systems are:

- Capacitance Discharge Ignition System
- Transistorized System

As in this project the interest is in igniting the fuel-air mixture, it is essential to understand how this is achieved in the different ignition systems discussed in this section.

- **Spark generation:**

For the spark plug, as its own name indicates, the ignition is generated by a spark, happening between the central electrode and the metal tongue (also known as side electrode). The central electrode of the plug gets charged with high voltage with one of the methods already explained (transistorized system or capacitance discharge system), creating a voltage differential between the central electrode and the side electrode. When this happens, the gap between both electrodes is filled with a fuel-air mixture, which actuates as an insulator. The voltage in the central electrode keeps increasing, starting to modify the structure of the gases between the electrodes until the voltage exceeds the *Dielectric Strength* (DS).

The DS is a physics term that is defined as the minimum applied electric field that results in a breakdown. This characteristic is a property directly related with the material of the insulation and the material and disposition of the electrodes.

Once the DS is achieved in the spark plug, the breakdown happens. At breakdown, electrons are freed from the electric field and due to the high electric field applied free electrons from background radiation (ionized radiation which exists everywhere) become accelerated, liberating additional electrons during collisions with neutral atoms and molecules. This process is scientifically known as avalanche breakdown. This breakdown happens abruptly (usually in the order of nanoseconds), resulting in the electrically conductive path. As the electrons current

goes through the gap, the temperature is increased up to 60,000 ºC. This intense heat generates the ionized gas to expand abruptly, generating a small explosion. In *Figure 2.2.* it's possible to see a draft of how the current develops during this process. Region 1 represents the beginning of the process, when there are free ions that can be accelerated by the field and induce a current. Region 2 shows the saturation of these, giving a constant current. Region 3 and 4 are caused by the ion avalanche (abrupt increase in the current, generation the small explosion).

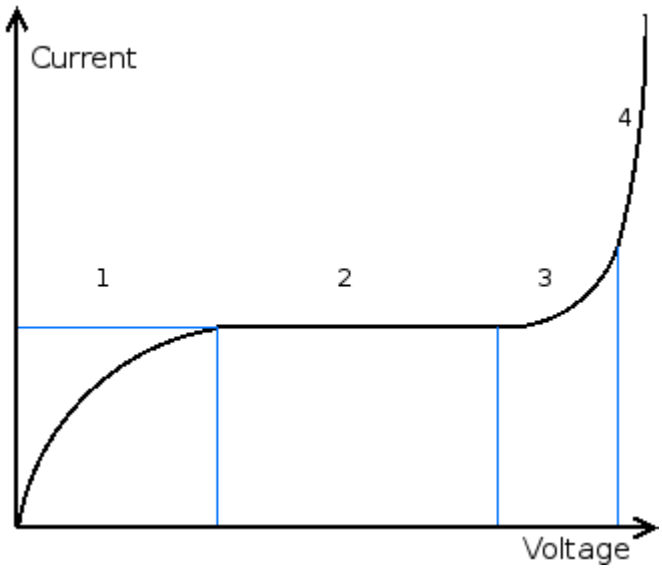

Figure 2.2. *Draft of current development in breakdown avalanche*

As a result of this process, with a spark plug the initial ignition obtained is a small sphere of fire in the spark gap which will make the gases to burn on their own. The size of this fire-sphere depends on the turbulence and the mixture of the gases (see *Chapter 1.3.* for specification of different type of turbulence).

The voltage spark plugs require is usually around 20,000 Volts, being able to go up to 45,000 Volts to ensure a correct ignition. This will depend on the type of engine where the spark plug is used.

The first commercially viable patent was done by Gottlob Honold (*US 1193548 A*) in 1902, making possible the development of the spark-ignition system for vehicles. Another scientific involved with the development was Nikola Tesla, who also published a patent related to spark plug, but that was not applicable to vehicles (*US 609250 A*). All these documents can be found in the annex section of this project for reference.

2.2. Alternative ignition systems

As part of the continuous research and development of new ways to improve the efficiency of the engine, some alternative ignition systems have been studied, one of which is the object of this project.

In this section an overview of the most relevant advances in the ignition efficiency is done, taking special interest in the system object of this project.

These systems are:

- Piezoelectric Ignition system
- Laser Ignition System
- Pulse Plug Ignition System
- Corona Ignition System

2.2.1. Piezoelectric Ignition System

The development of synthetic piezoelectric materials producing about 22 kV by mechanical loading of a small crystal resulted in some ignition systems using this methodology.

The way the charge develops to ignite the fuel-air mixture is exactly the same as specified in the previous chapter. The difference with this alternative ignition system is the way the voltage is generated.

In the Piezoelectric Ignition System the electric charge is accumulated in a specific solid material, such as a piezoelectric crystal or ceramic materials. The name piezoelectricity means electricity resulting from pressure, and that is the characteristics of piezoelectric crystals, under a certain pressure the crystals can generate a determined voltage that can create the ignition of the fuel-air.

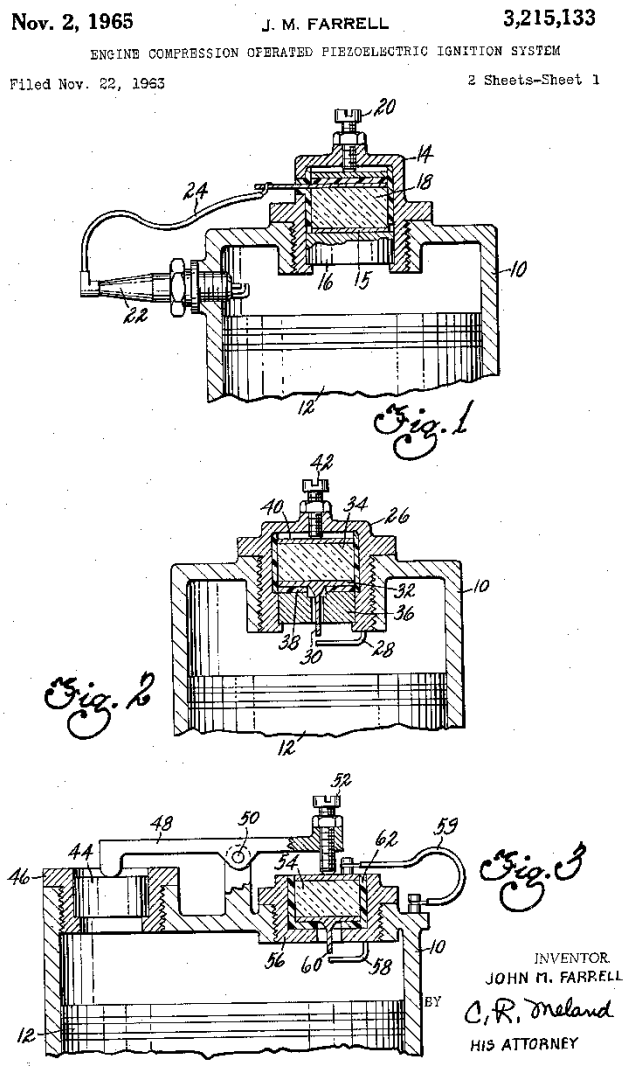

Figure 2.3. *Example of different piezoelectric ignition systems. Image taken from patent US 3215133 A.*

Some patents related to piezoelectric ignition systems are:

- *Engine compression operated piezoelectric ignition system* published by John M. Farrell (*US 3215133 A*).
- *Ignition apparatus for an internal combustion engine* published by Sanjar Ghaem (*US 5291872 A).*
- *Piezoelectric crystal spark plug* published by Norris G. Elwood (EP 0047020 A1).
- *Piezoelectric ignition and sensing device* published by Mide Technology Corporation (US 6138654 A).

Some of these schematics can be found in the annex of this project for reference, although not all the patent document has been added due to the long extension of it and low relevance to the thesis. If the reader is further interested in the patents, they are available online for reading at no extra cost.

All of them focus on using different methods of applying pressure to the piezoelectric crystal or ceramic element, most of them trying to use the own compression of the piston, which would result in enough pressure to generate the HV. Some others focus in using other external sources to generate the pressure (an example is using magnetic field stimulated electrically to generate the pressure to the crystal or ceramic material).

The main disadvantage this system has is the need of a mechanical system to generate this pressure. So far, it hasn't been found a material or mechanical system that can support the high work interval that an internal combustion engine requires, so this alternative ignition system is still a research study that at this moment in time doesn't have a feasible application to normal combustion engines.

2.2.2. Laser Ignition System

This system, together with the Corona Discharge system, is one of the most investigated systems nowadays due to its great potential and effectiveness.

Figure 2.4. *Three beam laser plug*

With this system more of the mixture in the chamber would be ignited simultaneously as this system has the capability of focusing several beams to the cylinder, making the ignition very effective compared to a traditional spark plug (only gap between electrodes is ignited in traditional spark plugs). Also, the technology allows to generate these beams at different heights inside the cylinder, while the traditional spark plug system has always the same height position.

To understand the disadvantages and advantages of this system more accurately it is required to look at how the ignition is generated with this system:

- **Ignition generation**

The most common way for generating the laser spark is the non-resonant multi-photon ionization, as it offers high interval speeds with high power. The other way of generating a laser spark is called resonance enhanced multi-photon ionization, but this will not be discussed in this document.

The first step to generate a non-resonant multi-photon ionization spark is the multi-photon ionization of the medium, resulting in the release of the first free electrons. For example, the energies for oxygen and nitrogen are 13.6 eV and 14.5 eV respectively. It is known that when using a Neodymium Yttrium Aluminium Garnet laser (NYAG), the wavelength obtained is 1064 nm, which corresponds to a photon energy of approximately 1.2 eV. Having understood this statement, it will be known that 13 photons of NYAG light ionize a nitrogen molecule to generate a free electron.

The multi-photon ionization process is then followed by electron cascade where, in the presence of the electric field of the laser pulse the free electrons are accelerated and collide with neutral particles generating more ions and electrons, resulting in an avalanche of electrons or breakdown. In *Figure 2.5.* it's possible to see a schematic representation of the electron avalanche.

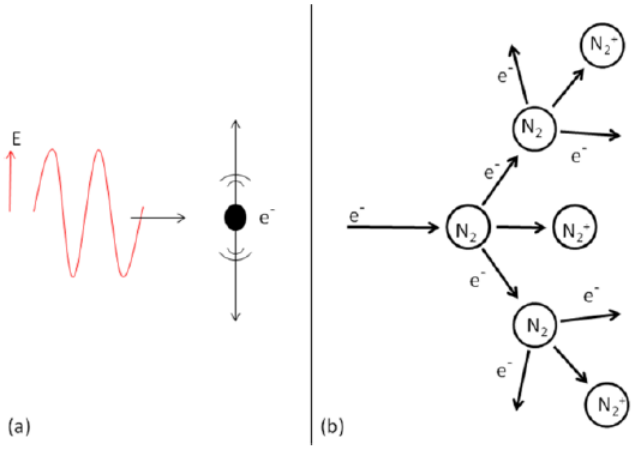

Figure 2.5. *(a) Electron oscillating due to electric field of the laser. (b) Electron avalanche in Nitrogen environment.*

Some studies have been conducted to represent the plasma temperature and electrode density. For example, in an ambient pressure of 34.5 bar and 3 microseconds after the breakdown, the plasma has a temperature of approximately 13.000 degrees Celsius with electron density of $4x10^{17}$ cm^{-3}.

After this introduction in how the laser plugs work, this document will not focus any longer on how laser ignition is developed, as this is not the main object of study. For more information consult the bibliography [14].

Once understood the development of the laser ignition, it is clear to see that the main input that will control the ignition is the laser wavelength, which will allow to regulate the plasma generated.

A big advantage that this system offers is the reduction in heat loss due to quenching, since there are no electrodes and the beam can be located at an optimal position away from the engine cylinder walls. Some Japanese prototypes have been able to focus two and three beams into an engine's cylinder at variable depths, fact that increases the completeness of combustion and nearly avoids the issue of degradation with time.

Another advantage is the interval time of this system. The laser ignition system can operate in nanoseconds, while the traditional spark plug system works in milliseconds. However, high pulse lasers are needed. In other words, a great amount of energy is needed to generate the ignition, which creates a disadvantage for this system.

In order for the lasers to be capable of supporting the combustion chamber heat, these are made of ceramic powders that are pressed into spark plug sized cylinders.

Although the achievements so far have been successful, this system still needs some research in order to be finally applied to conventional engines.

Find listed some patents related to laser ignition system:

- *Laser spark plug for an internal combustion engine and operating method for the same* published by Rene Hartke (*US 20130291818 A1*).
- *Laser ignition apparatus for an internal combustion engine* published by Nippon Soken, Inc. (*US 4416226 A*).
- *Laser spark plug for an internal combustion engine* published by Friedrich Gruber (*US 8826876 B2*).
- *Pre-chamber module for a laser spark plug and method for producing same* published by Pascal Woerner, Joerg Englehardt and Martin Weinrotter. (*US 20140225497 A1)*.

2.2.3. Pulse Plug Ignition System

These type of plugs, commercialised by Pulstar©, offer a little increase in the efficiency and performance of the engine. This improvement is about 5-15% depending on the manufacturer and type of the engine.

The first important difference with a normal spark plug is the peak power they offer. Pulse plugs offer 10 times more peak power than a conventional spark plug, resulting in a better performance which when applied in cars it is possible to obtain a slightly better torque and slightly more horsepower. As for the same situation as with a normal spark plug you offer more power, the CO_2 emissions are reduced.

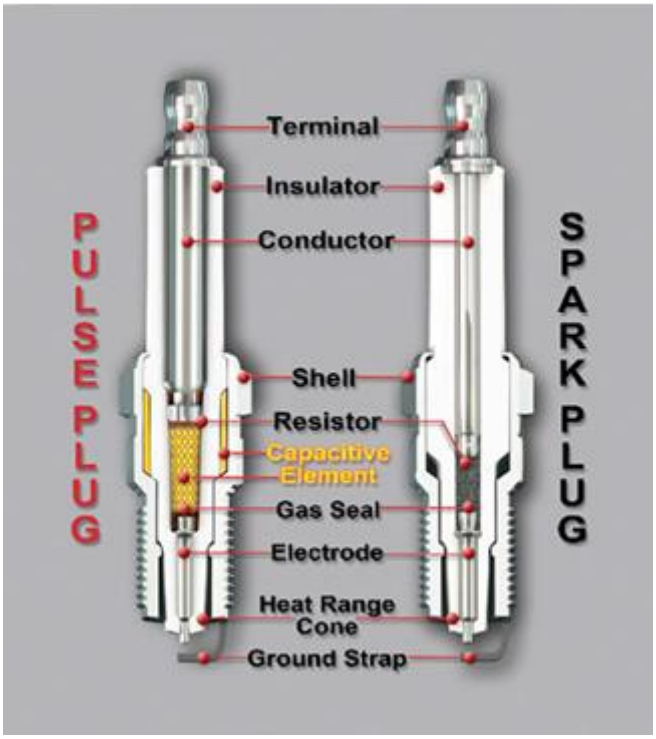

Figure 2.6. *Pulse plug composition in front of normal spark plug*

This type of spark plug stores energy in the capacitive element. When the energy is needed, it is released in about 2 nanoseconds, which results in a powerful and quick high-energy pulse.

In terms of generation of the ignition, this is exactly the same as the traditional spark plug. The only difference is it has a small modification to generate higher energy and, by doing so, improve the performance.

Compared to the laser and the corona ignition, this system doesn't produce an important improvement in the efficiency of the engine. On the good side, this system doesn't involve any modification in the actual ignition system.

2.2.4. Corona Ignition System

This system comes from the idea that with the continuous improvements of gasoline engine efficiency, in a near future these will work with more aggressive charge dilutions, resulting in traditional spark plugs not being able to ignite the mixture. In order to be able to work at such aggressive dilutions and higher MEP, the ignition will have to change to a faster ignition. In order to solve this problem, the corona ignition system has appeared.

At the moment, Federal-Mogul has developed a functional ignition system based in multiple long plasma jets instead of a single spark (*Figure 2.7.)*. This system is called by them ACIS (Advanced Corona Ignition System).

Figure 2.7. *Corona Discharge Plug by Federal-Mogul*

This system basically consists of two main components. The two-piece ignite assembly, which is mounted in the cylinder head very much like the traditional spark plug, and a controller which computes the trigger signal from the engine control unit and converts the 12 V DC electrical supply into the required AC voltage at a resonant frequency of around 1 MHz, which is fed forward the ignite.

By operating at this frequency, a strong electrical field up to 72 kV at the tips of the firing end is emitted. Because it's disposition in four electrodes, the field extends into a large volume of the combustion chamber, increasing by these way the ignition area and, consequently, the ignition speed. All this process only takes several nanoseconds as opposed to the nearly 1 millisecond in the case of the spark ignition arc breakdown.

In *Figure 2.8.*, an overview of the ACIS components can be seen.

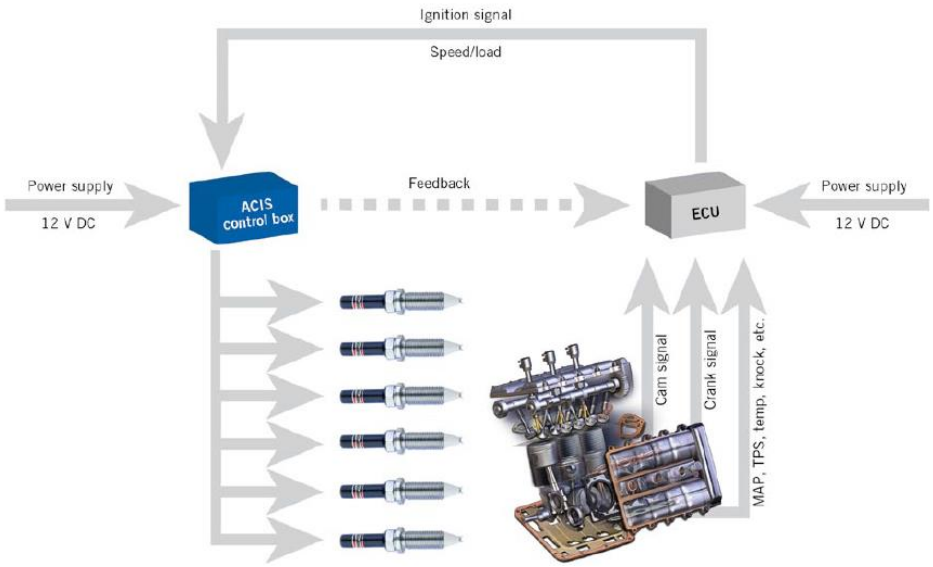

Figure 2.8. *Overview of the ACIS components*

Because of the low current and low heat discharge, there is no electrical erosion. Therefore, ACIS can be developed to serve as a lifetime component. However, its biggest benefit is the vast volume which is reached by the corona. Measuring the energy consumption of a spark plug and an ACIS for different on-times with a stoichiometric charge, results in the comparison shown in *Figure 2.9.*

	MAXIMUM VOLTAGE [V]	MAXIMUM CURRENT [A]	MAXIMUM POWER [W]	AVG. ENERGY/ IGNITION EVENT [MJ]
Spark (~ 3 ms)	14	8.7	102	192
ACIS (0.5 ms)	53	2	101	160
ACIS (0.25 ms)	53	2	100	93

Figure 2.9. *Energy comparison between ACIS and a traditional spark plug*

By integrating ACIS in an engine, it enables more aggressive measures to increase thermodynamic efficiency. As explained above, the ACIS ignition is much faster than with a conventional spark plug. This offers more freedom to control ignition timing.

In addition, ACIS permits ignition up to the double amount of air than in the stoichiometric relation air/fuel. The fuel economy improvement is calculated to be between 5 and 10 %, but it not only improves the fuel economy, ACIS is also an enabling technology, which facilitates more comprehensive technology paths that can result in a much higher fuel economy benefits.

As stated, this technology supposes a great improvement in the conception of engines and its performance, but obviously a big change in the ignition conception is needed.

This project will look further into the CD plug and see what other changes in the controlling could improve the efficiency of gasoline engines.

2.3. Patents and scientific publications involving Corona Discharge plugs or similar strategies

At the moment, some studies have been done involving plugs working with the CD effect. In previous sections, the example of the Federal-Mogul plug has been used, but this is not the only one. In this section, some of the actual publications relating with corona discharge or similar characteristics (wide gap arc discharge) are exposed.

Due to the complexity of each document, only a brief explanation of each is done. In case the reader is willing to know more information, it is possible to read some of the patents in the annex of this project or in one of the online references.

2.3.1. Patents

· Publication US3974412 A - Spark plug employing both corona discharge and arc discharge

This patent property of the Massachusetts Institute of Technology, presented on 1975, states a spark plug that uses both the arc discharge (commonly known as spark) and the corona discharge effect. The main difference with a normal spark plug is that it has a much longer arc discharge which can be electronically controlled to improve its length and disposition for different uses.

The patent states an object to provide a substantially long arc that once initiated can be moved and have its length altered to enhance the combustion. The proposal consists on a high voltage elongate axial electrode (referred as "1" in *Figure 2.10.*, all references made from now on are referenced to this figure) which extends from the base body of the spark plug. This extending part of the electrode is covered by a 1 mm insulating jacket except for the small exposed portion at its end. The electrode 2 (ground electrode in the embodiment) is adjacent to the HV electrode 1, displaced from the exposed portion 1A by a significant gap 6, having the insulating jacket 3 so that the distance between the ground electrode to the axial electrode between region 5 is less than the distance from the ground electrode across the gap 6 to the exposed portion.

With this distribution, the CD can be created between the HV electrode and the ground electrode. The corona effect begins in the region 5 and spreads along the insulating jacket toward the exposed portion 1A. Once the corona reaches it, an arc discharge occurs, referenced as 30 in the figure below. The path of this arc is determined, occurring in close proximity to the electrode 1, thereby causing it initially to contact the surface of the insulator.

The way this is distributed, an electric current upward in the electrode 1 at the stem portion shown at 1B will interact electromagnetically with a current downward in the arc 30, meaning this that the arc will move radially outward from the stem portion 1B of the electrode.

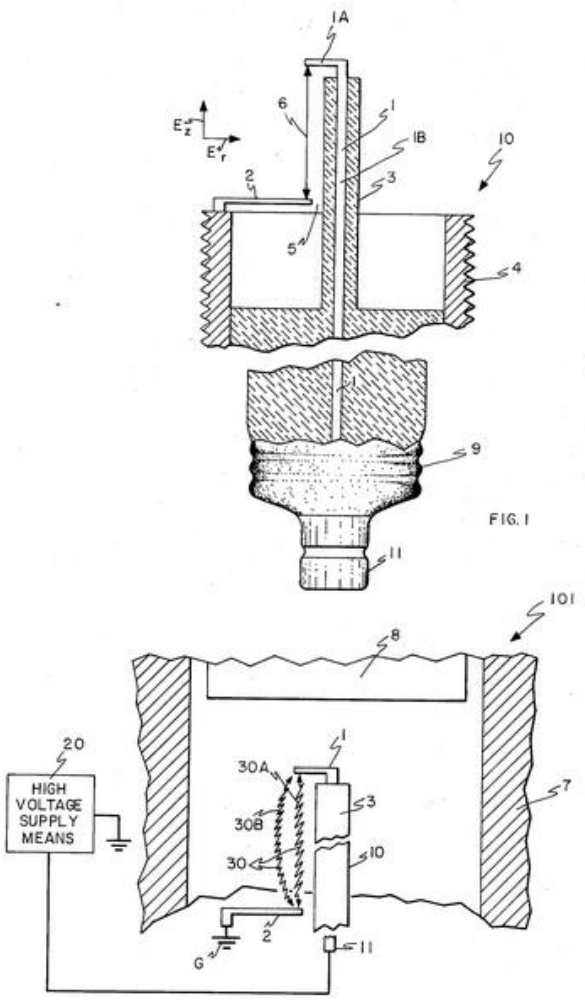

Figure 2.10. *Patent US3974412 diagram*

Other details included in the patent is the information that the insulation can be made of the same ceramic material as conventional spark plugs, so this wouldn't be a road-block for this new design. Also, the base is the same as the common spark plugs, threading into an engine block at electrical ground. This means that it can be used as well in a rotatory engine.

The patent ends with a special mention on the possible applications that the design could have in the future, like being able to program the ECU with not only the spark timing, but also the amount of corona, length of the arc discharge and duration of the arc discharge. This can be done by modifying the capacitor used to generate the HV.

· **Publication US3538372 A - Wide gap discharge spark plug**

Presented on 1968 by Kunio Terao, this patent includes the invention of a spark plug that works in a way that the gap between the electrodes is much bigger than the normal gap (0.6 mm to 0.9 mm). This plug is intended to work as a normal spark plug, but creating a big arc discharge so that a bigger quantity of mixture is ignited and, as an advantage, higher relations air/fuel can be used.

Looking into depth in the patent, it is indicated that the proposal offered can increase the gap up to 2 or 3 times the size of a conventional one. The distribution of this proposal consists in a central electrode and a ground electrode, the first electrode having an outer terminal end free of insulation and an intermediate portion coated with insulating material and the second electrode having a tip end adjacent the outer surface (see *Figure 2.11.).*

Referring to *Figure 2.12*, the central electrode referred as 1 extends through an insulator sleeve jacket 2 made of mica, hard porcelain, alumina porcelain or similar. The upper end of the electrode 1 has and enlarged head 3 not coated with insulation. This head 3 is sized to extend radially beyond the neck portion of the first electrode and the outer surface of the insulation sleeve 2. The ground electrode, referred as 4, extends from the housing 5, a distance around one half the distance of the height of the central electrode 1 from the end of the housing 5 (distance of projection). The gap between electrode 4 and the insulation jacket 2 is achieved by turning inwardly the electrode 4, radially toward the electrode 1 central line. The result of this configuration is that the electrode 4 and the uninsulated peripheral edge 7 of the head 3 is free and clear of obstruction by insulation, which contrasts with the insulation barrier caused by the jacket of insulation between the tip end 6 of terminal 4 and the nearest conductive portion of the central electrode 1.

The disposition specified in this patent results in a minimum gat between both electrodes from 2 to 3 mm (normal spark plugs offer 0.6 to 0.9 mm gap). This increased gap will require a considerable voltage difference between both electrodes. The way the spark will be generated is no different to the one already explained in the normal spark plug generation. The air in the gap will begin ionizing, progressing toward the weaker portion of the electric field. When the air between the upper end 6 of the ground electrode 4 and the head 3 of the central electrode 1 is

ionized, the CD effect starts generating, resulting in an arc that goes advancing through the gap. When this electric arc reaches the other tip of the electrode, the spark is generated. Because this gap is bigger than a conventional spark plug, more of the combustion gases can be ionized, increasing the ignition energy.

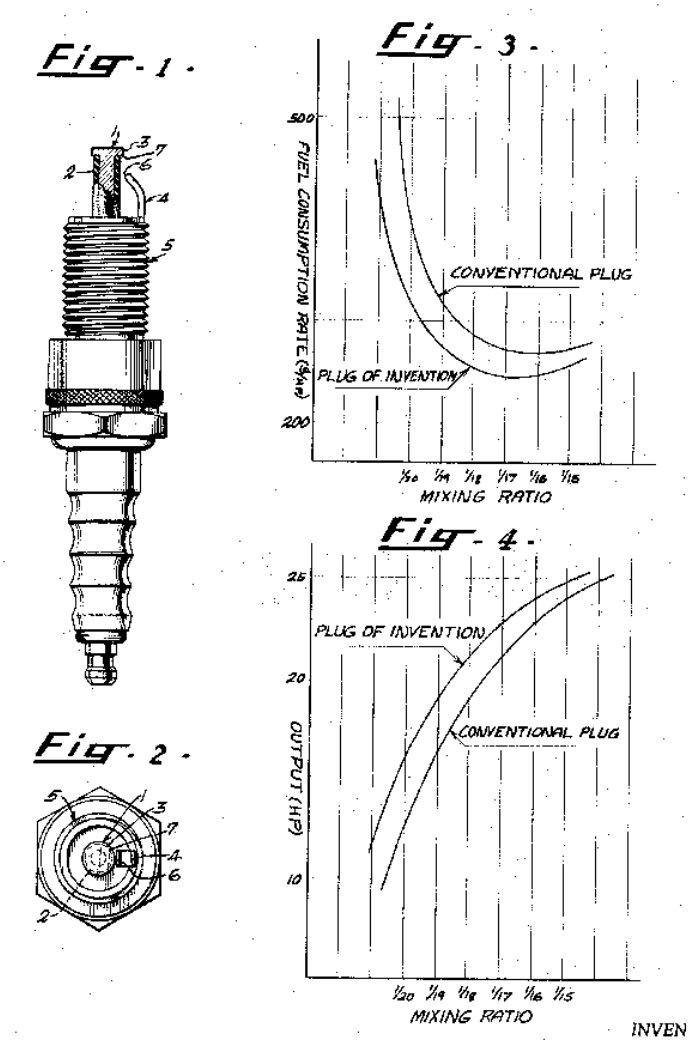

Figure 2.11. *Patent US3538372 schematic representation*

In this patent document it is also possible to find an indication of the required discharge voltage to make this work. The discharge voltage must be in the order of 7,000 V to 8,000 V.

To finalise the patent, the inventor exposes some graphic comparison of the improvements that have been found while running some testing with this new invention (1,200 cc engine with 4 cylinders, running at 3,000rpm). The results showed that the mixing ration can be increased (more air units per fuel unit) when compared to a conventional plug, the reasons behind this is the fact that the electric arc generated covers a much wider gap than the conventional spark plug, so we don't need to have as much fuel concentration in the gas as we would have in conventional spark plugs.

· **<u>Publication EP 0430899 A1</u> - A spark plug, particularly for supercharged and racing engines**

This patent presented by Magneti Marelli S.p.a. is presented in 1990. It describes a spark plug with a disc-shaped electrode that creates an axial discharge, igniting a bigger area of mixture. This spark plug has also a tubular body with an insulating element disposed in the centre which projects the axial discharge. Because the advantages already explained about having a bigger ignition area, the patents remarks its advantageous use in turbocharged engines, so they can use a bigger relation air/fuel.

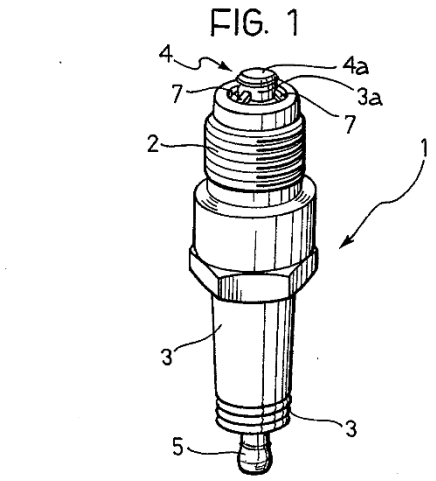

Figure 2.12. *Patent EP 0430899 representation*

The design of this invention is almost identical to the invention specified in publication *US3538372*, so this will not be explained as in detail as before. In case the reader wants to know more details about this specific publication, he can check the Patent in the Annex section of the Project.

· **<u>Publication US 5596974 A</u>– Corona generator system for fuel engines**

Presented by Lulu Trust in 1996, this patent contains the invention of an automotive ignition system in which a high voltage source supplies a continuous high voltage source to each spark plug wire. This continuous application of high voltage to the spark plug produces a continuous corona discharge at the tip of each spark plug. The patent also includes the possibility of using the engine head as a corona discharge surface.

This invention, in contrast to the ones seen so far, refers to the high voltage source instead of the plug itself. The invention consists in a high voltage source connected ti the ignition system that continuously supplies an RF voltage for each spark plug. This high voltage is capacitively connected by placing a metal clip on each spark plug wire and connecting the high voltage source to the metal clips. The metal clip and conductor act as the two plates of the capacitor and the insulation material in the spark plug acts as the dielectric of the capacitor. This high voltage system is designed to generate a continuous corona discharge at the tip of the spark plug internal to the engine, enhancing the combustion efficiency through the production of ozone, electrolytes and other elements, so that when the spark plug finally fires, the burning of the gasoline vapour is much more efficient.

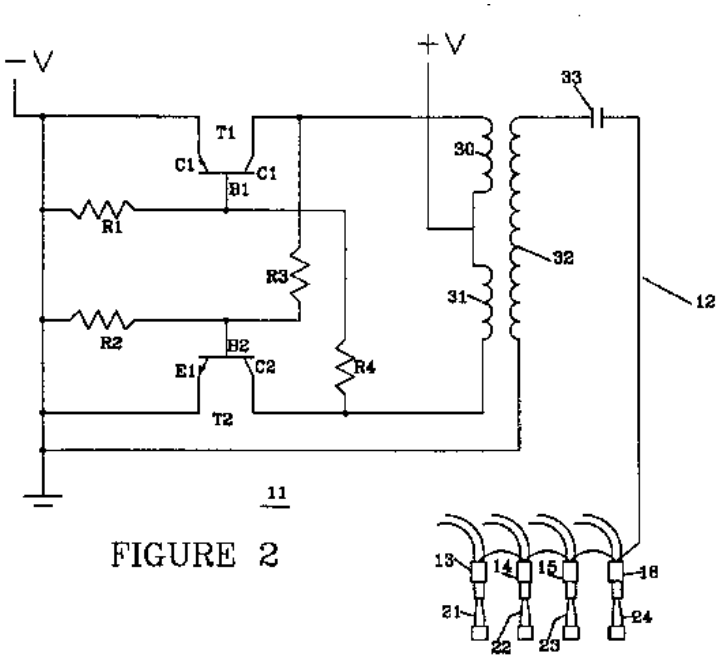

FIGURE 2

Figure 2.13. *Patent US 5596974 high voltage embodiment representation*

The way this high voltage invention works is operation from the D.C. source voltage of the vehicle. The output has a continuous A.C. component magnetic wave with rise times up to 50,000 V, and this is connected to each spark plug by semi-circular metal clip on the outside of the spark plug wire insulation to couple the high voltage through the spark plug wire to produce a corona discharge at the spark plug tip inside the engine.

Figure 2.13. shows an embodiment of the RF voltage source. It is possible to see that the embodiment is composed by to transistors (T1 and T2) that make a relaxation oscillator. Each emitter of the transistors is connected to ground and the negative voltage terminal –V. Each collector C1 and C2 is connected to one end of split primary coils 30 and 31 of transformer Tr1. The base B2 is connected through resistor R3 to collector C1 of transistor T1 and base B1 of transistor T1 is connected through resistor R4 to collector C2 of transistor T2. The RF voltage is conducted from the high voltage source 11 by conductor 12 through coupling capacitor 33. This conductor 12 is then connected to the clips 13,14, 15 and 16 (in this case it is specified 4 clips because the example used is a 4 cylinder engine, but there is no limit to the number of cylinders this can be applied to) which are fastened to spark plug wires 17-20, respectively.

This representation specified in *Figure 2.13*. is just a proposal made by this invention and is not limited to this disposition, so it specifies that any RF source may be used.

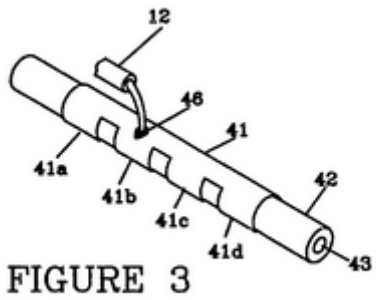

Figure 2.14. *Patent 5596974 RF attachment to spark plug wire*

Looking now at *Figure 2.14*, it is possible to visualize how this RF high voltage source is attached to the main spark plug wire (conventional spark plug wire that common spark plugs already have). Clip 41 is electrically connected to conductor 12. This clip is then clamped around the spark plug wire 42. The other plate is conductor 43 inside of the spark plug wire 42. The insulation material on wire 42 serves as the dielectric of the capacitor. This capacitor will couple the RF energy onto conductor 43 providing the corona in the engine at the spark plug discharge point.

The publication ends the main description of the embodiment specifying that the voltage through the conductor 12 is in the range of 1kV to 50 kV. The frequency of this voltage will provide the continuous corona discharge represented as 26, 27, 28 and 29 in *Figure 2.15*. In the invention object of the publication, frequencies up to 20,000 kHz have been found suitable, being possible to use higher frequencies if needed.

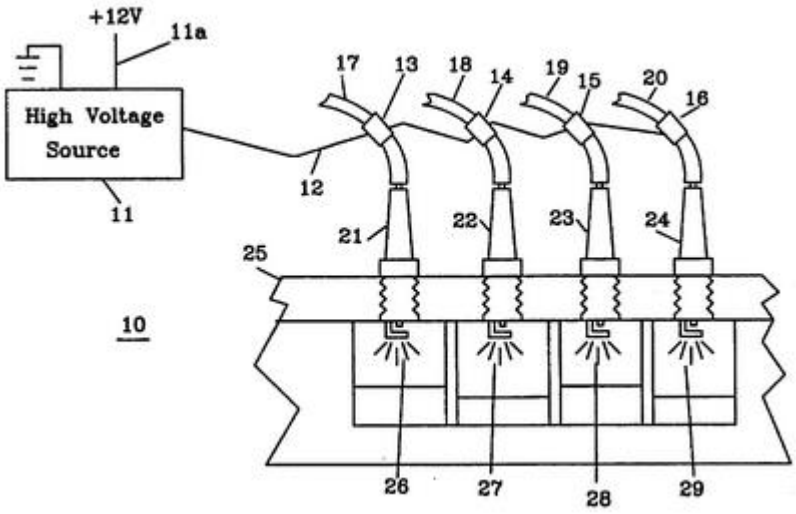

Figure 2.15. *Patent 5596974 RF representation*

The main advantage of the invention is that the corona discharge at one spark plug is independent of the other spark plugs. In the prior art systems to the one of this publication, the corona discharge only happened when the spark was produced at a spark plug, inducing a voltage to the other spark plugs. On the other hand, the limiting factor for this invention is when a corona discharge is produced on conductor 12 or one of the clips 13-16 between the conductor or clips and another metallic object in the engine compartment.

2.3.2. Scientific publications

· ***"Spark Plug and Corona Abilities to Ignite Lean Methane/Air Mixtures"*** **- Laboratoire de combustion et detonique, France**

This publication studies the behaviour of the ignition of extremely lean fuel/methane mixtures. The energetic efficiency and ignition ability is analysed for both normal spark plug ignition and CD ignition.

In the experiment a premixed methane/air mixture of equivalence ratios of 0.55 to 0.517 [1] is ignited by a spark plug or positive corona. The combustion occurs in a cylindrical combustion chamber of 80 mm in diameter and 30 mm in height. In order to have a fair comparison between both technologies, the same electrodes have been used for spark and corona ignition. One discharge electrode is placed along the axis of symmetry of the combustion chamber and the chamber wall is used as another discharge electrode. Discharge gap is in all tests 20mm.

As part of the control of the spark plug ignition, a high voltage converter coil is used allowing up to 25kV. To control the stored energy in the ignition system the value of the capacitor discharging through the primary circuit is used. As results in this study, the maximal energy stored is 80 mJ with a duration of the discharge of 50-100 µs. Peak discharge current is around 16 A.

To generate the corona discharge an "*Entwicklung Leistungselectronik"* type power supply is used in a single pulse mode. The duration of the corona pulse can vary so on the experiment thre different pulse durations were used, 3 ms, 10 ms and 20 ms.

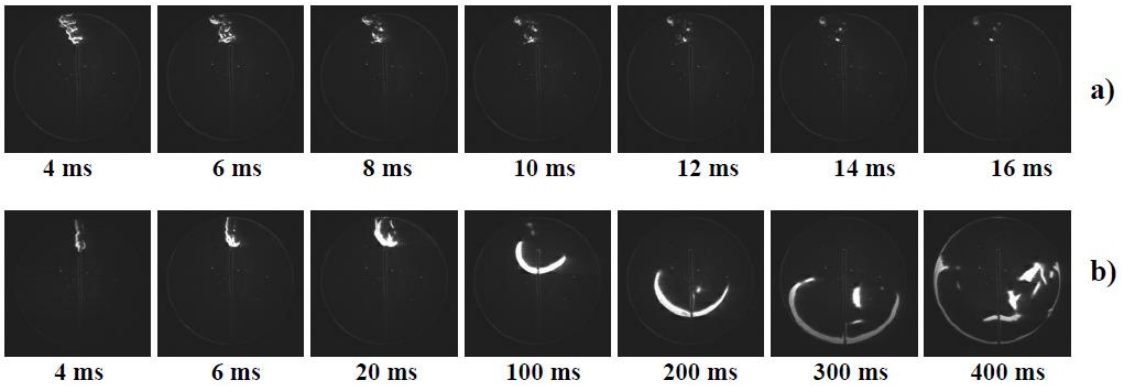

Figure 2.16. *Snapshots of ignition by spark plug (a) and corona (b) in Methane/Air mixture relation of 0.517*

The results of this study shows that the corona discharge allows more efficient ignition with much less discharge energy. This study also proves that the CD allows the regime of ignition and flame propagation on extremely lean mixtures, even when the spark discharge isn´t able to. Also it is specified that the pulse corona generates intensive turbulent flow around the discharge electrodes, which provides faster combustion.

· ***"NOx Reduction from IC Engines with DC Corona Discharge"*** **– The Pearlstone Center for Aeronautical Studies, Ben-Gurion University of Israel**

This scientific investigation does an experimental study of NOx reduction from diesel engine exhaust. Although this study doesn´t look for the same objective as this project, its functionality is very similar to the one that could be used on gasoline engines.

In this case, the objective of the CD is not to ignite the mixture, but to "burn" the gases that come out of the combustion. Doing this, some of the emissions are reduced, in concrete, the NOx. It is found that the cleanness off the gases is independent on the engine load but dependent on the CD reactor length, electrodes' separation distance and needle density. In order to prove this method works, the effectiveness of the NOx decomposition was mapped and optimal geometrical parameters for the best reactor performance were obtained.

As an experimental setup, a Mitsubishi 3 cylinder diesel engine with total volume of 1300 cc was used. In *Figure 2.17.* a sketch of the test rig is shown.

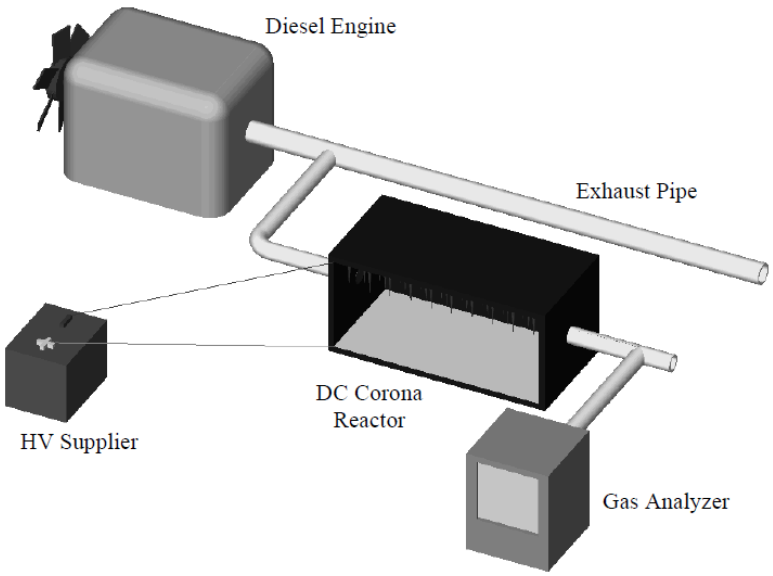

Figure 2.17. *Experimental rig setup*

The reactor was built as a box that has a rectangular cross section with 100x100 mm inner dimensions, made of Perspex. Medical needles of 0.6 mm external diameter are installed on the plate in the disposition shown in *Figure 2.18.*

The results of the experiment shows an important improvement on the cleanness of the exhaust gases, but this alone doesn´t provide enough information for a feasible design. The energy consumption must also be considered. As a result, the energy consumption varies between 15 and 30 gr NOx/kW-h, which is good enough. However, a DC corona reactor results an important expensive solution and also there is the consideration of the space it occupies.

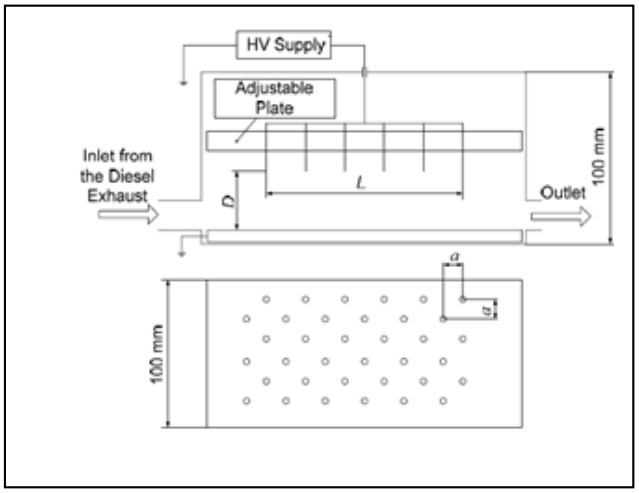

Figure 2.18. *Experimental rig needles setup*

· **"*Transient Plasma Ignition of Quiescent and Flowing Air/Fuel Mixtures*" – IEEE Transactions on Plasma Science, Vol.33, Nº 2, April 2005**

This study focuses on using a pulse ignited CD in a pulse detonation engine (PDE), using a methane/air mixture.

This study is very similar to the first scientific publication exposed in this section, for that reason the lector might find some similitudes between them.

The ignition of a pulse detonation engine (PDE) is a useful potential application of transient plasma technology. The PDE is attractive because it is potentially a low-cost alternative to turbojet and liquid-propellant rocket engines. As in automobile engines, PDEs require a premixed flame to undergo a deflagration-to detonation (DDT) transition in each cycle within the engine length. DDT length and time will determine the limits of engine size and operation cycle.

The setup of the experiment consists in create transient discharges with a pseudo spark switch-based pulse generator, as shown in *Figure 2.19.*, and the ignition chamber, made of steel with a cylindrical form of 63.5 mm inner diameter and 200 mm in length. On one end of the chamber it has ports for has supplies and vacuum pump, and on the other end transducers for measuring reactant partial pressures and the total gas pressures during combustion.

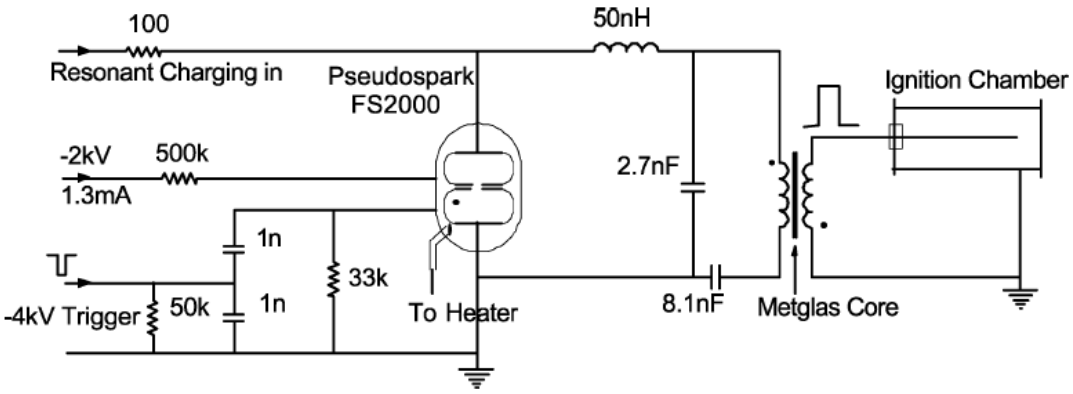

Figure 2.19. *Pulse generator circuit schematic for transient plasma assisted ignition experiments*

As a result to this study, reduction of ignition delay times were observed of the order of 4 times. The transient plasma ignition strategy is seen to provide an accelerated combustion sequence leading to the rapid generation of strong pressure waves and transition of laminar flame to turbulent flame.

After having a look at the presented publications and patents, it is possible to notice that the CD effect has been studied for a long time, being noticed the first spark plugs using corona discharge effect around 1970. Although in this project only the most relevant publications have been exposed, there are hundreds of studies implementing the CD effect in the ignition of a mixture of air/fuel, this indicates that there is a large interest on developing this area of the ignition technology, as it has great advantages that could be successfully applied on today´s engines. It is also noticeable that this research area is also growing very fast, as in the last 4 years new patents have been presented and new and interesting advancements have been done, for example the Federal-Mogul ACIS.

3. CORONA DISCHARGE ANALYSIS

Before being able to control the corona discharge effect, it is important to choose the way it is going to be studied. There are 3 configurations that can be used:

- **Atmospheric discharges:** Only air at 1 bar pressure is covering the discharge gap between the electrodes.
- **Dielectric barrier:** A dielectric barrier covers the discharge gap between the electrodes.
- **Packed bed reactor:** Very similar to the dielectric barrier, a packing material covers the gap between the electrodes. This material is usually glass particles (SiO2) or synthetized nanoparticles like γ-Al2O3.

These three configurations have been under investigation for the last 30-40 years and there is still the open question of which of the three offers the best efficiency. As it is not possible to choose by only looking at the efficiency, it is important to find which of the configurations offers a simple control and an easy implementation to the combustion engines (this is the final application this project aims to).

From the three configurations, the ones that offer better properties are the dielectric barrier and the atmospheric discharge. Looking at both, it appears that, although the barrier discharge achieves higher electrical power densities, it is more complicated to control since it is a combination of a gas discharge and a surface discharge. For that reason this project is focusing from now on in the atmospheric discharge.

3.1. Pulsed atmospheric discharge

This type of discharges have different appearances. The most known is lighting, which consists in an arc with short duration and high power density. This arcs are usually used for welding, high voltage circuit breakers and certain types of lamps. The arcs with duration of microsecond range are the commonly known sparks. Shorter discharges with duration of nanoseconds range are called transient discharges. This type of discharges stop before they have completed their arc, so they never get to produce the spark.

There are two ways to produce the transient discharges. One way is using a dielectric barrier (*dielectric barrier discharge*). The second way is to use an asymmetric electrode pair, making the discharge develop in the high field region near the sharp electrode, spreading towards the cathode. Using the second option, the way to avoid the transition to arc can be lowering the voltage enough to stop the spreading of the discharge somewhere before the cathode is reached.

It is also possible to avoid the transition by stopping or lowering the voltage when the cathode is reached.

Using the second way more energy can be put on to the discharge, but it is more difficult to make the power supply. This type of discharge is the one known as Corona Discharge (CD), which is the object of this project.

The CD can be called:

- **Positive Corona:** The electrode with the strongest curvature is connected to the positive output of the power supply.
- **Negative Corona:** The electrode with the strongest curvature is connected to the negative output of the power supply.

In relatively low voltage corona discharges, the discharge stops itself due to the build-up of space charge near the sharp electrode. This space charge then disappears due to diffusion and recombination and a new discharge appears. This effect can happen in both the positive and the negative corona and it is called self-repetitive corona.

3.2. Test layout

As explained in the previous point, we are going to use the pulsed atmospheric distribution, producing discharges of duration in the range of nanoseconds. Take in consideration that this test layout has been used as indicated in study documents included in the annex. To do the test we are using an asymmetric electrode pair where the transition to arc will be avoided by lowering the voltage when the cathode is reached.

Knowing this, the steps of this process are:

1. Asymmetric electrode configuration must be made
2. A high voltage must be applied
3. Some free electric charge must be present
4. An avalanche must build up and leave behind a space charge area
5. Photons from the avalanche create new charge carriers outside the space charge area
6. New avalanches develop closer to the cathode

3.2.1. Asymmetric electrode configuration must be made

It is required field enhancement near one electrode. To do so, the most conventional methods used are point-to-plane (convenient for comparisons with model calculations) and wire-in-cylinder geometries (suitable for gas treatment where the residence time in the cylinder is an

important parameter). Looking at the results from other studies relating corona discharge [2], we can see that the current density is approximately 10^9 A/m^2, which makes expect erosion of the anode. This would be a study of the long-term application, but this is not studied in this project.

3.2.2. High voltage must be applied

The order of the breakdown field strength in a uniform gap with atmospheric air is in the order of 3kV/mm. This means that a free electron gains several eV of energy from the field in-between collisions. The ionization energy of air molecules is approximately 10eV, but the electrons in the tail of the electron energy distribution function will have enough energy to cause ionization. Field emission cannot occur because the electrons are drawn towards the anode.

3.2.3. Free electric charge must be present

The first electron to start the discharge can be provided either by cosmic radiation or by field detachment from negative ions. The cosmic radiation leads to low background electron densities of 10^3-10^6 el/cm^3. This will mean that it takes some time for an electron to be at the right place. This time is known as inception time lag and in practice it varies from about 1ns to some microseconds. The other method, the field detachment from negative ions, is important when ions of a previous discharge are still present. It occurs in the self-repetitive DC corona and it causes the streamer to choose the path of its predecessor. In most applications of pulsed corona it does not occur due to the low repetition rate (approximately 100 Hz)

3.2.4. Avalanche must build up and leave behind a space charge area

When talking about an avalanche building up, this makes reference to the fact that when the first electron has caused an ionization, there are two electrons left that again start moving in the electric field and ionize again. This process continues until the space charge of the slow ions that are left behind cancels the applied electric field. The avalanche can also stop at the anode before it is complete (the avalanche extinguishes). The length required to build up a complete avalanche is called the critical length, which at 1 bar it is in the order of 1mm [3].

3.2.5. Photons from the avalanche create new charge carriers outside the space charge area

The space charge region cancels the field between itself and the anode, but it enhances the field in the direction towards the cathode. Having a free electron at the right position in this area can start a new avalanche. It will be required a process to provide a new electron because the background electron will be disappeared from the gap due to drift. This required process can be photoionization, which is caused by the resonance photons of nitrogen that are absorbed by oxygen. The problem with this process is that data on photoionization in these cases is

unavailable. Computer models of streamer propagation are also made without photoionization. An artificial background electron density is then required for starting new avalanches. Although such background is not realistic, the results are very similar to models that do include photoionization.

3.2.6. New avalanches develop closer to the cathode

The electrons of the new avalanche cancel the previous space charge but create a new one closer to the cathode. In order to continue the propagation of the streamer channel, it is found that a stability field of 5 kV/cm is enough [4]. If the power supply can continue to deliver current the temperature of the channel will increase due to Joule heating, then its resistance will drop and the discharge may develop in to an arc.

In this study, it is considered that the corona current stops after the streamer head reaches the cathode, but there are many processes that continue to occur in the gap after the discharge has stopped. The most important processes are:

- **Attachment:** This is the formation of negative ions when low energy electrons combine with atoms or molecules. It is important to know that not all particles form negative ions (noble gases and nitrogen). Some molecules that easily form negative ions are O_2, H_2O and CO_2. The capturing of low energy electrons will influence the conductivity of a plasma, as the light and mobile electrons are replaced by heavy ions. Therefore, the field strength for sustaining a certain current is much higher in an electronegative gas.

- **Recombination:** The recombination of positive ions and electrons leads to the neutral has as before the discharge pulse. It can cause some additional effects such as the emission of recombination radiation which can be used to determine the electron energy if its intensity is sufficient. In case of a CD this is not to be expected.

  The recombination time in the atmospheric corona discharge is estimated to be in the order of 1 μs. In other experiments it has been found that the time interval required for a corona pulse in order not to notice its predecessor is found in experiments to be in the order of 1 ms. The reason of this interval is probably due to negative ions and metastable that have much longer lifetimes than electrons.

- **Diffusion:** The active particles in a corona discharge are formed in a thin channel. The intention is to treat the whole gas volume, so it is possible to wonder if diffusion is able to spread the radicals significantly. From Schlieren pictures (these can be seen in the next section of this project 3.3.5) it is seen that the streamer diameter increases

approximately 2 mm in 0.2 seconds. This increases the treated volume but still a single discharge pulse treats only a volume fraction in the order of 10^{-3}. This is the explanation to why it is required a residence time of several seconds for a complete treatment. Until now this effect has not been studied in detail, but it is believed that the turbulence created but the corona discharge could help to mix the gas.

- **Vibrational relaxation:** The high-energy electrons that are in the streamer head cause ionization and excitation to higher electric states. These excitation also leads to high vibrational relaxation by which these states decay through collisions to rational and translational excitation. This is the same as saying that the gas is heated.

- **Metastable quenching:** It is not possible for excited metastable states to lose their energy by emission of a photon. Another process able to do so is by collisional quenching. A collision with low energy electron can cause them to become resonant and lose the energy by emitting a VUV photon and become ground state, as metastables are often close to resonant levels. Another option is to transfer all their energy to another molecule which could cause dissociation of a water molecule. No quantitative studies are available at the present to evaluate this and se in a more extensive way which effects has over the CD.

- **Radical reactions:** The radicals are formed by electron impact dissociation of molecules in the streamer head region. Primary radicals are the ones created directly by these collisions. They may react rapidly with molecules to form secondary radicals such as HO_2 or O_3. If gas contamination is present (SO_2 or NO) the previous gases can oxidize them to acids. How much this happens will depend on the gas composition.

3.3. Diagnostics

As it is explained in the previous section of this project, this test layout and the results of it have been obtained from the research documents that will be included in the annex.

From those studies, the effects that were observed in the testing are explained in the following points. In order to analyse the testing there have been used different methods, each of one shows different characteristics of the CD generation. The ways of reading the results and the diagnostics of these results are:

3.3.1. Cloud Chamber tracks

The first recording of avalanches, shown here in *Figure 3.1.*, were made by Raether [5]. To do so, a cloud chamber was used to grow droplets around the ions that are left behind. These droplets were photographed through light scattering. A disadvantage of these pictures is that they don´t have time resolution, but as an advantage they are extremely sensitive.

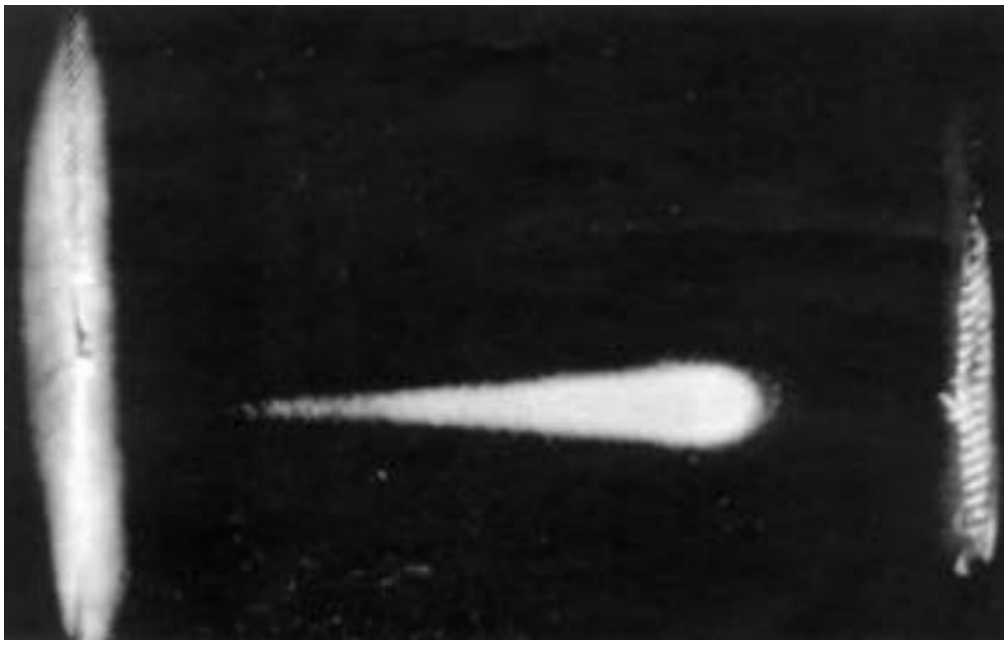

Figure 3.1. *Cloud track picture of a single avalanche (picture taken by H.Raether, [5])*

In *Figure 3.1.* it's possible to see an avalanche obtained by Raether from 1939. The length of the avalanche is of the order of 1 cm.

3.3.2. Photography

It is very difficult to obtain detailed experiment results of the streamer discharge using the photography method due to the short duration of this. As an average, the total duration is around 10 ns, and the streamer head moves along its own thickness in 0.1 ns. At present day, intensified high speed cameras can obtain pictures in 1ns intervals. This sensitivity is close to the photomultipliers required. This speed will be sufficient to allow a single shot exposure.

Figure 3.2. *Streamer propagation in a point-to-plane gap. Real size per frame approx. 3x3 cm^2 (picture by A.H.F.M. Baede [6])*

In *Figure 3.2* it is possible to see a photograph of a point-plane CD in a 25 mm gap in ambient air using a voltage pulse of 25 kV with a rise time of 30 ns. The camera that was used here had the specifications of 1024 x 1024 pixels, pixel size 13 µm x 13 µm, sensitivity of 180-850 nm and a minimum optical gate 0.8 ns. The resulting gain of the camera resulted in up to 3600.

The three trigger moments represented in the figure have a total gap of approximately 40 ns. The dark spots of the streamer heads are exposed in these pictures, therefore they look larger than they are. An analysis of their full width at half maximum shows a value of 150 µm for all stramers observed under this condition [6].

Looking now at *Figure 3.3* it is possible to see two examples of pictures taken with exposure times of 100 ns, which is representative of a time integrated picture of the discharge crossing the gap. In the left part it is possible to see that the streamers spread out to a width that is larger than the point-wire distance, while in the right figure the streamers bend out in the middle of the gap but they redirect towards the wire.

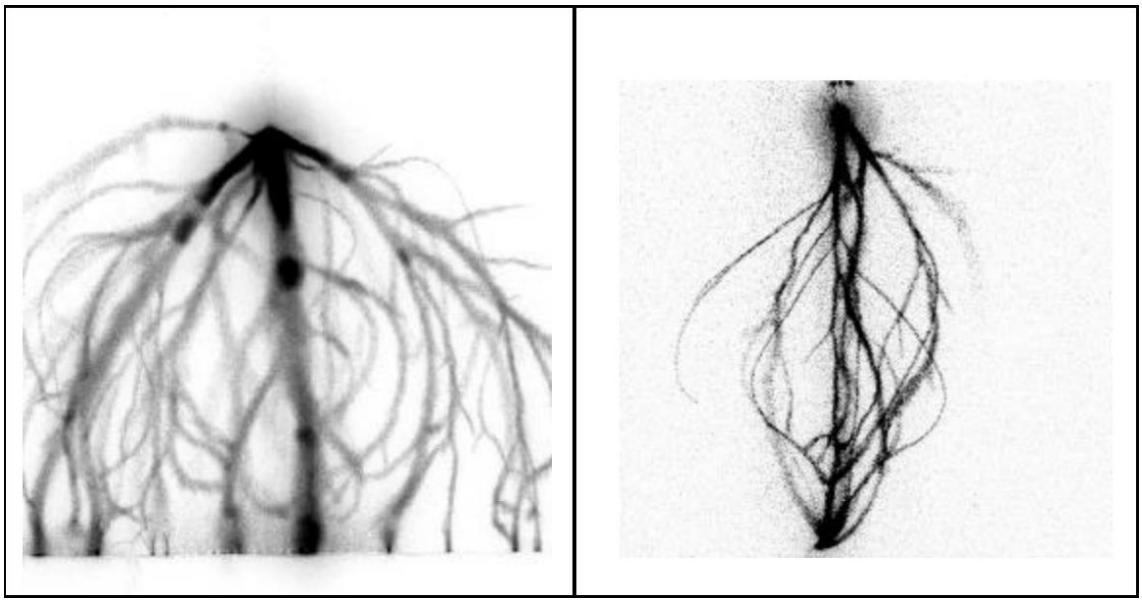

Figure 3.3. *High speed photographs of a point-wire corona discharge in a 25 mm point-wire gap in air. (Left: view perpendicular to wire / Right: view parallel with wire)*

3.3.3. Streak pictures

The streak method consists in using an image-intensified camera. This method was used by Wagner [7]. The results of this type of photography is an image showing one spatial dimension against time. In *Figure 3.4* it can be seen that in the case of plane electrodes the streamer starts in the middle of the gap and it develops towards cathode and anode. Two phases of developments are distinguished: from 60 to 70 ns with a propagation velocity of approx. 2-3 x 10^5 m/s and from 70 to 80 ns the speed becomes to approx. 10^5 m/s.

Figure 3.4. *Streak picture of cathode (bottom) and anode (top) directed streamer n a 30 mm plane gap. (Picture by K.H. Wagner [7])*

3.3.4. Emission spectroscopy

A way of analysing the optical emission of the corona streamer is using spectroscopic techniques. Monochromators have sufficient resolution for a discharge at 1 bar but main problems are the low intensity and short duration. A good technique that suits this case is the time-correlated single-photon counting method.

The single-photon counting method uses an optical trigger to determine the timing of the photon to be counted. A time-to-amplitude converter can be included to obtain a time resolution down to 0.1 ns. Several slightly different version of this method are also used for the self-repetitive discharge [8-10] as well as for the corona discharge [3].

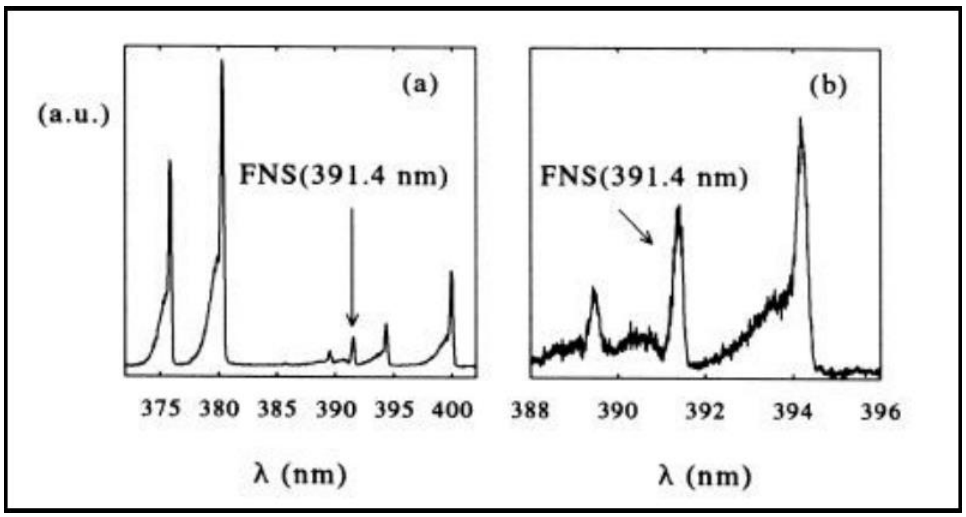

Figure 3.5. *Emission spectrum of a pulsed corona discharge showing parts of N2 SPS and FNS (picture by Creyghton [3])*

The *Figure 3.5* shows an example of a part of the nitrogen spectrum in the near UV. –because this systems have very different excitation levels the ratio of their intensities is a measure of the electron energy. Using this effect it is obtained approximately 10 eV for electrons in the streamer head [3].

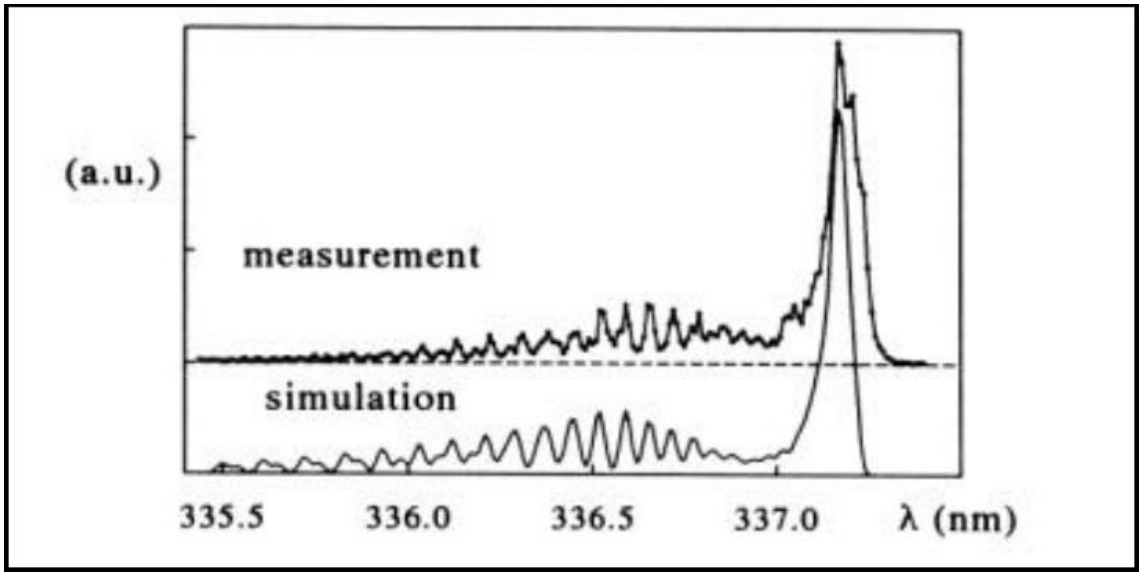

Figure 3.6. *Measured and calculated rotational structure of the N2 SPS (0-0) transition in the secondary streamer phase of a pulsed corona (picture by Creyghton [3]).*

Figure 3.6 shows the resolution of the SPS rotational structure. This is compared with a calculated spectrum with a rotational temperature of 350 K. The spectrum is recorded in a time interval of 50-200 ns after rise of the voltage pulse, so the secondary streamer is observed [3], showing that the gas is still hardly heated at this instant. The width of the measured spectral line can also be used.

3.3.5. Schlieren photography

The path created by the corona streamer has a composition that is different from the surrounding gas and it can also have an enhanced temperature. This will mean that its index differs from its background. In order to visualize this difference the Schlieren photography offers this possibility. This can be performed in three different ways:

1. **S**tandard Schlieren methods are sensitive to the gradient in the refractive index, *dn/dx*.
2. Interferometry, which is related directly to the refractive index *n*.
3. Shadowgraph, which is proportional to *d2n/dx2* [3].

Figure 3.7 was obtained by a standard knife-edge method.

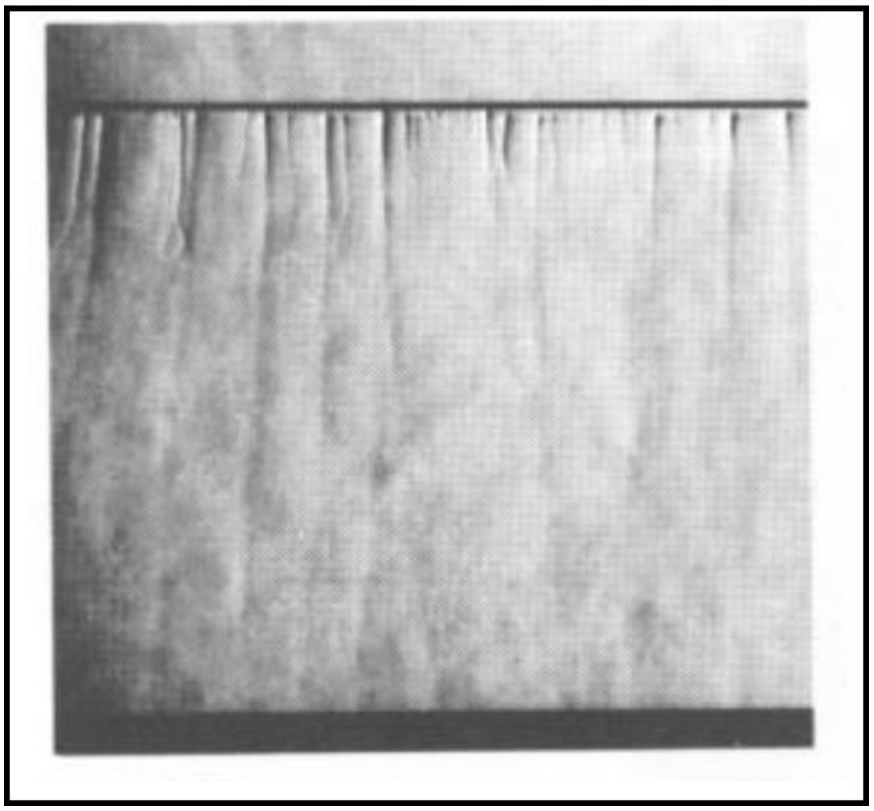

Figure 3.7. *Schlieren photograph of wire-plane pulsed corona taken 100 µs after the voltage pulse (picture by Creyghton [3]).*

The remarkable result of Schlieren pictures of a CD is that its appearance is most clearly 50 to 100 µs after the voltage pulse. It is possible to notice that within 1 ms the streamer paths are not observed. The explanation for this is that the fast electrons first cause ionization and vibrational excitation that does not affect n. After vibrational de-excitation to rotations and translations the streamer channel gets heated and shows up more clearly. A time constant of 100 ms for this process is reasonable.

3.3.6. Absorption spectroscopy

The advantage of absorption spectroscopy is that it easily gives quantitative information on the lower level of the transition involved. Calibration is usually straightforward from known cross sections or gas mixtures. This method can be used to detect all kinds of species in a discharge system. The most used are Ozone, NO, NO_2, SO_2 and NH_3 [11]. Short living excited states and radicals, created by the discharge can also be measured. Absorption spectra can also be used to determine rotational temperatures.

3.3.7. Laser induced fluorescence

Although absorption spectroscopy is relatively easy it cannot be used in many cases because the absorption of low-density species is weak. The molecule that has absorbed radiation can emit this in other directions and also at other wavelengths, this comes to be the so-called fluorescence. In that case, using a strong source like a laser can increase the signal. The sensitivity of this method is many orders of magnitude higher than the classical absorption technique. The first example of its use in a barrier discharge is the detection of OH radicals [12, 13].

3.4. Test remarks

The outcome that it is possible to obtain from the analysed research documents is that the CD is something that is in use at atmospheric pressure and that it has been under investigation for a long time. The most recent use of it is with a pulsed power supply.

It is easy to think that given all the information and with all the research already done in the CD the situation is well known, but this is a big mistake. A lot of the processes that happen in the CD and that have been explained in this project are only assumed or estimated. An example of this is the field emission, photoionization, collisional de-excitation, etc. The reason for not having all of the information is that the tools available at the present aren't enough to analyse in detail all the points of the CD. So, the way to face this is to make a theory and experiment analysis with all the available tools to make the results more quantitative. All the methods that have been mentioned can be used and it is possible that after this project is finished more techniques become available.

Now that the knowledge of CD generation is clear, the thesis can propose a generation model to be used in the laboratory for studying the effect as explained above. The next section will focus on this generation circuit and how it must be to help generating the Corona effect.

4. CIRCUIT FOR THE CORONA DISCHARGE GENERATION

After all the main research done it is now possible to understand the main weaknesses of this system and investigate where the main focus needs to be. This section will focus on proposing a corona discharge generator and control system that allows us the capability of controlling the effect in the ignition plug.

From all the patents and studies investigated, there is one that will be used as a base to start this proposal of the electric circuit. Concretely, the patent used as a start is *Publication US 5596974 A.* The proposed design in the patent states a high voltage source with a continuous supply of RF voltage to each spark plug wire, generating then a continuous corona discharge when the spark plug is activated. The new proposal will try to use the same idea but instead of generating a continuous corona discharge, the objective will be to generate a variable discharge by making the RF voltage variable as well so that the design can be used to make further studies on this effect and verify the combustion at different frequencies to help understanding better how to control this effect.

4.1. Elements of the electric circuit

With this concept of the electrical circuit, it is needed a variable generator that allows to modify RF independently from the voltage. The RF formed between the electrode and the ground produces a RF electric field in-between that creates non-thermal plasma.

The second important element in the generating system will be the transformer that increases the voltage from the main RF generator (between 5-15 V) to the required voltage for the CD to develop (approximately 20,000 V peak to peak). It is very important that the core of this transformer is made from ferrite, as this will allow the usage of the high frequency. Regarding the RF generation, this must also be variable as this will help controlling the CD development in the cylinder and it will provide the capability of setting it up so that depending on the conditions in where the vehicle is running (engine speed, air temperature …) the corona discharge is always generated. From the studies realised in section 3 it is known that the air and RF characteristics will have direct effect in how the CD starts and develops.

The third element important for the generation will be the coupling of the generated RF voltage with the main ignition wires voltage, so that when the discharge is activated in the spark plug the RF couples with the discharge, resulting in the CD effect in the plug. This third part of the circuit will also have to contain a Shunt resistor for making the appropriate measurements.

In the next section of this document it is possible to see the study realised for this circuit, with some proposals on how to proceed. As mentioned above, this proposal is made in order to study the effect of the CD at different frequencies and voltage. No further development is made in this thesis as this is not something considered in the objectives. The complete development of the circuit would be subject to another thesis and it would be recommended to use one of the verification methods discussed in section 3 of this document.

4.2. Schematic for the CD generation

In this section, the proposal for the circuit is explained in detail. The Software Multisim© has been used to represent some of the circuits and also to verify each module.

As mentioned in the previous section, the CD circuit will consist in 3 different modules: The RF generation module, the transformer to HV module and the HV circuit module, containing the CD plug and the Shunt ammeter for current measurements. In the following points, each module is explained separately with a proposal on how to implement it.

4.2.1. RF generation module

In order to generate the RF signal, two different proposals have been investigated. The first one consists in using an operational amplifier to generate the low voltage sinusoidal signal we require. In order to do this and to be able to regulate the frequency generated, a potentiometer is needed so that we can vary the resistance offered by it and by this way, making frequency of the output signal increase or decrease.

Before going into the design of this module, it is required to define the main frequency that is required and also the voltage that will give the output. Ideally, the voltage in the output should be as high as possible to reduce the size of the transformer. From similar circuits the range of the voltage obtained is 5 to 15 V peak to peak. Regarding the frequency, ideally it is required to be able to regulate the frequency from 50 HZ to 500 kHz. Higher frequencies might be able to be implemented as well but this is the main range that the generation module should work in.

In *Figure 4.1.* it is possible to see one circuit proposal. This circuit consists in an operational amplifier IC (Integrated Circuit), LMH6622MA. The first operational amplifier U1A is used to generate a square wave which is then transformed to a sinusoidal wave in the operational amplifier U1B. The output frequency is controlled by potentiometer R1. Unfortunately, this system doesn't allow to control frequency and voltage independently, so the more output frequency, the less voltage peak to peak there will be.

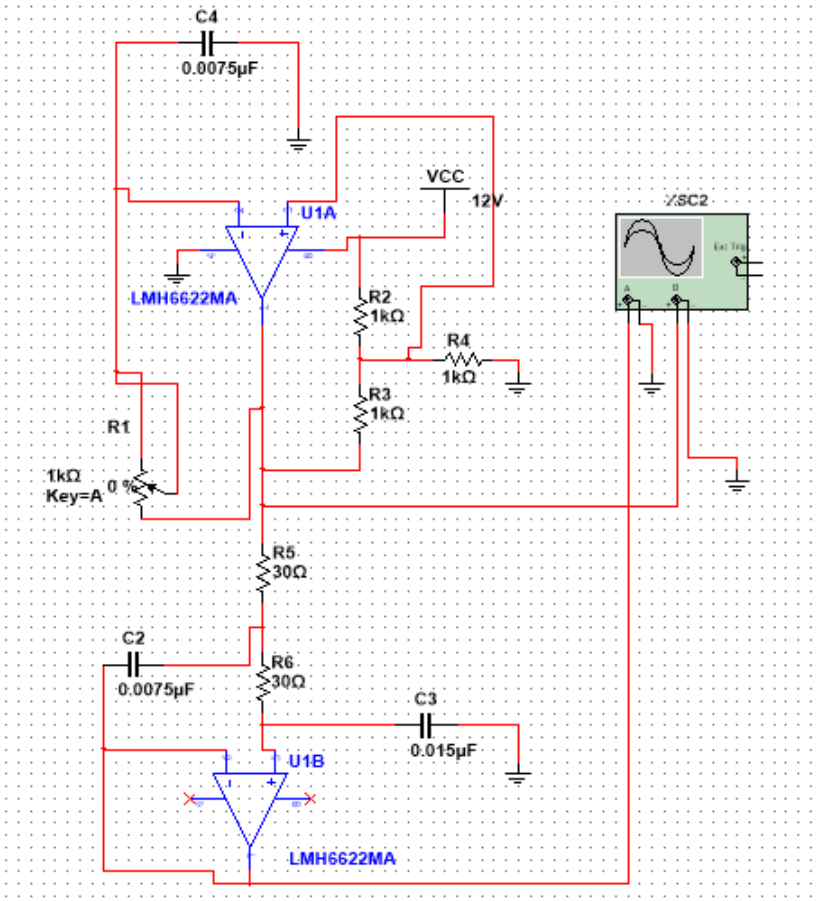

Figure 4.1. *Sinusoidal generator using operational amplifiers*

As an example of the results obtained with this circuit, *Figure 4.2.* and *Figure 4.3.* show the wave obtained for the potentiometer at 25 % and at 75 % respectively.

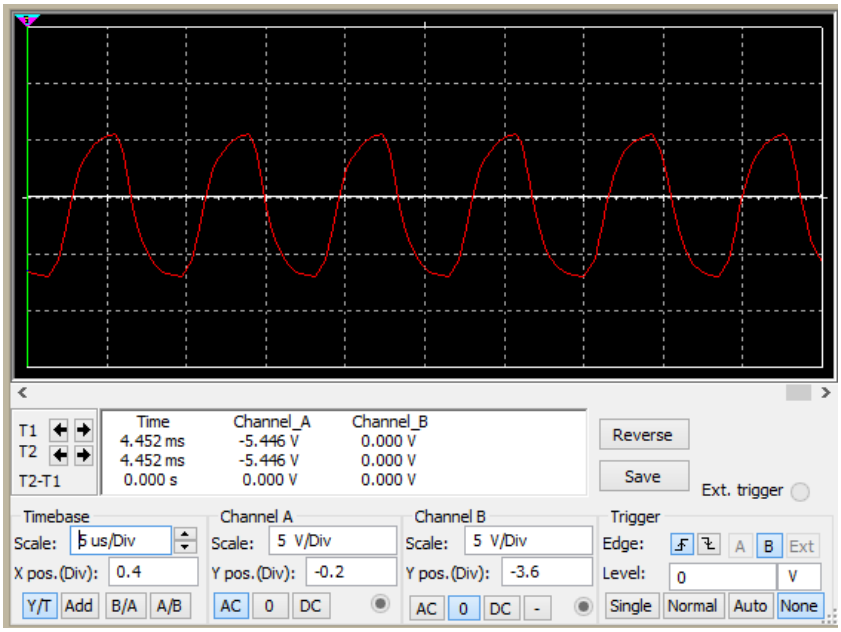

Figure 4.2. *Wave obtained using* LMH6622MA IC when potentiometer at 25%

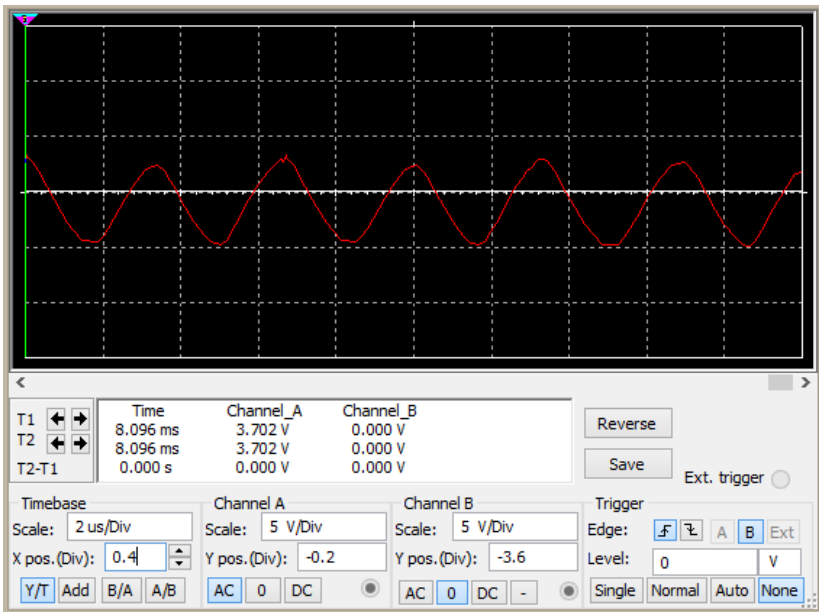

Figure 4.3. *Wave obtained using* LMH6622MA IC when potentiometer at 75%

From the above waves, it is possible to see the direct effect the potentiometer has in the output voltage (approximately 50 % voltage difference between both waves). Also, the frequency for *Figure 4.2.* is approximately 100 kHz and for *Figure 4.3.* is approximately 250 kHz. These frequencies are inside the main range required, but it doesn't meet all the range as this is way above the minimum frequency stablished in the initial assumptions.

Another drawback of the circuit is that the wave generated has a lot of noise and the sinusoidal wave is affected negatively by it, creating some possible fluctuations in the CD generation that could result in inaccurate testing.

As an alternative and another cheap way to generate a sinusoidal wave, it is possible to use a Wien Bridge oscillator structure. This would offer a higher voltage sinusoidal wave which would help reduce the required transformer size. *Figure 4.4.* shows a Wien Bridge oscillator with its respective results, where the resistor R17 is used to tune the sine wave generated.

The frequency of the sinusoidal wave generated is directly related to the resistances and the capacitors, following the following formulas:

$$R13 = R14 = R \qquad \text{(Eq. 4.1)}$$

$$C7 = C8 = C \qquad \text{(Eq. 4.2)}$$

$$f = \frac{1}{2\pi CR} \qquad \text{(Eq. 4.3)}$$

$$R17 = 2 \cdot R16 \qquad \text{(Eq. 4.4)}$$

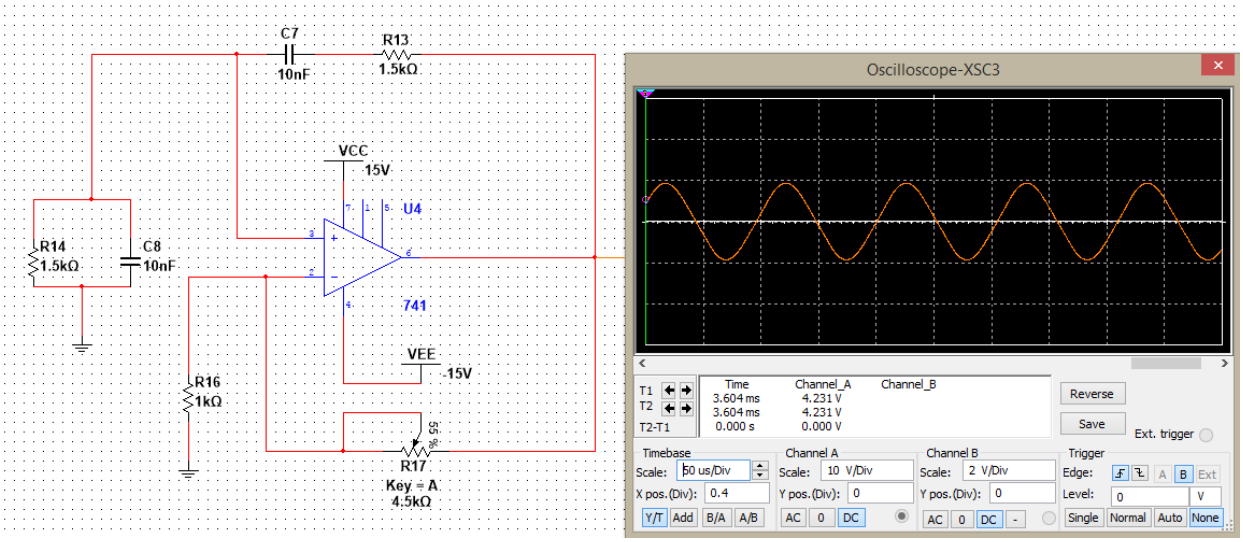

Figure 4.4. *Wien Bridge oscillator circuit using IC 741*

The main drawback of this circuit will be the frequency regulation, as in order to change the frequency it is required to change either the condensers or the resistances at the same time so that it still applies the frequency formula mentioned above. Also a big problem is the frequency capabilities of the operational amplifier used, which will limit our range capabilities.

After considering both options, the proposal of this project has been focused on using the Wien Bridge oscillator structure, but in order to implement it as appropriate to the project, some modifications have been made, resulting in the circuit shown in *Figure 4.5*.

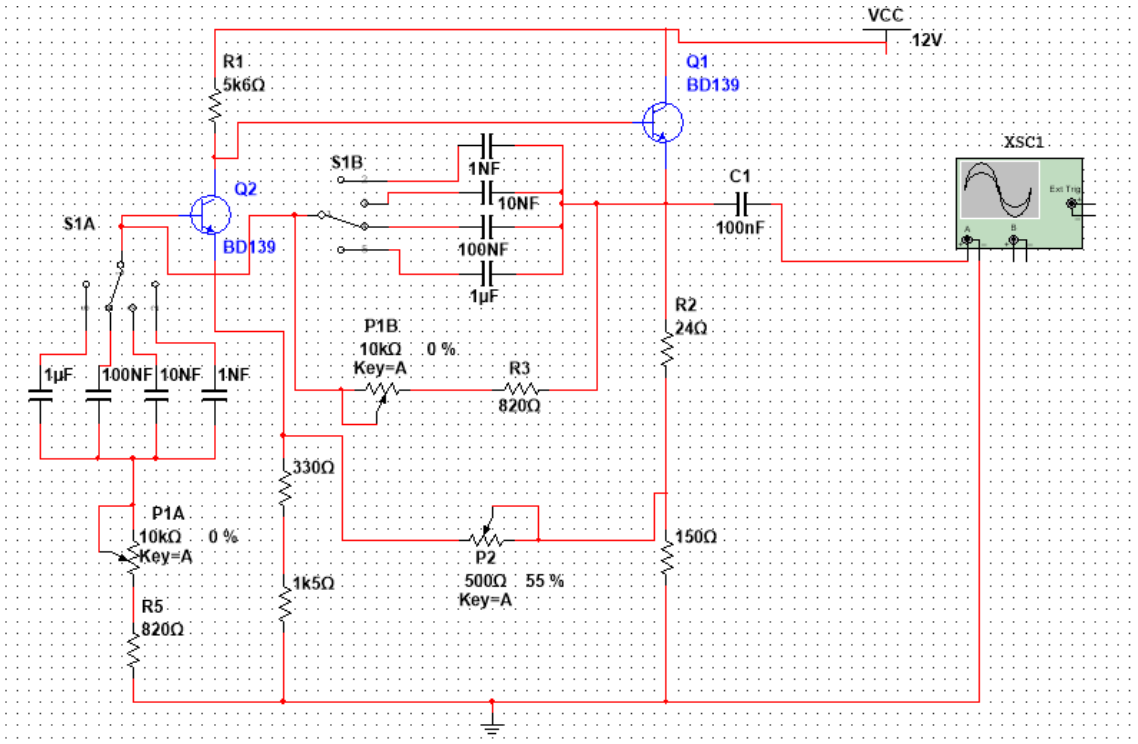

Figure 4.5. *Sine Wave generation (Wien Bridge) module with range from 15 HZ to 200 kHz.*

The main difference in the circuit is in the replacement of the operational amplifier for transistors, as this will simplify the elements of the circuit and it will allow to use higher frequencies than the one limited by the operational amplifier, giving room to future and simple modifications if the range is too short and it is desired to increase it to higher frequencies. In terms of the circuit it still uses the Wien Bridge oscillator schematic. Another noticeable difference is the addition of Switch S1A and S1B (coupled switches that change at the same time and at the same pin), and the addition of potentiometer P1A and P1B (coupled potentiometers that change at the same time and value).

As discussed at the beginning of this section, the frequency in the Wien bridge depends in the Capacitor value and the Resistor value, so in order to be able to control in different ranges the circuit has implemented the Selector 1 (S1) as a selection of different capacitors, offering different range of frequencies, and the Potentiometer 1 (P1) to move along the range stablished by the selector selection. So, in case in the future higher frequencies are required, by simply modifying the switch and adding another position with a capacitor of lower capacity, the frequency can be increased, always taking in consideration the limitation from the components in the system (transistors BD139).

The result of the generator ranges depending on the selector position will be:

- **Selector in position A (10 uF capacitor):** 15 Hz - 200 Hz
- **Selector in position B (100 nF capacitor):** 200Hz – 2 kHz
- **Selector in position C (10 nF capacitor):** 2kHz – 20 kHz
- **Selector in position D (1 nF capacitor):** 20 kHz – 200 kHz

The potentiometer P2 is used to refine the sine wave, as in the low frequencies it has been observed some small distortion of the sine wave that could need some refinement.

As for the tension, the circuit can be connected to a 12 V source, being possible to use the car battery for the purpose when implementing the circuit. In the output the value depends on the frequency. At low frequency the tension is 9 V, but when going to higher frequencies the voltage drops down to 7 V.

A full report of the generator system working conditions and calculations can be found in the annex of this document.

4.2.2. High voltage transformer module

The transformer will consist in a ferrite core so that it allows the high frequencies, a primary coil and a secondary coil, each of them with a determined number of cable turns.

In order to design this module, it has been considered that the output from the first generation module is approximately 8 V peak to peak. On the output of the transformer it has also been estimated that we need a value of 15,000 V to 20,000 V peak to peak with approximately a current of 10 mA. After calculating the required number of turns, calibre of the cables and core area (calculations shown in Annex), it has been obtained that:

- **Transformer power:** 200 W
- **Core dimensions:** 3.8 cm x 5 cm
- **Primary coil turns:** 9 turns
- **Primary cable calibre:** Calibre 9 (From AWG Table in annex)
- **Secondary coil turns:** 22500 turns
- **Secondary cable calibre:** Calibre 30 (From AWG table in annex)

In *Figure 4.6.* a representation of the transformer is shown, verifying the output of the increased voltage is approximately 20 kV with an input voltage of 8 V.

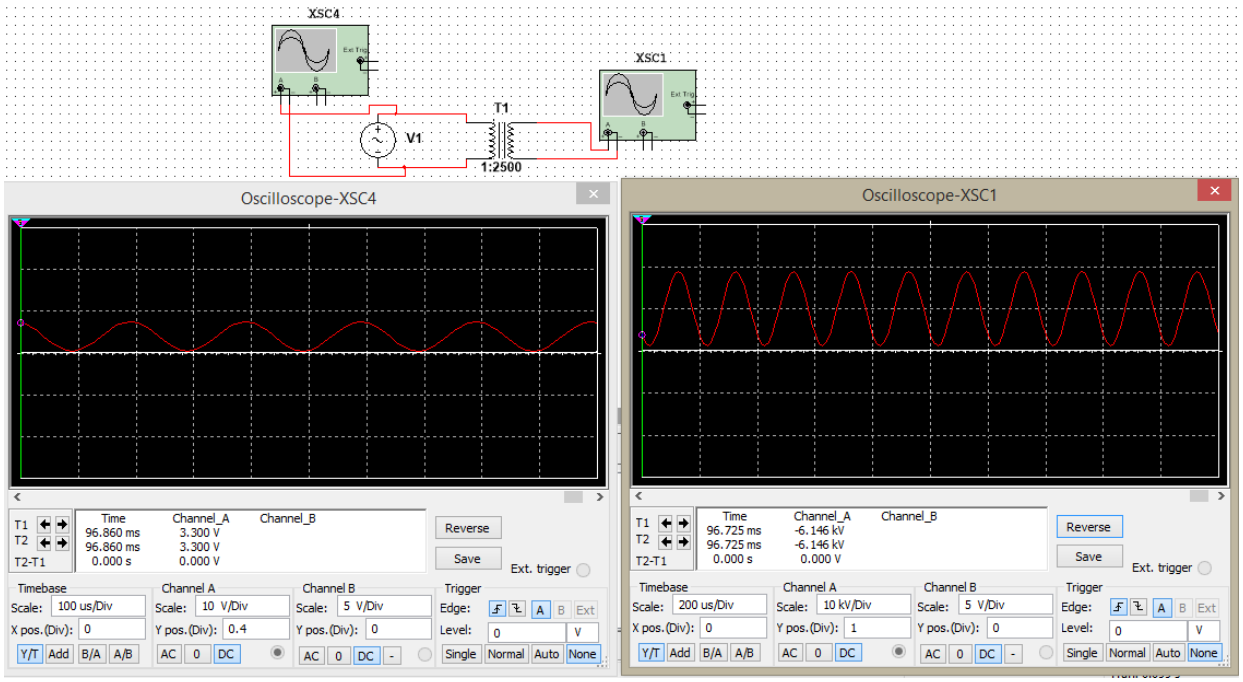

Figure 4.6. *Transformer module verification*

4.2.3. High Voltage circuit module

The third and last module will consist in the CD plug, its wires and the Shunt ammeter. It must be understood that the RF generation specified above is not a direct replacement of the ignition wires. The proposed generation circuit will couple to the traditional ignition wires to control the spark plugs. This concept will be the same as the one stated in Patent US 5596974, where after generating the RF HV this is coupled to the spark plug wires using a special clamp (see *Figure 2.15.*).

The purpose of clipping this together is to create a "capacitor" where the isolation of the plug wire will act as the dielectric. The way this will work is that when the ignition plug is at its discharge point, the clip attaching to the ignition wire will couple the RF energy from the generation system to the conductor in the ignition wire, resulting in a CD effect for the ignition plug while it is at its discharge point.

In another patent which the reader can check in the Annex (US 3949718), a similar coupler is used. This is represented in *Figure 4.7.*

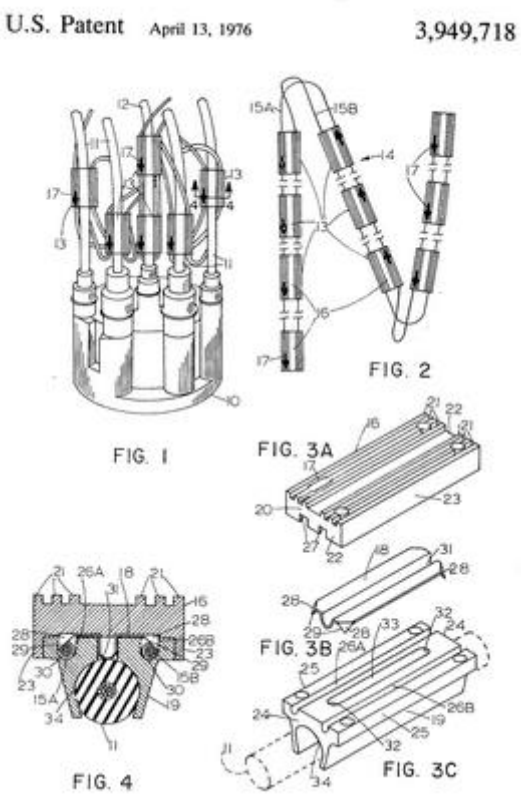

Figure 4.7. *Patent US 3949718 Engine spark ignition system corona coupler*

In order to measure the current supplied by the RF HV circuit, a Shunt ammeter is required. A Shunt ammeter consists in a Resistor of precise known resistance that is put in series to the load. In this case, the resistance will need to be put before the clip coupling to the ignition plug wires. Shown in *Figure 4.8.* is a representation of this third module and how it would look like.

The Voltmeter must have a scale calibrated to read current (amperes). In our case, with a voltage of approximately 20,000 V peak to peak and an estimated current of 10 mA, the Shunt resistance we will need is of 2 MΩ.

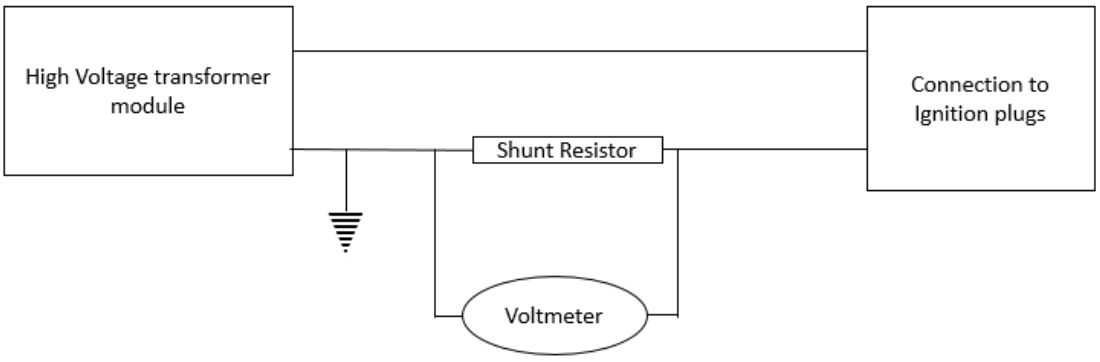

Figure 4.8. *Shunt ammeter connection in module*

4.3. Summary of the Corona Discharge generation circuit proposal

This section is used as a summary of the three modules explained in the previous sections. With the proposed design proposal it is possible to obtain an estimated generation of voltages up to 20,000 V peak to peak with frequencies that will vary from 15 Hz up to 200 kHz. The connection of the modules will be as shown in *Figure 4.9.*

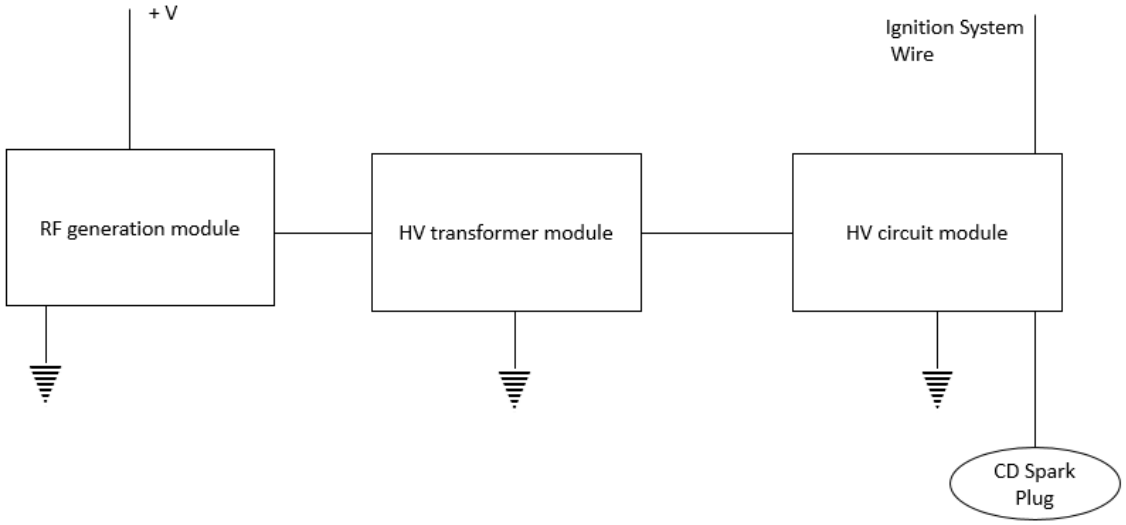

Figure 4.9. *Summary of the connection of the proposed circuit modules*

It must be understood that this proposed circuit might be subject to some modifications or updates during the physical testing, as it might be found that the range of frequencies offered by the first module is not wide enough, or maybe that the voltage available is too low. These must be considered in another thesis with the purpose of developing the testing to finalise the design of the Corona Discharge Ignition System. This proposal is designed with the purpose of giving a starting point for future investigation on the generation of the Corona effect and understand which are the frequency and voltage required for different engine conditions.

5. BUDGET

The budget stated in this section represents only the development and the generation circuit cost, as this thesis only focuses in the main study of the corona discharge generation. Before implementation to an engine, further research and development needs to be done which would add additional cost to the one stated.

Understanding this, the results can be seen in *Table 5.1*, where all the hourly costs are assuming a qualified engineer.

Cost type	Cost per hour (€/h)	Worked hours (h)	Total Cost (€)
Documentation research	50	25	1,250
Experimental documentation	50	50	2,500
Elaboration of computer model of circuit	50	10	500
Perform adjustments of circuit to adequate output	50	100	5,000
Calculations for the simulation and set-up	50	20	1,000
Results verification	50	10	500
Study redaction	50	150	7,500
Physical circuit elaboration	50	20	1,000
TOTAL BEFORE TAX	-	-	19,250
+ 21 % IVA	-	-	4,040
Computer software	-	-	2,000
Material for the circuit	-	-	60
TOTAL	**-**	**-**	**25,350 €**

Table 5.1. *Budget breakdown*

From the *Table 5.1*, each item refers to:

- **Documentation research:** Research of the automotive ignition systems and how they generate.
- **Experimental documentation:** Research of patents and other universities and companies studies.
- **Elaboration of computer model of circuit:** Design the initial structure of the circuit in the software used.
- **Perform adjustments of circuit to adequate output:** Calibrate the circuit to get the desired output.
- **Calculations for the simulation and set-up:** Development process to select the component values.
- **Results verification:** Analyse the results obtained in the software.
- **Study redaction:** Elaborate and expose the different points of the thesis in a text document.
- **Physical circuit elaboration:** Construction of the generation system,
- **Computer software:** License for the simulation software used.
- **Material for the circuit:** Parts used for the circuit construction.

6. ENVIRONMENTAL IMPACT

The development of this thesis gives a good start point for a technology that with further research could give a high improvement in the engine emissions. This objective of this thesis was not the development of the complete system and the implication to the engine, the main objective was to study the corona discharge generation and understand the improvements it offers.

From the section 2 and 3 from this document, it is possible to see the advantages the system offers in terms of performance (faster ignition speed, higher rate, no erosion …). All of these advantages could offer an estimated improvement of 3% up to 10 % in fuel efficiency (as indicated by the actual leader company in this sector *Federal-Mogul*), so considering an in-between value of 6% it is possible to see how much improvement this can offer to a vehicle .

For the following study in *Table 6.1* it has been considered a conventional vehicle designed to circulate only in an urban area.

	Conventional car[1]	**Modified car with Corona ignition**
Consumption	5,9 L/100 Km	5,55 L /100 Km
Emissions	139 g CO_2/Km	131 g CO_2/Km
Average daily distance	10 Km	
TOTAL EMISSIONS	1.39 Kg CO_2/day	1.31 Kg CO_2/day

Table 6.1. *Estimated emissions comparison for a modified car with Corona discharge technology*

Considering this 6% reduction in the consumption (and by consequence to the emissions), if this technology was to be implemented to a high volume of cars, the amount of CO_2 generated would be importantly reduced, having a great impact to the overall contamination.

Also the technology opens a way for improvement of the ignition in the engine, which with further investigation on increasing the stratification of the engine and with making the mixture more aggressive by including more air can decrease even more the consumption of the vehicle, bringing the emissions even to a lower value.

[1] Values for a Ford Fiesta 1.6 Ti-VCT as per source http://coches.idae.es/

CONCLUSIONS

After all the research done in this document, it is now possible to have a clear understanding on how the ignition works in combustion engines and also in any application where a spark or plasma plug is used. Although there are different technologies for the ignition system, all of them share the same ionization principle and it is very important to understand it properly so that it is possible to implement correctly alternative ignition systems understanding exactly why they offer an improvement.

In case of this project, it has been possible to understand and implement the Corona Discharge effect into the combustion chamber to increase the number of fuel ignited and, by this way, increase the efficiency of the engine. During the development of the project it has been possible to see other ignition methods that are also very interesting, like the laser ignition, which could also have been the subject of this project. Actually, there are already a lot of automotive companies investigating in the implementation of the technologies discussed in the project, so this is a clear clarification that the ignition system will be one of the main focuses of improvement for the next years.

As a closure of the project, an investigation of the modification required in the common system has been made. The result of this has been a circuit consisting on three different modules that used in parallel to the common ignition system would allow the implementation of an alternate ignition plug design that could help the CD effect to spread along the combustion chamber more efficiently. The result of this work is meant to be used by the next engineer interested in moving forward the design of the ignition system by building a physical circuit to generate the corona discharge and investigating any more modifications required in either the combustion chamber or the ignition plug.

ACKNOWLEDGMENTS

Special thanks to the director of this project Jesus Álvarez, who has shown his support along all the way and has advised accordingly any question although working from distance. The elaboration of this project would have not been possible without the help given by him.

Also special appreciation to my partner, who has supported me during the development of this project and has kept pushing me to complete it in time. As my partner, I thank my family for also showing me their support and not letting me down so that this project was successfully completed.

At last but not least, special thanks to my supervisors and colleagues of AVL UK, who have allowed me to work in a flexi time schedule so that I could manage my time better for the development of the project and for the experience provided in other projects that has helped me to finish this document.

BIBLIOGRAPHY

[1] Laboratoire de combustion et detonique, France "*Spark Plug and Corona Abilities to Ignite Lean Methane/Air Mixtures"*

[2] E.M. van Veldhuizen, W.R. Rutgers "*Corona Discharges: Fundamentals and diagnostics"* Faculty of Applied Physics, Technische Universiteit Eindhoven.

[3] Y.L.M. Creyghton, *"Pulsed Positive Corona Discharges: Fundamental Study and Application to Flue Gas Treatment"*, Ph.D. thesis TUE, Eindhoven, September 1994.

[4] I. Odrobina, M. Cernak, "*Numerical simulation of streamer–cathode interaction"*, J. Appl. Phys. 78(1995)3635.

[5] H. Raether, "*The development of electron avalanche in a spark channel (from observations in a cloud chamber)"*, Zeitschrift fur Physik 112(1939)464. (Reproduced in: Electric Breakdown in gases, J.A. Rees, The Macmillan Press, London, 1973).

[6] E.M. van Veldhuizen, A.H.F.M. Baede, D. Hayashi, W.R. Rutgers,*" Fast imaging of streamer propagation"*, APP Spring Meeting, Bad Honnef, 2001, p. 231-234.

[7] K.H. Wagner, "*Vorstadium des Funken, untersucht mit dem Bildverstaerker"*, Zeitschrift fur Physik 204(1967)177

[8] K. Kondo, N. Ikuta, "*Highly resolved observation of the primary wave emission in atmospheric positive streamer corona"*, J. Phys. D: Appl. Phys. 13(1980)

[9] F. Tochikubo, T.H. Teich, "*Optical emission from a pulsed corona discharge and its associated reactions"*, Jpn. J. Appl. Phys. 39(2000)1343-1350.

[10] R. Brandenburg, K.V. Kozlov, P. Michel, H.-E. Wagner, "*Diagnostics of the single filament barrier discharge in air by cross-correlation spectroscopy"*, HAKONE VII, Greifswald, Germany, sept. 2000, p.189-193.

[11] I.P. Vinogradov, K. Wiesemann, "*Classical absorption and emission spectroscopy of barrier discharges in N2/NO and O2/NOx mixtures"*, Plasma Sources Sci. Technol. (1997).

[12] J.J. Coogan, A.D. Sappey, "*Distribution of OH within silent discharge plasma reactors"*, IEEE Trans. Plasma Sci. (1996)91-92

[13] R. Sankaranarayanan, B. Pashaie, S.K. Dhali, *"Laser-induced fluorescence of OH radicals in a dielectric barrier discharge"*, Appl. Phys. Lett. (2000)2970-2972.

[14] Frank C. Loccisano, *"Investigation of optical pre-chamber spark plug and dual laser pulses for ignition"*, Colorado State Unversity, Department of Mechanical Engineering Thesis (2009) p.3-13.

ANNEXS

ANNEXS SUMMARY

A. PATENTS

This section contains some short presentations of the patents referred in the main body of the thesis. The full patent document hasn't been attached due to the length of some patents. If further information is required for the reader, patents are available online for reading at no extra cost.

A.1 Common spark ignition

A.1.1 Patent US 1193548- "*Lighting system for moving vehicles*" by Gottlob Honol.

G. HONOLD.
LIGHTING SYSTEM FOR MOVING VEHICLES.
APPLICATION FILED JUNE 7, 1915.

1,193,548. Patented Aug. 8, 1916.

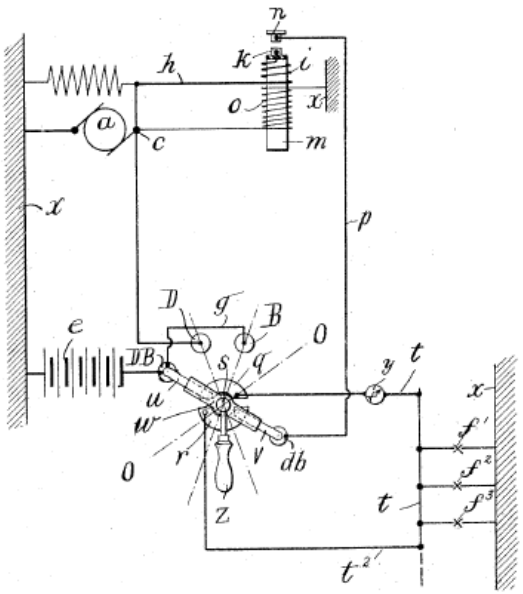

Gottlob Honold INVENTOR
BY
ATTORNEY

A.1.2 Patent US 609250 – "*Electrical Igniter for Gas Engines*" by Nikola Tesla.

No. 609,250. Patented Aug. 16, 1898.

N. TESLA.

ELECTRICAL IGNITER FOR GAS ENGINES.

(Application filed Feb. 17, 1897. Renewed June 15, 1898.)

(No Model.)

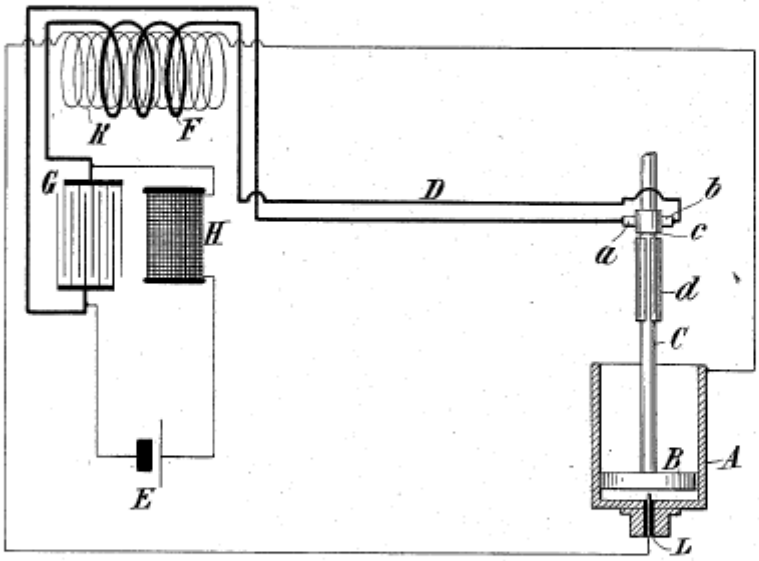

Witnesses:
M. Lamon Dyer.
Edwin B. Hopkinson.

Nikola Tesla, Inventor
by Kerr, Curtis & Page Attys

A.2 Piezoelectric ignition

A.2.1 Patent US 3215133 – "*Engine compression operated piezoelectric ignition system*" by J.M. Farrell

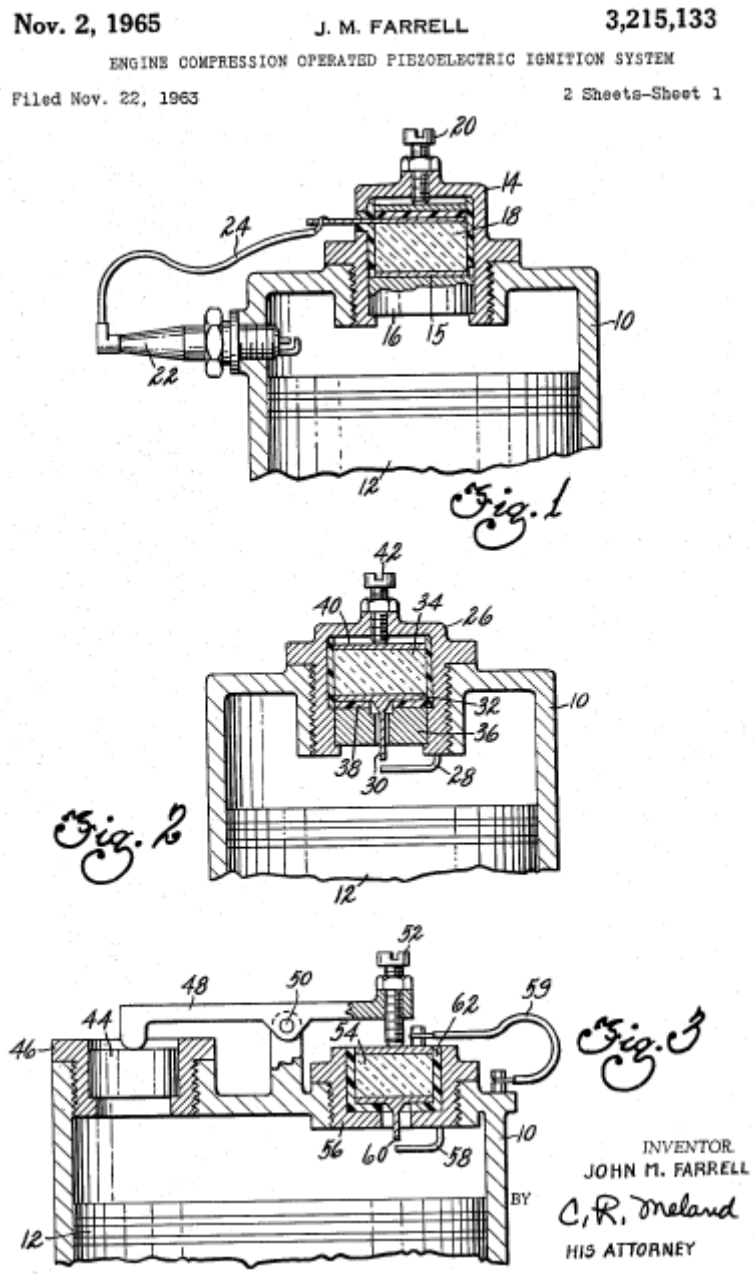

Nov. 2, 1965 J. M. FARRELL 3,215,133

ENGINE COMPRESSION OPERATED PIEZOELECTRIC IGNITION SYSTEM

Filed Nov. 22, 1963 2 Sheets-Sheet 1

Fig. 1

Fig. 2

Fig. 3

INVENTOR
JOHN M. FARRELL
BY C. R. Meland
HIS ATTORNEY

A.3.3 Patent US 5291872 – "*Ignition apparatus for an internal combustion engine*" by Sanjar Gahem

U.S. Patent Mar. 8, 1994 Sheet 1 of 6 5,291,872

FIG. 1

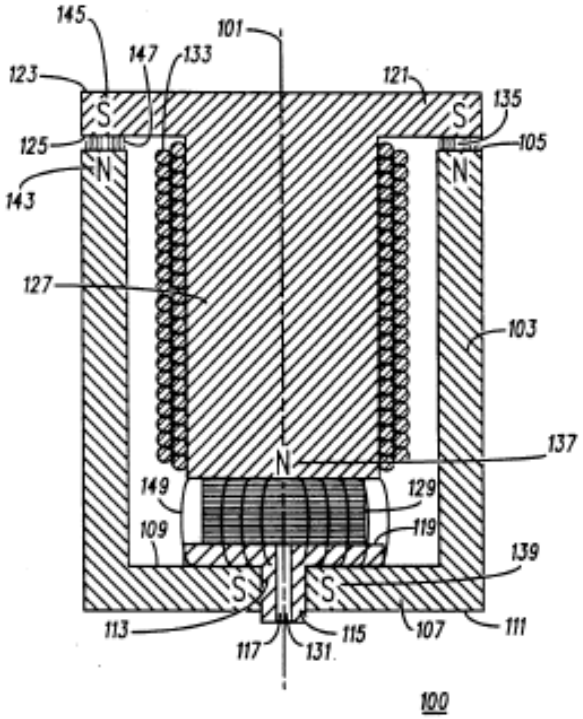

A.3 Laser ignition

A.3.1 Patent US 4416226 – "*Laser ignition apparatus for an internal combustion engine*" Minoru Nishida, Tadashi Hattori and Shinichi Mukalmakano.

United States Patent [19] [11] **4,416,226**
Nishida et al. [45] **Nov. 22, 1983**

[54] **LASER IGNITION APPARATUS FOR AN INTERNAL COMBUSTION ENGINE**

[75] Inventors: **Minoru Nishida; Tadashi Hattori; Shinichi Mukainakano,** all of Okazaki; **Toru Mizuno,** Aichi; **Tukasa Goto,** Kariya, all of Japan

[73] Assignees: **Nippon Soken, Inc.,** Nishio; **Nippondenso Co., Ltd.,** Kariya, both of Japan

[21] Appl. No.: **383,835**

[22] Filed: **Jun. 1, 1982**

[30] **Foreign Application Priority Data**

Jun. 2, 1981 [JP] Japan 56-85308

[51] **Int. Cl.**³ **F02P 23/00**
[52] **U.S. Cl.** ..... **123/143 B**; 123/143 R
[58] **Field of Search** ..... 123/143 B, 143 R, 637, 123/638

[56] **References Cited**

U.S. PATENT DOCUMENTS

3,280,809	10/1966	Issler	123/637
3,861,371	1/1975	Gamell	123/143 B
4,122,816	10/1978	Fitzgerald	123/143 B
4,314,530	2/1982	Giacchehi	123/143 B

FOREIGN PATENT DOCUMENTS

964539	3/1975	Canada	123/143 B
2207392	8/1973	Fed. Rep. of Germany	123/143 B
2924910	1/1981	Fed. Rep. of Germany	123/143 B

Primary Examiner—Ronald B. Cox
Attorney, Agent, or Firm—Cushman, Darby & Cushman

[57] **ABSTRACT**

A laser ignition apparatus includes a laser oscillator which generates at least two successive pulse-shaped laser beams during each compression stroke of the engine. A first pulse-shaped laser beam is generated by a Q switching action of the laser oscillator and thus has a high peak output and a second pulse-shaped laser beam is generated without the Q switching action and has a low peak output but a larger pulse duration than the first laser beam. The first and second pulse-shaped laser beams are guided and directed into the combustion chamber of the engine and the first laser beam of a high energy density causes the breakdown of the air-fuel mixture in the combustion chamber to develop a plasma and the second laser beam further increases the energy of the plasma thereby to ensure the setting fire of the air-fuel mixture.

5 Claims, 15 Drawing Figures

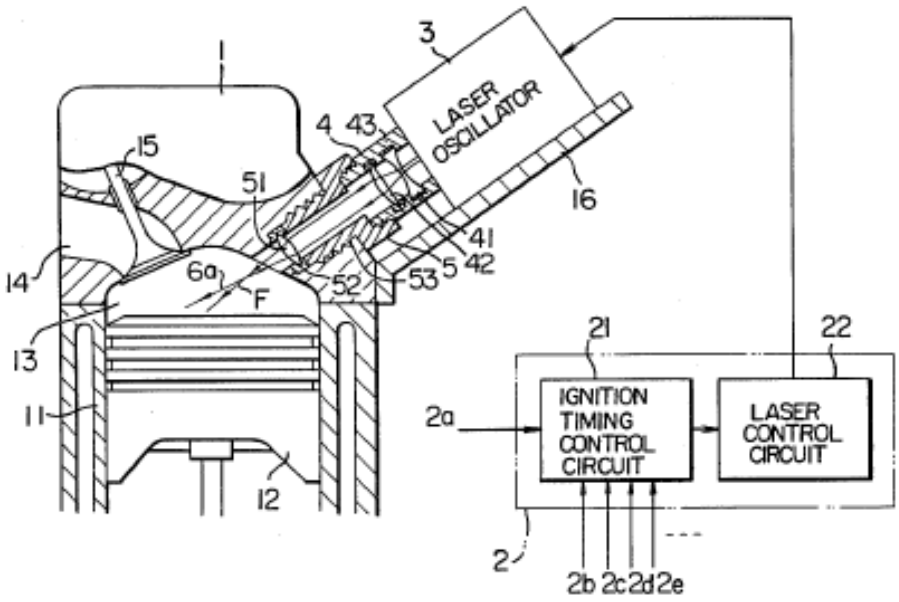

A.3.2 Patent US 8826876 – "*Laser spark plug for an internal combustion engine*" by Friedrich Gruber and Markus Kraus.

(12) **United States Patent**
Gruber et al.

(10) **Patent No.: US 8,826,876 B2**
(45) **Date of Patent: *Sep. 9, 2014**

(54) **LASER SPARK PLUG FOR AN INTERNAL COMBUSTION ENGINE**

(75) Inventors: **Friedrich Gruber**, Hippach (AT); **Markus Kraus**, Wiesing (AT)

(73) Assignee: **GE Jenbacher GmbH & Co OHG**, Jenbach (AT)

(*) Notice: Subject to any disclaimer, the term of this patent is extended or adjusted under 35 U.S.C. 154(b) by 0 days.

This patent is subject to a terminal disclaimer.

(21) Appl. No.: **13/425,571**

(22) Filed: **Mar. 21, 2012**

(65) **Prior Publication Data**

US 2012/0210969 A1 Aug. 23, 2012

Related U.S. Application Data

(63) Continuation of application No. PCT/AT2010/000351, filed on Sep. 27, 2010.

(30) **Foreign Application Priority Data**

Oct. 7, 2009 (AT) ..... A 1579/2009

(51) **Int. Cl.**
F02B 23/00 (2006.01)
F02P 23/04 (2006.01)

(52) **U.S. Cl.**
CPC ***F02P 23/04*** (2013.01)
USPC ..... **123/143 R**; 123/143 B; 313/118

(58) **Field of Classification Search**
USPC ..... 123/143 R, 143 B, 647; 313/118, 129
See application file for complete search history.

(56) **References Cited**

U.S. PATENT DOCUMENTS

7,806,094	B2 *	10/2010	Gruber	123/143 B
8,146,554	B2 *	4/2012	Gruber	123/143 B
8,181,617	B2 *	5/2012	Kuhnert et al.	123/143 B
2006/0132930	A1 *	6/2006	Kopecek et al.	359/718
2007/0064746	A1 *	3/2007	Winklhofer et al.	372/10
2009/0107436	A1	4/2009	Schultz	

(Continued)

FOREIGN PATENT DOCUMENTS

AT	505 766	4/2009
AT	506 200	9/2009

(Continued)

OTHER PUBLICATIONS

International Search Report issued Apr. 27, 2011 in International (PCT) Application No. PCT/AT2010/000351.

(Continued)

Primary Examiner — John Kwon
(74) *Attorney, Agent, or Firm* — Wenderoth, Lind & Ponack, LLP.

(57) **ABSTRACT**

A laser spark plug includes a laser light-producing device and a spark plug housing at the end of which facing the combustion chamber an injection lens for injecting laser light into the combustion chamber of an internal combustion engine is arranged. The spark plug housing includes a fastening zone for fastening the laser spark plug in a cylinder head of the internal combustion engine. A projection on the end of the spark plug housing facing the combustion chamber houses the injection lens. The outer diameter (D1) of the projection is smaller in the area of the injection lens than the outer diameter (D2) of the spark plug housing in the fastening zone.

17 Claims, 6 Drawing Sheets

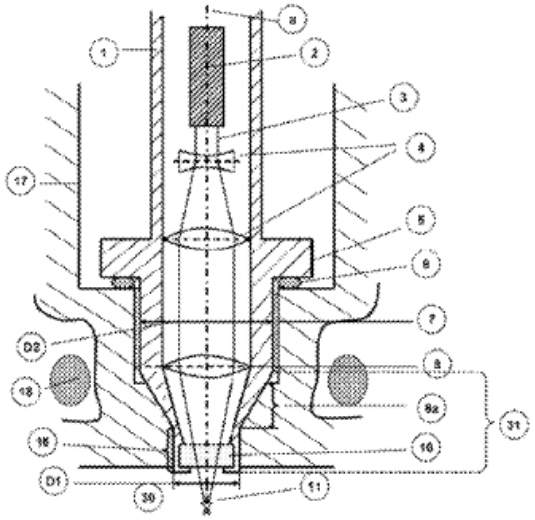

A.4 Corona discharge ignition

A.4.1 Patent US 5596974 – "*Corona generator system for fuel engines*" by L. Trust

United States Patent [19]
Hall et al.

[11] **Patent Number: 5,596,974**
[45] **Date of Patent: Jan. 28, 1997**

[54] **CORONA GENERATOR SYSTEM FOR FUEL ENGINES**

[75] Inventors: **Richard Z. Hall**, Arlington; **Carl E. Gali**, Garland, both of Tex.

[73] Assignee: **LuLu Trust**, Garland, Tex.

[21] Appl. No.: **546,891**

[22] Filed: **Oct. 23, 1995**

[51] **Int. Cl.**[6] **F02P 3/02**
[52] **U.S. Cl.** **123/620**
[58] **Field of Search** ..... 123/620, 594, 123/598, 605, 606, 607, 619, 628, 597, 596; 315/209 CD, 209 T; 361/207, 251, 253, 256, 257, 263

[56] **References Cited**

U.S. PATENT DOCUMENTS

3,408,536	10/1968	Tibbs	123/607
3,949,718	4/1976	Turner	123/620
4,245,609	1/1981	Gerry	123/594
4,269,160	5/1981	Irvin, Jr.	123/620
4,320,735	3/1982	Canup	123/607
4,446,826	5/1984	Kimura et al.	123/606
4,457,285	7/1984	Hamai et al.	123/598
4,502,454	3/1985	Hamai et al.	123/597
4,710,681	12/1987	Zivkovich	315/209 T
5,207,208	5/1993	Ward	123/596
5,471,362	11/1995	Gowan	123/598
5,513,618	5/1996	Rich et al.	123/598

Primary Examiner—Raymond A. Nelli
Attorney, Agent, or Firm—John E. Vandigriff

[57] **ABSTRACT**

The invention is to a system in which a high voltage source is connected to and continuously supplies a RF voltage to each spark plug wire in an automotive ignition. The high voltage is capacitively connected by placing a metal clip on each spark plug wire and connecting the high voltage source to the metal clips. The metal clip and conductor in the spark plug wire forms the two plates for the capacitor and the insulating material on the spark plug wire is the dielectric of the capacitor. The application of the high voltage to the spark plug wire produces a continuous corona discharge at the tip of the spark plug internal to the engine. A corona discharge surface may also be on one surface of the engine head in the combustion chamber.

23 Claims, 5 Drawing Sheets

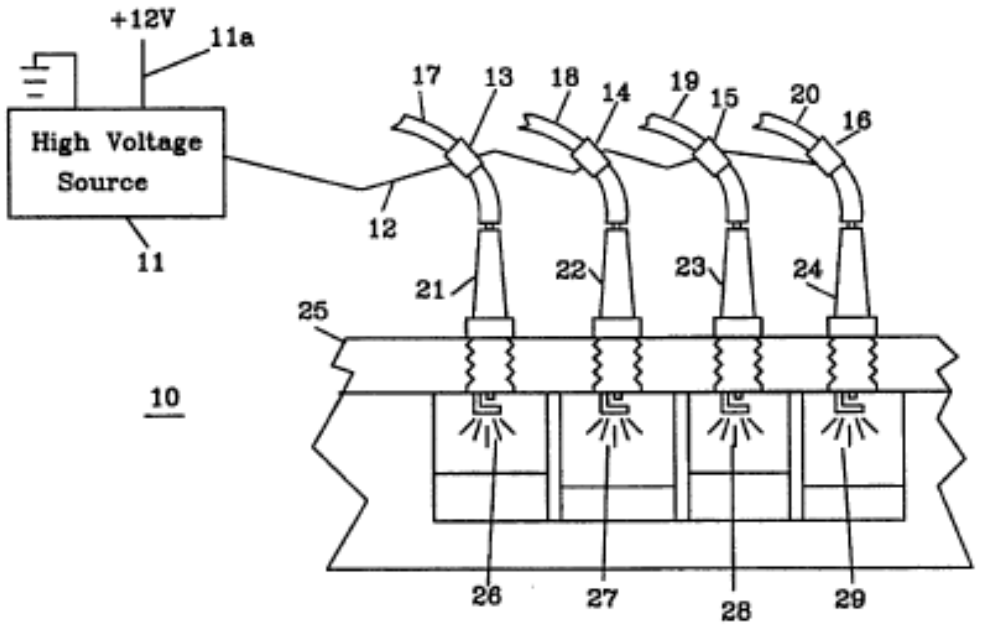

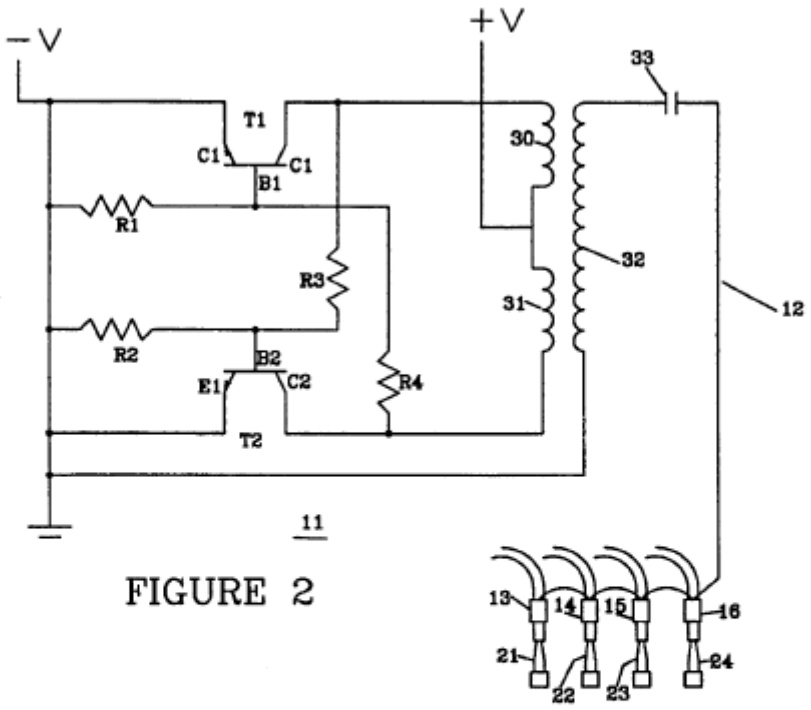

FIGURE 2

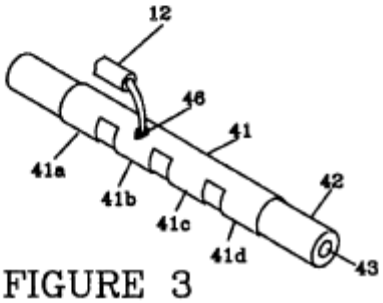

FIGURE 3

A.4.2 Patent US 3974412 – "*Spark plug employing both corona discharge and arc discharge*" by Massachussets institute of technology.

United States Patent [19]
Pratt, Jr.

[11] **3,974,412**
[45] **Aug. 10, 1976**

[54] **SPARK PLUG EMPLOYING BOTH CORONA DISCHARGE AND ARC DISCHARGE AND A SYSTEM EMPLOYING THE SAME**

[75] Inventor: **George W. Pratt, Jr.**, Wayland, Mass.

[73] Assignee: **Massachusetts Institute of Technology**, Cambridge, Mass.

[22] Filed: **Feb. 3, 1975**

[21] Appl. No.: **546,232**

[52] **U.S. Cl.** ..... **313/131 R**; 123/169 EL; 123/169 MG; 313/138; 313/139; 313/141
[51] **Int. Cl.²** **H01T 13/20**
[58] **Field of Search** ..... 313/118, 131 R, 131 A, 313/134, 141, 145, 133, 138, 139, 140, 142; 123/169 R, 169 EL, 169 MG

[56] **References Cited**
UNITED STATES PATENTS

1,247,975	11/1917	Linn	313/143 X
1,905,957	4/1933	Anderson	313/131 R
2,129,576	9/1938	Gorny et al.	313/131 R X
2,798,980	7/1957	Beardslee	313/145 X
2,926,275	2/1960	Péras	313/131 R
3,049,644	8/1962	Bowlus et al.	313/131 R X
3,538,372	11/1970	Terao	313/142 X

Primary Examiner—Siegfried H. Grimm
Attorney, Agent, or Firm—Arthur A. Smith, Jr.; Robert Shaw; Martin M. Santa

[57] **ABSTRACT**

A spark plug wherein corona discharge is employed to create a long arc and to determine, in part, the path of the arc, electrodes of the spark plug being shaped, oriented and positioned to create an arc of desired length and at a desired location as well as to effect electromagnetic interaction between electric current in the arc and the electrodes to provide a force on the arc which acts to control its spatial behavior. The spark plug includes means to enhance the electromagnetic interaction.

31 Claims, 9 Drawing Figures

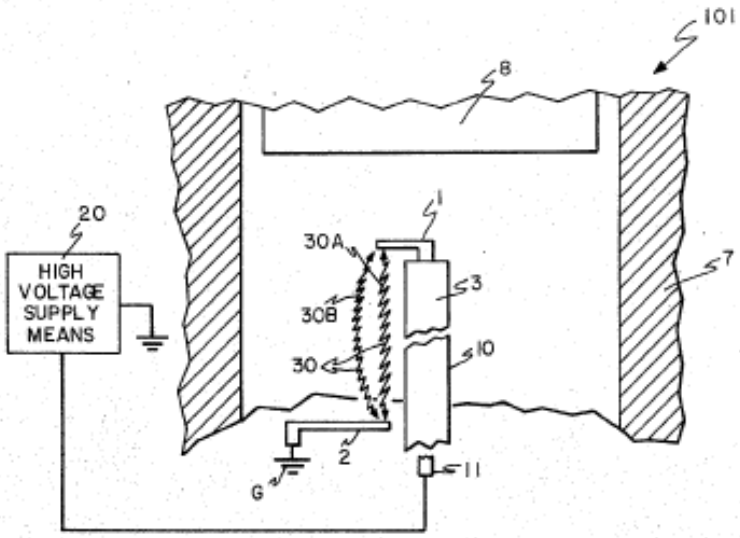

U.S. Patent Aug. 10, 1976 Sheet 2 of 4 3,974,412

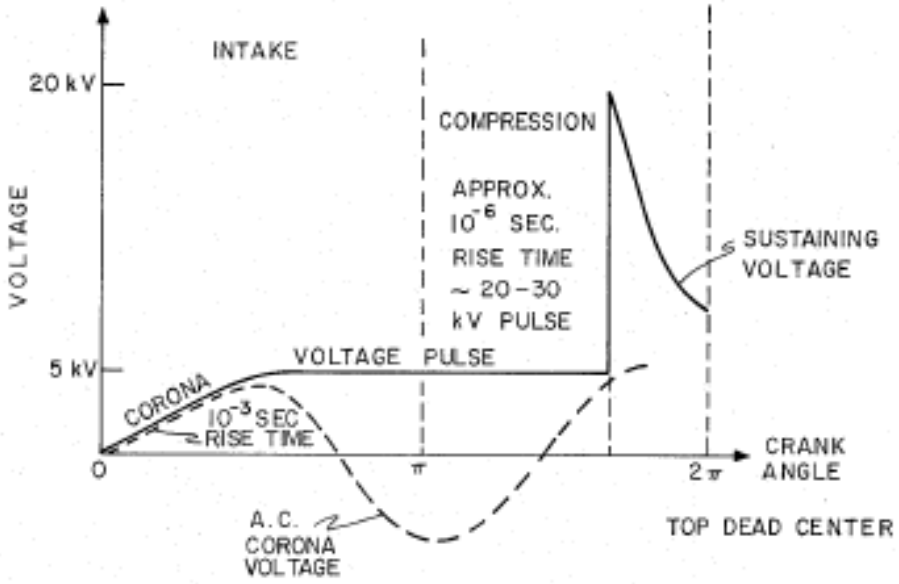

FIG. 3

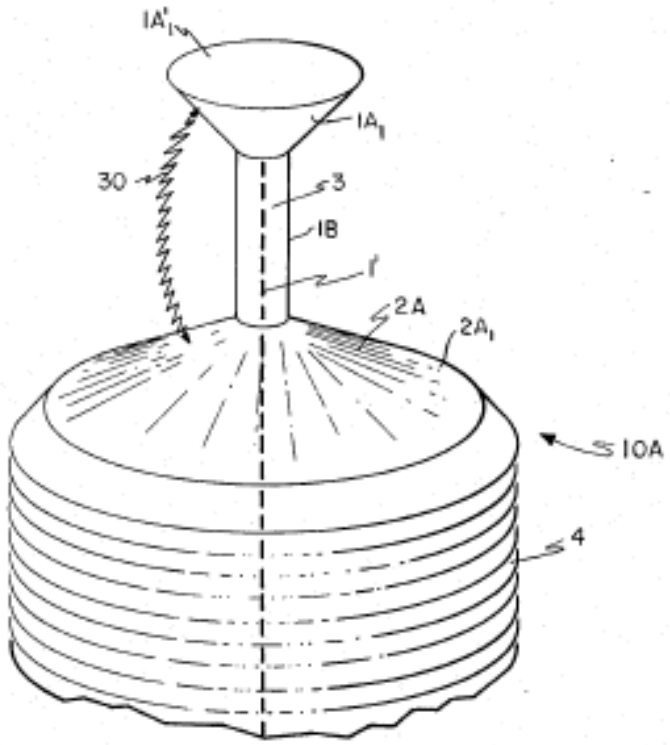

FIG. 4

A.4.3 Patent US 3538372 – *"Wide gap discharge spark plug"* by Kunio Terao

Nov. 3, 1970 KUNIO TERAO 3,538,372

WIDE GAP DISCHARGE SPARK PLUG

Filed Jan. 8, 1968 2 Sheets-Sheet 1

Fig. 1.

Fig. 2.

Fig. 3.

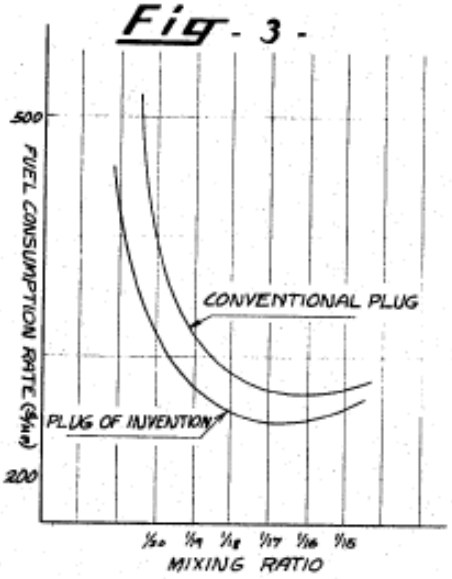

Fig. 4.

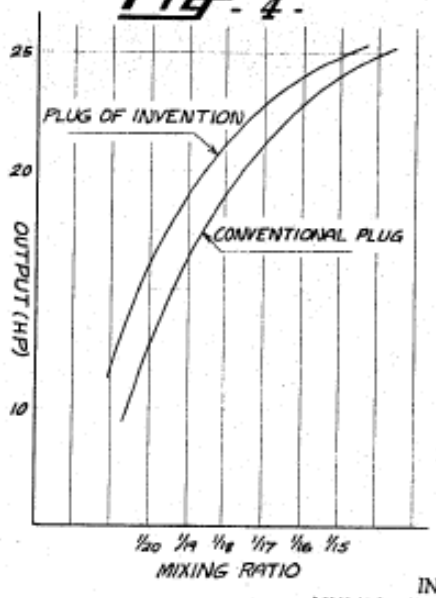

INVENTOR
KUNIO TERAO

United States Patent Office 3,538,372 Patented Nov. 3, 1970

3,538,372

WIDE GAP DISCHARGE SPARK PLUG

Kunio Terao, Yokosuka-shi, Japan, assignor of fifty percent to Okamura Manufacturing Company Limited, Yokohama, Japan

Filed Jan. 8, 1968, Ser. No. 696,385
Int. Cl. H01t 13/32, 13/52
U.S. Cl. 313—131 5 Claims

ABSTRACT OF THE DISCLOSURE

A wide gap spark plug for generating a strong spark across a gap of two or three times the width of the gap on a conventional type of spark plug without loss of electrostatic energy for generating the sparks. A strong spark across a wide gap as provided by the spark plug of this invention has the ignition energy sufficient to ignite a mixture of fuel and air in a most efficient proportion to provide improved combustion for greater economy and to decrease air pollution.

This invention relates to an improved spark plug for internal combustion engines and, particularly, to a spark plug for discharging across a relatively wide gap in relation to prior art spark plugs.

The spark gap or the distance between the electrodes of a spark plug for internal combustion engine depends primarily upon the potential difference or voltage which has been established between the electrodes of the spark plug, the gap being ordinarily approximately 0.6 mm. to 0.9 mm. However, a gap of such short distance is not adequate to generate sparks of maximum ignition energy for igniting a mixture of fuel and air in the most efficient proportions. Therefore, most internal combustion engines are operated by much thicker mixed gases than that which is theoretically required.

When the volume ratio of fuel to air exceeds a predetermined proporation, imperfact or incomplete combustion will occur with an accompanying exhaust of noxious combustion gases thereby adding pollution to the atmosphere and causing a loss of efficiency and waste of combustible materials.

If a long spark of strong ignition energy is generated across a wider inter-electrode gap, the actual volume of the mixed gas exposed to the spark and activated thereby is increased substantially and the fuel gases will burn more evenly and perfectly in a short time and, therefore, the above mentioned disadvantages would be removed. On the other hand, if only the distance between the electrodes is increased and a larger gap thus achieved, there is an accompanying loss of energy resulting in incomplete ionization of air between the electrodes which in turn reduces the spark generating power. If conventional spark plugs are utilized with increased gaps, the enlarged gap will accelerate the diffusion of activated mixed gases; thus, the amount of mixed gases as the source of ignition will be reduced and the ignition capacity will be lowered.

A principal object of this invention is to provide an improved plug for generating a strong spark across an enlarged gap preferably in the order of 2 or 3 times the width of the gap of a conventional plug to increase the

tion and spaced from the outer surface of the jacketed first electrode a distance which is less than the distance from the terminal end of the ground electrode and the uninsulated terminal end of the first or central electrode. The shapes and sizes of both electrodes as well as the insulating coating jacketing the intermediate portion of the central electrode and the relationship of the distances between the electrodes, it will be seen, are so designed that there exists no insulation on the line of the shortest distance between the terminal or tip ends of both electrodes, notwithstanding the fact that the distance from the central elecrode through the insulating coating or jacket to the tip end of the ground electrode is shorter or less than the distance between the uninsulated tip ends of the electrodes.

It is a general object of this invention to provide an improved spark plug which is simple in construction, inexpensive to manufacture, provides for improved fuel consumption, and is adapted for use in increasing spark plug performance and of power plants on which it is installed.

It is another object of this invention to provide an improved spark plug which is characterized by a first central electrode, the intermediate portion of the length of which is jacketed by insulating material and a second or ground electrode having a tip end at about the medial portion of the length of the insulating material and spaced from the outer surface of the first electrode a distance which, as measured from the tip of the second electrode through the insulating material, is less than the distance from the terminal ends of the electrodes, and to provide various preferred configurations for achieving the results described herein which derive from the improved spark plug construction.

Other objects and advantages of this invention will become apparent from the following detailed description thereof when read in conjunction with the attached drawings in which:

FIG. 1 is a side elevation partly in section of the wide gap discharge spark plug of the present invention;

FIG. 2 is a plan view of FIG. 1;

FIG. 3 and FIG. 4 are diagrams showing the fuel consumption rate and output, comparing the test of the improved spark plug of the instant invention to a conventional plug;

FIG. 5 is a plan view illustrating a modified type of a wide gap discharge spark plug according to this invention;

FIG. 6 is a fragmentary side elevation, partly in section, of the plug of FIG. 5;

FIG. 7 is a plan view illustrating a further modification of a wide gap discharge spark plug; and

FIG. 8 is a fragmentary elevation, partly in section, of the plug of FIG. 7.

Referring first to the embodiment shown in FIGS. 1 and 2, the central eelctrode **1** extends through an insulator sleeve or jacket **2**, which is made of mica, hard porcelain, alumina porcelain or the like. The upper end of the central or first electrode **1** is provided with an enlarged head **3** which is not coated with insulation, that is, which is electrically conductive. The peripheral edge of the head **3** is preferably sized so as to extend radially beyond the neck portion of the first electrode and the outer surface of the insulation sleeve or packet **2**. A ground electrode **4** extends from the housing **5**, a distance substantially one-

A.4.4 Patent US3949718 – "*Engine spark ignition system corona coupler*" by James Edward Turner

United States Patent [19]
Turner

[11] **3,949,718**
[45] **Apr. 13, 1976**

[54] **ENGINE SPARK IGNITION SYSTEM CORONA COUPLER**

[76] Inventor: **James E. Turner**, 720 S. Kimball, Southlake, Tex. 76051

[22] Filed: **May 21, 1974**

[21] Appl. No.: **471,865**

[52] **U.S. Cl. 123/119 E**; 123/146.5 A; 123/148 AC
[51] **Int. Cl.²** **F02M 27/04**
[58] **Field of Search** ..... 123/143 B, 143 C, 148 A, 123/119 E, 148 E, 148 AC, 148 DC

[56] **References Cited**
UNITED STATES PATENTS

2,451,482	10/1948	Flint	123/148 DC
2,799,792	7/1957	Flint	123/148 AC
3,019,276	1/1962	Harlow	123/148 A
3,613,653	10/1971	Irvin, Jr. et al.	123/146.5 A

Primary Examiner—Charles J. Myhre
Assistant Examiner—Tony Argenbright
Attorney, Agent, or Firm—Warren H. Kintzinger

[57] **ABSTRACT**

A corona coupling system with a plurality of corona coupling unit blocks, individually snapped on spark plug wires and coil wires, interconnected by wire for corona coupling distribution between the spark plug and coil wires. The blocks are interconnected by two generally parallel, insulated wires clamped in place running through each two-piece block by a stamped conductive metal plate having formed-down corners biting into and through insulation on the block interconnecting wires as plastic top and bottom parts of each block are pressed and sonically welded together. The stamped conductive metal plate is formed with a downward longitudinally extended ridge positioned in the blocks so that the bottom edge rests against and along the insulation of the wire on which each block is mounted.

16 Claims, 6 Drawing Figures

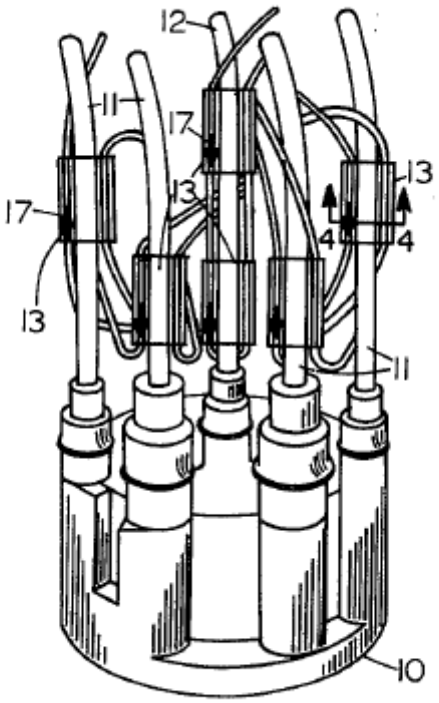

U.S. Patent April 13, 1976 3,949,718

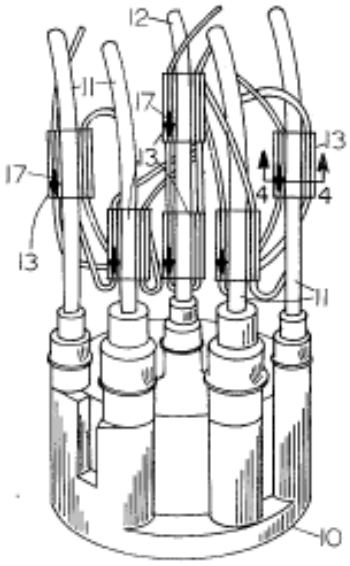

FIG. 1

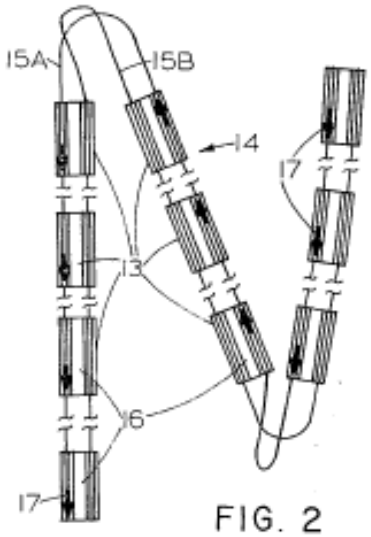

FIG. 2

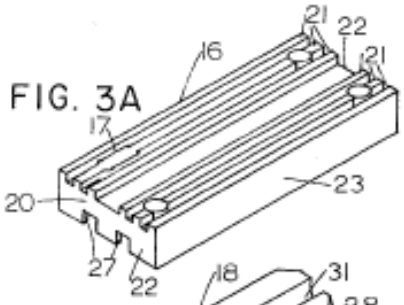

FIG. 3A

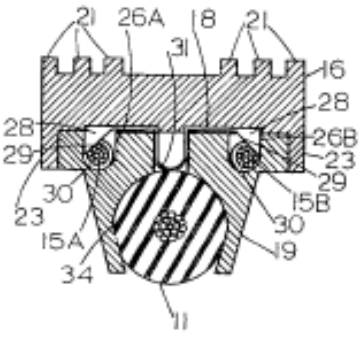

FIG. 4

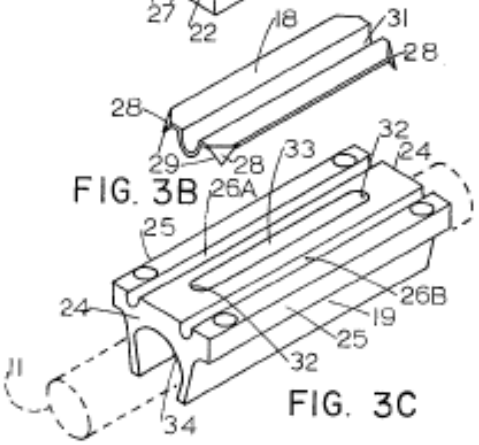

FIG. 3B

FIG. 3C

B. CORONA DISCHARGE SCIENTIFIC PUBLICATIONS

In this section scientific publications that have been reviewed during the elaboration of the thesis have been included. These publications offer a deeper research on the corona discharge generation in case the reader wants to investigate further.

B.1 Packed Bed Corona Discharge reactor

Packed Bed Corona Discharge reactor for gas-phase acetaldehyde decomposition at atmospheric pressure and ambient temperature

C. Klett, M. Redolfi, A. Vega, S. Touchard, X. Duten, K. Hassouni

[1]*LIMHP, CNRS UPR 1311, Université Paris 13, 99 Av. JB Clément, 93430 Villetaneuse, France*

Abstract: The aim of this study is to investigate the effect of a packed bed on the acetaldehyde degradation in atmospheric pulsed plasma. Acetaldehyde was chosen as this pollutant is produced during the biofuels combustion. Nano-TiO_2 deposited on SiO_2 or γ-Al_2O_3 balls will be used as packed bed. Major sub-products of acetaldehyde degradation will be identified and major reaction paths will be discussed.

Keywords: corona, packed bed, acetaldehyde, oxidation, atmospheric pressure

1. Introduction

The emission of Volatile Organic Compounds (VOCs) in the atmosphere is restricted by environmental regulations to very low values, due to the toxicity of these compounds and their contribution to global warming mechanisms. We investigate the remediation of acetaldehyde (CH_3CHO), as a model VOC, using different Packed Bed Corona Discharge systems (PBCD). PBCD takes advantage of a synergy between non-thermal plasma chemistry and surface chemistry in the porous bed at relatively low temperature conditions.

VOCs include many toxic species and are, with nitrogen oxide, the main ozone precursors. VOCs emission limits are therefore becoming more stringent and development of new VOC removal process is needed to satisfy the limits projected in the near future either in industrial activities (solvent industry) or transport application (mobile emission). Several studies were carried out to investigate the potentiality of non-thermal plasma as a tool for an advanced oxidation of VOC [1-5].

Most of the systems discussed in the literature made use of dielectric barrier discharge [6]. Corona coupled discharges were rarely considered in these studies. Corona systems operated in a pulsed mode give the possibility of a very precise control of the energy deposition in the system. They also enable achieving high activation efficiency when processed with very short rise time voltage chocks [7].

The aim of the work presented in this paper is to investigate the efficiency of a pulsed corona system for the oxidation of acetaldehyde molecule. Our choice of acetaldehyde was motivated by the fact that the oxidation of this species under discharge conditions has almost never been investigated.

The corona systems considered here include Packed Bed Wire-To-Cylinder configurations. Catalytic packed materials were considered in this study. The oxidation efficiencies of the corona systems were characterized in term of CO_2 and CO production yield.

2. Gas flow system and chemical analysis

The feed gas considered in this study mainly consists of N2/O2 mixture. The flow rate entering the discharge cell is monitored with three digital mass flow-meters (**Fig.1**). The base values of oxygen and acetaldehyde concentrations in the feed gas are 0%-10% and 1000 ppmC (i.e. 500 ppm of acetaldehyde). The total flow rate is fixed at 100 mL/min, corresponding to a residence time in the empty reactor of 64 seconds.

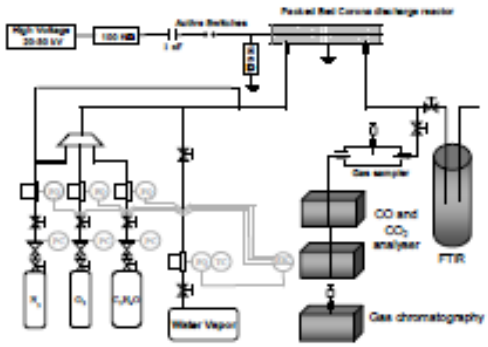

Fig.1 Experimental setup for acetaldehyde removal in the Packed Bed Corona Discharge Reactor.

The oxidation of acetaldehyde was evaluated by measuring the CO, CO_2 using an infra-red absorption analyser (Environnement S.A MIR 9000), and the residual acetaldehyde by gas chromatography (Shimadzu GC 2010) at the cell exit. The gas phase chromatograph is also used to detect and quantify the hydrocarbons that may result from the

interaction between acetaldehyde and the atmospheric pressure pulsed corona discharges. Ozone concentration at the cell exit was measured by ultra-violet absorption spectroscopy using an InUSA IN 2000 analyser.

3. Packed Bed Corona Reactor

The reactor consists of two coaxial electrodes and small sized beds. The outer electrode is a stainless steel tube, and the inner electrode is a 100 µm diameter tungsten wire. The inner diameter of the reactor is 20 mm, resulting in a 10 mm discharge gap. The discharge length is 200 mm.

Two packing material were used in the packed bed wire-to-cylinder configuration: (i) a 2 mm diameter spherical SiO_2 glass particles, (ii) a 2 mm diameter spherical non porous γ-Al_2O_3 particles as a packing material.

TiO_2 catalyst was deposited [8] on both packing materials to enhance the degradation efficiency or modify the degradation kinetics of acetaldehyde.

The Packed Bed material is analysed before and after being used in the corona reactor, by Scanning Electron Microscopy (SEM – Figure 2), BET, X-ray diffraction, IR-absorption and Raman spectroscopy.

Fig.2: SEM image of γ-Al_2O_3 packing material

The energy deposited during one discharge pulse is estimated from the measured voltage and current. **Figure 3(a) and 3(b)** show a typical voltage and current waveforms associated respectively to a pulsed corona discharge and a SiO_2 packed bed corona discharge. In both configurations, the discharge voltage and current reaches a maximum of 22 kV and 65 A.
They cancel after 200 ns duration. The typical value for the energy deposited in the discharge ranges between 20 mJ and 60 mJ per pulse, corresponding to a maximum power of 3 W for a ten Hz frequency.

We observe that the use of a packed bed does not significantly modify the current and voltage waveforms.

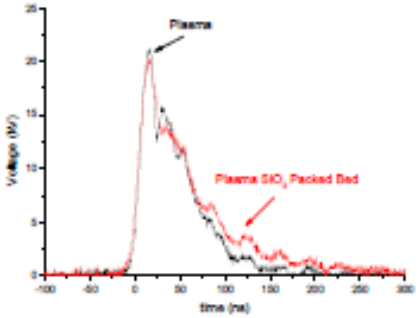

Fig.3(a): voltage waveforms in plasma and plasma SiO_2 packed bed configurations.

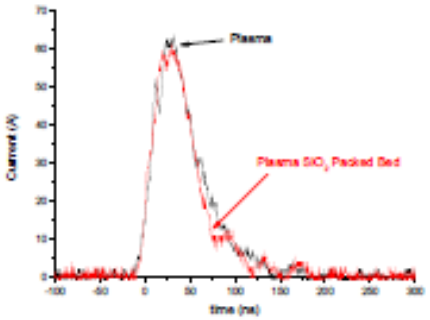

Fig.3(b): current waveforms in plasma and plasma SiO_2 packed bed configurations.

4. Degradation of acetaldehyde in different packing material

We propose here to present some of the results that will be discussed during the poster session. In the following, the oxygen content was fixed at 5%, acetaldehyde was introduced at 1000 ppmC and experiments were performed at room temperature. Results obtained with plasma alone and with SiO_2 packed bed plasma reactor will be compared.
The Figure 4 presents the residual acetaldehyde measured at the exit of the reactor using a plasma discharge (open symbols) and a plasma coupled with a SiO_2 packed bed. At low specific energy, the residual acetaldehyde decreases at the same rate with and without a packed bed.
The fact that residual acetaldehyde is the same at low energy using plasma and plasma packed bed reactors means that the main species responsible for the degradation of acetaldehyde is not much influenced by the packing material (i.e. SiO_2 in this example). In corona discharges, active species that may degrade acetaldehyde are mostly O, OH radicals, O_3 and N and N_2 metastable.

B.2 Spark Plug and Corona Abilities to ignite Lean Methane/Air Mixtures

Spark Plug and Corona Abilities to Ignite Lean Methane/Air Mixtures

M. Bellenoue, S. Labuda, B. Ruttun, J. Sotton
Laboratoire de combustion et détonique, 86961Futuroscope Chasseneuil Cedex, France

Corresponding author, S. Labuda: labuda@lcd.ensma.fr

Introduction

Corona discharge in gases has many applications in plasma reactors, ozone generation, anti-pollution systems, etc. One of the most interesting practical applications is the use of corona discharge for the ignition of combustible mixtures in engines. A short pulsed corona was used first by Liu et al. (2002) for the ignition of CH_4-air mixtures. As mentioned in this work, potential advantages of corona ignition are the following. A corona has a better coupling with the gas because the cross-section for dissociation and ionization more closely matches the electron energy distribution function in the discharge. Corona discharge also has lower energy losses through lower radiation and lower anode and cathode losses. It is worth noting that a corona produces numerous streamers, each of which has similar energy content, as opposed to a single, unnecessarily large and intense arc. Moreover, a corona allows initiation of combustion in a large volume; the ignition volume can be tailored using the anode and cathode geometry. Finally, a corona generates a gas flow (corona wind) characterized by intensive turbulence. For nanosecond or microsecond duration discharge, the corona wind is negligible, whereas for a millisecond pulsed corona, the corona wind starts to be significant (Bellenoue[a)], 2004). Generated by a corona discharge, turbulent gas flow influences the initial flame kernel development positively. Due to the characteristics mentioned above, the use of corona discharge for ignition of combustible mixtures looks very attractive.

Currently, there are only a few studies related to corona ignition (Liu, 2002; Starikovskii, 2003, Bellenoue[b)], 2004). In these works, some advantages of pulsed corona ignition over spark plug ignition have been demonstrated. The scarcity of experimental data does not allow comparative analysis of spark plug and corona ignition efficiency and the determination of the corona ignition mechanism. In this work, spark plugs and coronas have been used for the ignition of extremely lean fuel methane/air mixtures. Energetic efficiency and ignition ability have been analysed for these ignition systems.

Experimental set-up

In our experiments, a quiescent premixed methane/air mixture of equivalence ratios 0.55 or 0.517 is ignited by a spark plug or positive corona. Experiments are carried out with an initial pressure of 0.15 MPa. Combustion occurs in a cylindrical combustion chamber of 80 mm in diameter and 30 mm in height. Glass windows mounted on the side-wall of the chamber allow observation of all cross-sections of the combustion vessel. The same electrodes have been used for spark and corona ignition. One of the discharge electrodes (constantan wire of 0.35 mm in diameter, lateral surface of the wire is covered by Teflon isolation) is placed along the axis of symmetry of the combustion chamber. The chamber wall is used as another discharge electrode. In all tests, the discharge gap is 20 mm.

In spark plug ignition tests, capacitive discharge is used. The spark plug ignition unit is based on the high voltage converter coil allowing a voltage up to 25 kV across the discharge gap. Discharge energy stored in the ignition system is controlled by the value of the capacitor discharging through the primary circuit. In our tests, the value of the maximal energy stored is 80 mJ, the duration of the discharge is about 50-100 μs, the peak discharge current value is 16-16.5 A, and the discharge energy is 16-17 mJ.

An ***Entwicklung Leistungselectronik*** type power supply is used to generate the corona discharge in single pulse mode. In our experiments, positive corona pulse durations of 3 ms, 10 ms, and 20 ms have been used for ignition. Depending on the discharge duration, the discharge energy igniting the combustible mixture varies in the range of 0.5-0.7 mJ.

Two diagnostics have been used to study the ignition and to follow the flame kernel development. One is the record of pressure time evolution during combustion. The ***dP/dt*** value obtained from the pressure signal is used as the characteristic of combustion efficiency. Another diagnostic used is Schlieren visualization of the combustion process. A Kodak camera (Kodak Ektapro HS Motion Analyser) performing 500-40500 frames/s has been used for Schlieren image recording. A continuous wave Ar laser supplied by a break cell producing highlight pulses of 3 μs in duration is used as a light source.

Results

Schlieren snapshots of spark plug and corona ignition of a 0.55 equivalence ratio mixture are shown in Fig. 1 and Fig. 2, respectively. It appears that the spark ignites the combustible mixture simultaneously in all cross-sections of the spark gap (see Fig. 1). It is worth noting that ignition occurs at the last stage of the discharge, when the plasma is rather cold. Non-straight line spark shape causes initial flame front wrinkling.

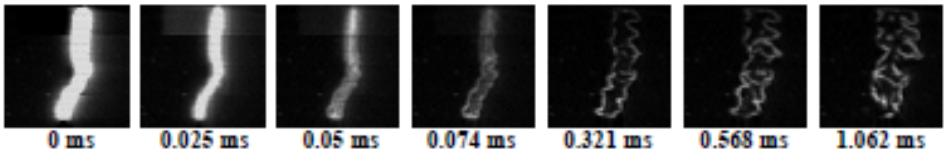

Figure 1. Spark plug ignition of CH_4/Air mixture of equivalence ratio 0.55.

In Fig. 2, Schlieren snapshots of corona ignition of the same mixture for discharge duration of 3 ms are shown with corresponding oscilloscope traces of the corona discharge trigger signal (curve "a"), voltage across the gap (curve "b"), and discharge current (curve "c"). Dashed vertical lines in oscilloscope traces mark the time instants when corresponding Schlieren images have been obtained. It can be seen that corona streamer discharge is characterised by a brush of current pulses of 0.5-2 mA in amplitude. At the beginning of the discharge no change in mixture density across the discharge gap has been recorded. The first changes in gas density can be observed in the anode region 2.5 ms after the beginning of the discharge. Our preliminary tests carried out in Argon at the same discharge parameters (discharge current and corona pulse duration) and using the same Schlieren optical scheme does not detect the gas heating in the discharge. Thus, the change in gas density observed in the combustible mixture

B.3 NOx Reduction from IC Engines With DC Corona Discharge

NO_X REDUCTION FROM CI ENGINES WITH DC CORONA DISCHARGE - AN EXPERIMENTAL STUDY.

Jan Vinogradov, Eran Sher, Boris Rivin
The Pearlstone Center for Aeronautical Studies, the Department of Mechanical Engineering,
Ben-Gurion University of the Negev, Beer-Sheva, Israel.
jan@bgumail.bgu.ac.il

ABSTRACT

An experimental study of DC corona discharge technology for NO_x reduction from diesel engine exhaust is presented. The DC corona reactor consists of a flat electrode against a multi-needle electrode.

The results are presented in terms of the cleanness (the mass of removed NO_x referred to its initial mass), and the energy consumption (the mass of NO_x per unity corona electric energy). For both cleanness and energy consumption, negative polarity (negative needles) is preferable. The cleanness was found to be independent of the engine load. The results show that the performance of a DC corona reactor depends on the reactor length, electrodes' separation distance, and needle's density. The effectiveness of the NO_x decomposition was mapped, and optimal geometrical parameters for the best reactor performance have been obtained.

It is concluded that for best performance, the residence time of the exhaust gas inside the reactor should be longer than 1.2 seconds; the electrodes' separation distance must be less than 30mm (in order for the electric field intensity to remain sufficiently high for dissociation reactions); and the needles separation distance must not exceed 20mm (in order to provide sufficiently dense distribution of plasma regions from each needle). The cleanness and energy consumption values for the optimal geometry lay between 55%, 17.2gr-NOx/kW-h, and 46%, 27gr-NOx/kW-h for needles separation distance of 10 and 20mm, respectively.

INTRODUCTION

In response to public pressure, controlling hazardous substances from being emitted into the ambient environment has become a major focus of the scientific community. One of the major pollutants is NO_x, known for its perilous effects on human health and environment. The term NO_x denotes nitric oxides NO and NO_2, which are produced in combustion process due to high temperatures inside the combustion chamber. These oxides cause eye, throat, and lung irritation and produced mainly by motor vehicles [1].

In last two decades the possibility of NO_x reduction from exhaust gases ($DeNO_x$ process) by means of electric discharge has been intensively studied [2,3]. It has been revealed that chemically active radicals produced in the ionized gaseous media interact with pollutant molecules, converting them to non hazardous substances. Keeping in mind that the Diesel exhaust gas contains water vapor, oxygen, CO_2, nitrogen, and traces of pollutants, the ionization processes in it, resulting in radicals' production, is similar to the one taking place in humid air.

The ionization initiates when free electrons, accelerated by electric field, collide with neutral species. The source for free electrons may be either naturally produced electrons from cosmic radiation, or electron emitter, like one used in electron beam devices. Cosmic radiation produces electrons at a rate of ~1 el/mm^{3}s. This leads to rather low background electron densities of 10^3-10^6 el/cm^3. This can imply that it takes some time for an electron to be at the right place, i.e. a region where the electric field is high enough. This time is called *inception time lag* and in practice it varies from about 1 ns to many microseconds [4]. The

electron-molecule collisions can result in molecule excitation or its ionization, as well as they can be absolutely elastic and then, only kinetic energy is transmitted. Since average molecule is thousands times heavier than electron, the mean velocity, which molecule gains from elastic collision with the electron, due to energy exchange with it, is comparable to its thermal velocity. In case of ionized molecule, at atmospheric pressure, where the concentration of neutral species is high and therefore ion's mean free path (m.f.p.) is short, ionized species' velocity at the end of its m.f.p. is also low. Thus, in either case, both ionized and neutral species remain slow or cold in sense of their velocity, and this charge transform is referred to as cold plasma. In cold plasma the ionization of one molecule by collision with another can be neglected.

By using an asymmetric electrode pair a non-uniform electric field is produced. Free electrons, which are present in the interelectrode space, are accelerated by electric field towards anode. Field enhancement near one electrode is required. The most common methods used in practice for this purpose are point-to-plane and wire-in-cylinder geometries. In order for an electron to accumulate sufficient energy along its m.f.p. for collisional ionization of neutral species, the electric field intensity should be higher than 24.4kV/cm [5]. At these conditions additional electrons are produced from the collision, and the so-called electron avalanche is initiated. For electric field higher than 24.4kV/cm ionization processes prevail over electron attachment, and therefore the total ionization coefficient α^*, which is defined as a subtraction between first ionization coefficient of Townsend α and attachment coefficient η, becomes positive. Within the interelectrode space, defined as ionization layer, in which the electric field is higher than 24.4kV/cm, recombination of electrons with positive ions is negligible [6]. Beyond the ionization boundary, attachment prevails over ionization and the number of electrons decreases with the decrease of electric field. Thus, only ions transfer the charge, and the interelectrode space beyond the ionization layer is referred to as drift region.

EXPERIMENTAL SETUP

Experimental investigation of CI engine exhaust treatment was made on Mitsubishi 3 cylinder diesel with total volume of 1300cc. The engine was mounted on a test bench and connected to a 3-phase generator, which provides the engine loading, when connected to external heaters. The heaters are capable of consuming a total amount of electric power up to 8kW, taken from 10kW of maximal engine power. The engine speed is kept constant and equal to 1500rpm, in order to maintain standard 50Hz AC supplied to the heaters.

A flow rate of 8L/min from approximately 1000L/min was set to pass through the DC reactor. High voltage supplier, capable of delivering maximum 50kV DC corona voltage is connected to the reactor. The limiting resistor of 6MΩ was connected in series, and the total current and voltage were measured. Thus, controlled by the current, the potential difference on the reactor can be easily calculated. The scheme of the experimental setup is shown in Fig.1. A luminescent type gas analyzer Sun-DGA1000 is connected to the exhaust pipe downstream the reactor. A thermocouple is installed at the entry to the reactor, in order to provide simultaneous temperature measurement.

C. CORONA GENERATION CIRCUIT PROPOSAL

C.1 Calculations

C.1.1 Module 1: Sine Wave generation

The sine wave generator consists in a Wien Bridge oscillator design using transistors.

From the theory of the Wien Bridge oscillator it is known that the frequency depends directly from capacitor C and resistance R, following the formula *Eq. C.1*.

$$f = \frac{1}{2\pi CR} \qquad \text{(Eq. C.1)}$$

In the proposal of this project, a two-transistor Wien Bridge Oscillator is used. Looking at the following example in *Figure C.1* of another two-transistor Wien Bridge Oscillator, the capacitor and the resistance that affect the frequency are the ones shown in the picture as C and R, respectively.

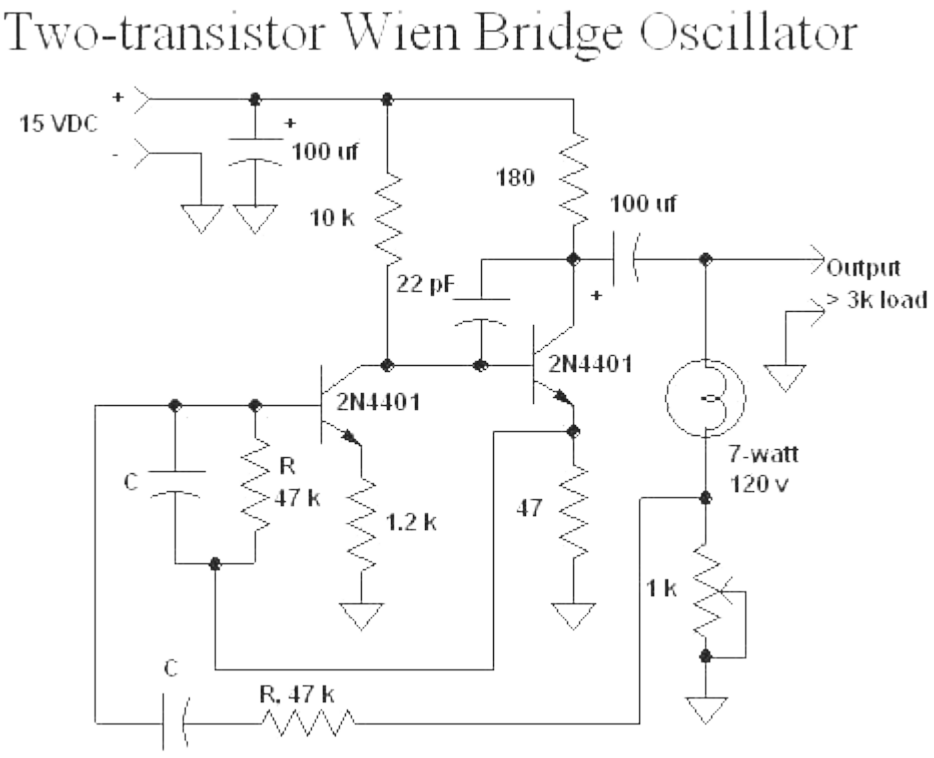

Figure C.1. *Example of Two Transistor Wien Bridge distribution*

Using this example as a start the proposal of this project is built. To allow the regulation of all the range required (initial estimation of 0Hz to 500 kHz), it is seen that either R or C will need to be variable.

After some testing run with Multisim© using only variable resistance, it is seen that the frequency range is very short compared to the desired one, so a solution where both capacitors and resistance are variable is investigated.

After different testing the final solution is shown in *Figure C.2*.

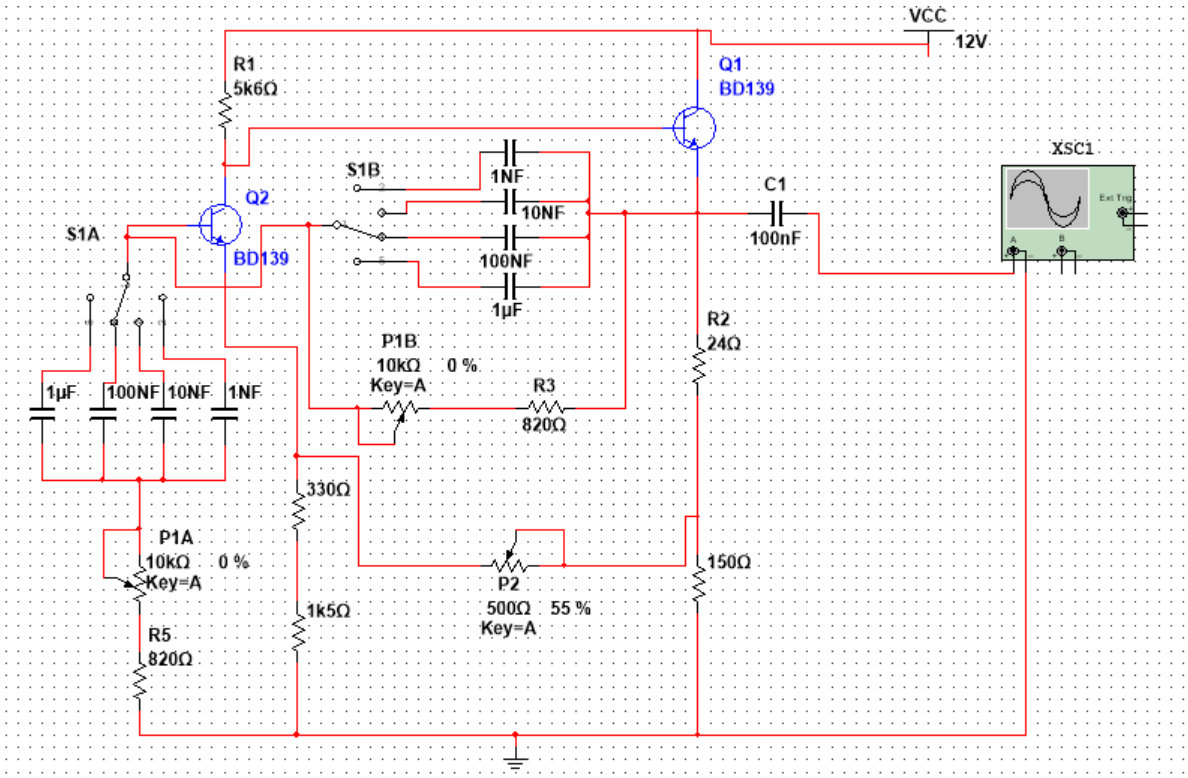

Figure C.2. *Proposed Sine wave generator system*

This still follows the same structure as the example seen above but has slight modifications:

- The capacitor C that will regulate the frequency will be selected with a selector S1. Because it has been seen that there are two capacitors C of the same value, for ease of construction it has been designed so that selector S1 is a double selector composed by 2 sub-selectors S1A and S1B that are coupled between them.
- The resistor R has been divided in potentiometer P1 and resistors R3 and R5, where R3=R5. It is possible to see that the idea of the coupled selector has also been applied to potentiometer P1, consisting this in a double potentiometer formed by 2 sub-potentiometer P1A and P1B. The reason of adding the resistance in series to the potentiometer is to control the frequency generation when the potentiometer is at 0 %, so that it doesn't create issues in the sine wave generation.
- A potentiometer P2 has been added to regulate the sine wave generation. This has been seen in some Wien bridge proposals and is used to calibrate the sine wave when distortion appears. This will depend on the frequency at which the circuit is running.

Once the circuit proposal is ready, to calculate the required potentiometer and resistor values an initial estimation of the capacitor is made, supposing this 1 uF. Starting from the bottom frequency the desired output would be 10 Hz. Adding this to the formula *Eq. C.1* mentioned above it is obtained:

· For 10 Hz frequency output:

$$10\ Hz = \frac{1}{2\pi \cdot 1x10^{-6} \cdot R} => \boldsymbol{R \approx\ 10610\ \Omega}$$

Now, in order to find the value of R3 and R5, the limit of this range must be chosen. In order to keep the values as simple as possible, the limit frequency is decided to be 200 Hz.

· For 200 Hz frequency output:

$$200\ Hz = \frac{1}{2\pi \cdot 1x10^{-6} \cdot R} => \boldsymbol{R \approx\ 820\ \Omega}$$

So, knowing that that the resistance when potentiometer is at 0% must be 820 $\boldsymbol{\Omega}$, it is possible to say that the potentiometer will be the result of:

$10610 - 820 = 9790\ \boldsymbol{\Omega} => \mathbf{P1 = 10\ k\Omega}$

And, $\mathbf{R3 = R5 = 820\ \Omega}$

For the next range and to keep the circuit simple, a capacitor of **100 nF** has been chosen. Looking now at the frequency formula *Eq. C.1* using the known values for the resistors it is possible to state:

$$f_{B,high} = \frac{1}{2\pi CR} = \frac{1}{2\pi \cdot 0.1x10^{-6} \cdot R3} = 1940\ Hz$$

$$f_{B,low} = \frac{1}{2\pi CR} = \frac{1}{2\pi \cdot 0.1x10^{-6} \cdot (R3 + P1)} = 147\ Hz$$

New range in selector **position B is 147 Hz – 1940 Hz.** The fact that this is 10 times higher than the previous range is no surprise, as the capacitor is the only thing that has changed by a factor of 10.

To complete the range, 2 more capacitors are added in the positions C and B of the selector with a 10 factor each one, so that the final range of the generator results in (values have been approximated and shown only to usable new range):

- **Selector in position A (10 uF capacitor):** 15 Hz - 200 Hz
- **Selector in position B (100 nF capacitor):** 200Hz – 2 kHz
- **Selector in position C (10 nF capacitor):** 2kHz – 20 kHz
- **Selector in position D (1 nF capacitor):** 20 kHz – 200 kHz

C.1.2 Module 2: Transformer to High Voltage

As a start of the calculation we have the following values:

Primary coil

$V_1 = 8\ V$

Secondary coil

$V_2 = 20\ kV$

$I_2 = 10\ mA$

With this initial values we can establish the power of the transformer and the estimated area of the core using the following formulas:

$$\boldsymbol{Power} = V \cdot I = 20x\ 10^3(V) \cdot 0.01\ (A) = \mathbf{200\ W} \qquad \text{(Eq. C.2)}$$

$$\boldsymbol{Core\ section\ area} = quality_{core}\sqrt{Power} = 1{,}2 \cdot \sqrt{200} = \mathbf{17\ cm^2} \qquad \text{(Eq. C.3)}$$

Where:

- *$quality_{core}$: Assumed a value of 1,2 because of the transformer power range.*

With the value of the core section area and the power of the transformer, referencing to the table in section C.3.2 of this document it is possible to stablish the normalised dimensions of the core **3,8 cm x 5 cm.**

To know the size of the cable in each coil required, the table shown in section C.3.3 is used cross-referencing the intensity of each cable and selecting the immediately above. For knowing the intensity of the primary coil, the following formula *Eq. C.4* is used:

$$\boldsymbol{I_1} = \frac{P}{V_1} = \frac{200}{8} = \mathbf{25\ A} \qquad \text{(Eq. C.4)}$$

The resulting required sizes are:

Primary coil: Calibre 9

Secondary coil: Calibre 30

To calculate the number of turns of the primary coil, the following formula *Eq. C.5* is used:

$$\boldsymbol{N_1} = \frac{V_1}{4 \cdot k \cdot f \cdot A_{core} \cdot \beta} \cdot 10^8 = \boldsymbol{8,85\ turns \sim 9\ turns} \qquad \text{(Eq. C.5)}$$

Where:

- *k= 1.11, because of ferrite core*
- *f= 120 Hz, considered the minimum workable frequency we will be using for studying the corona effect*
- *A_{core}= 17 cm^2. Area of the core section*
- *β=Induction in Gauss. Assumed a value of 10,000.*

To calculate the secondary turns the transformer relation below is used:

$$\frac{V_2}{V_1} = \frac{N_2}{N_1} \Rightarrow \quad \boldsymbol{N_2 = 22500\ turns} \qquad \text{(Eq. C.6)}$$

The final characteristics of the transformer are:

- **Transformer power:** 200 W
- **Core dimensions:** 3.8 cm x 5 cm
- **Primary coil turns:** 9 turns
- **Primary cable calibre:** Calibre 9 (From AWG Table in annex)
- **Secondary coil turns:** 22500 turns
- **Secondary cable calibre:** Calibre 30 (From AWG table in annex)

C.1.3 Module 3: High Voltage circuit

The only calculation referencing module 3 is for the Shunt resistor, which follows a simple Ohm law. As a result, the required resistance will be:

$$\boldsymbol{R_{shunt}} = \frac{V}{I} = \frac{20{,}000\ V}{0.01\ A} = \boldsymbol{2x10^6\ \Omega = 2\ M\Omega} \qquad \text{(Eq. C.7)}$$

No other calculation is made as the coupling to the spark plug wire is supposed to be as one of the already studied patents US 5596974 or US3949718.

C.2 Computer simulation measurements

C.2.1 Module 1: Sine Wave generation

By simulation it has been found that for all the frequency range, the refinement potentiometer can be left at 55 %, as this gives an accurate and stable sine wave. A lower value for the potentiometer P2 will result in a distorted wave, and a higher value will result in reduction of the amplitude and loss of the sine wave

- **30 Hz output**

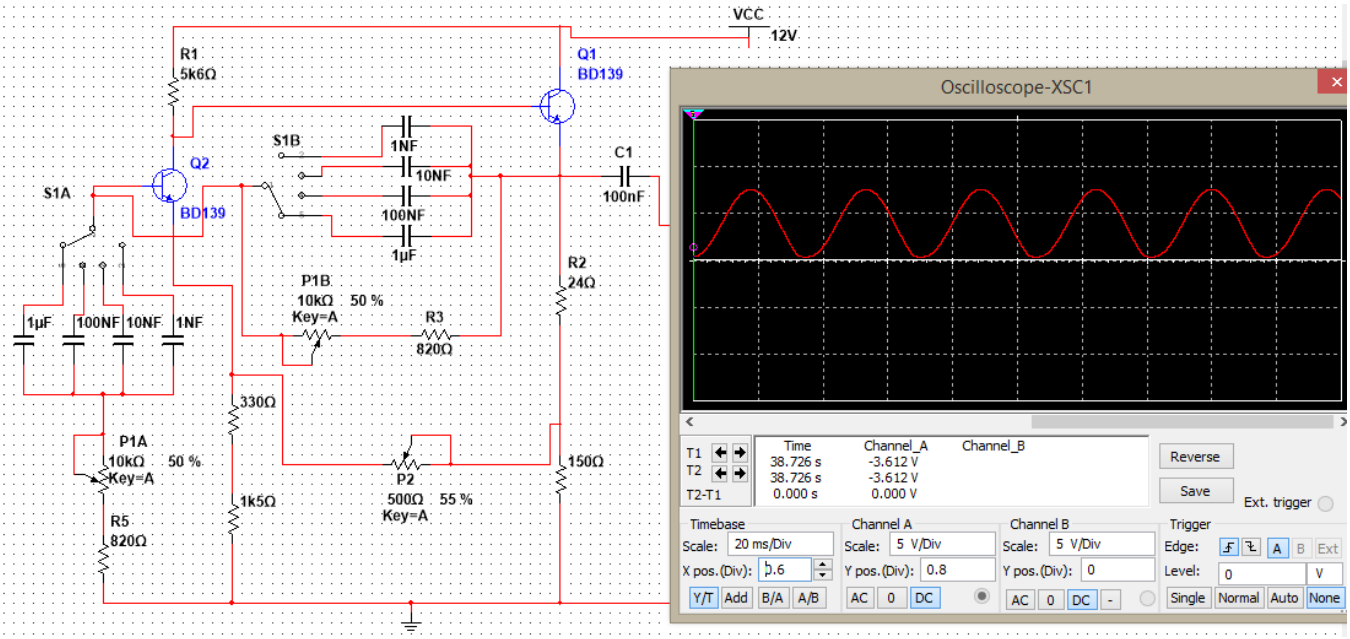

Figure C.3. *30 Hz sine wave generation configuration*

- P1 at 50 %
- S1 in position A (1 uF)
- Vout = 8V

- **250 Hz output**

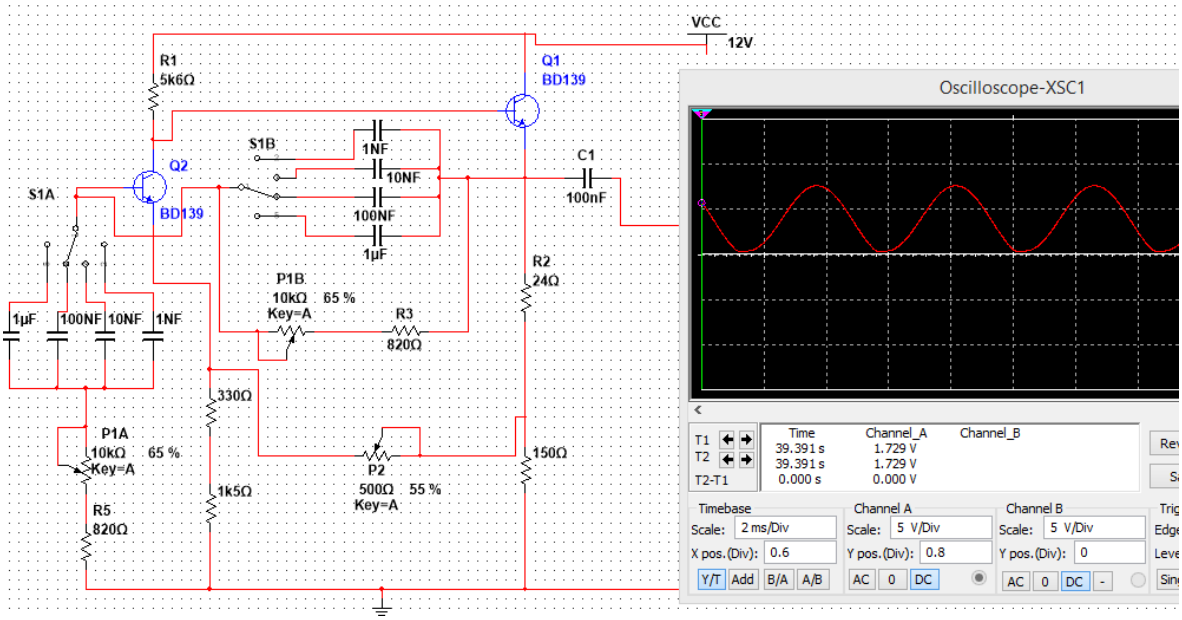

Figure C.4. *250 Hz sine wave generation configuration*

- P1 at 65 %
- S1 in position B (100 nF)
- Vout = 8V

- **10 kHz output**

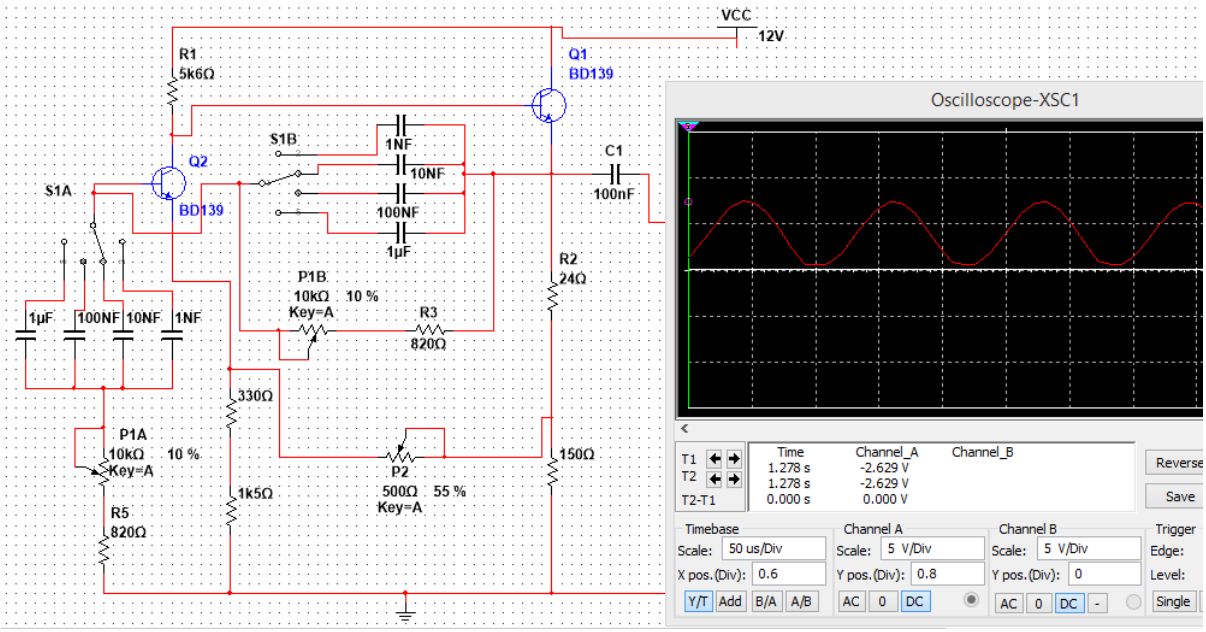

Figure C.5. *10 kHz sine wave generation configuration*

- P1 at 10 %
- S1 in position C (10 nF)
- Vout = 7 V

- **200 kHz output (Max output)**

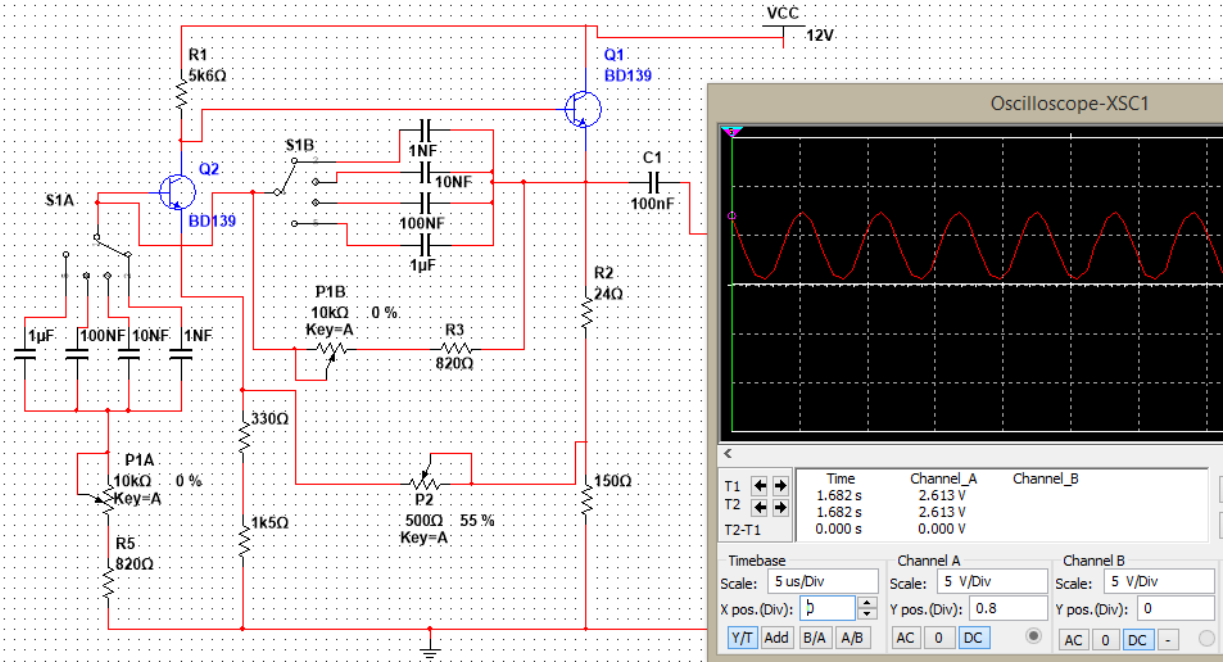

Figure C.6. *200 kHz sine wave generation configuration*

- P1 at 0%
- S1 in position D (1 nF)
- Vout = 7 V

For any other configuration select the correct S1 position depending on the range desired and move potentiometer P1 until the frequency of the output is as required.

Approximate ranges for the selector S1 as measured by simulation are:

- **Selector in position A (10 uF capacitor):** 15 Hz - 200 Hz
- **Selector in position B (100 nF capacitor):** 200Hz – 2 kHz
- **Selector in position C (10 nF capacitor):** 2kHz – 20 kHz
- **Selector in position D (1 nF capacitor):** 20 kHz – 200 kHz

C.2.2 Module 2: Transformer to High Voltage

To verify the transformer module, this has been attached to the output of the module discussed in the previous section, resulting in the following distribution.

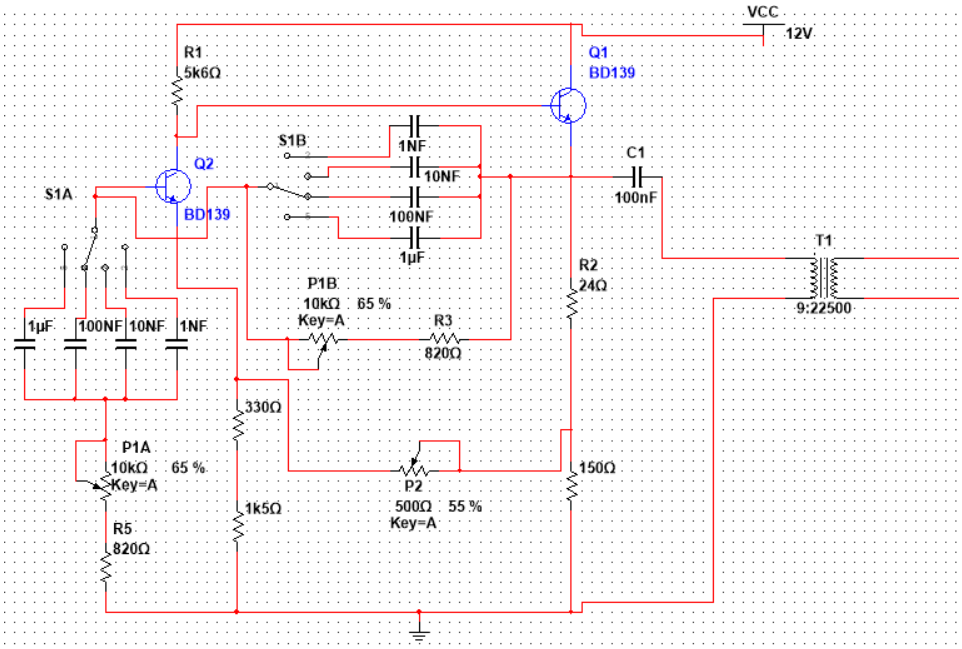

Figure C.7. *Module 1 with Module 2 connected*

By running the simulation for one high frequency and one low frequency we can verify if the transformer makes the transformation accurately.

- **Module 1 configured for 250 Hz output**

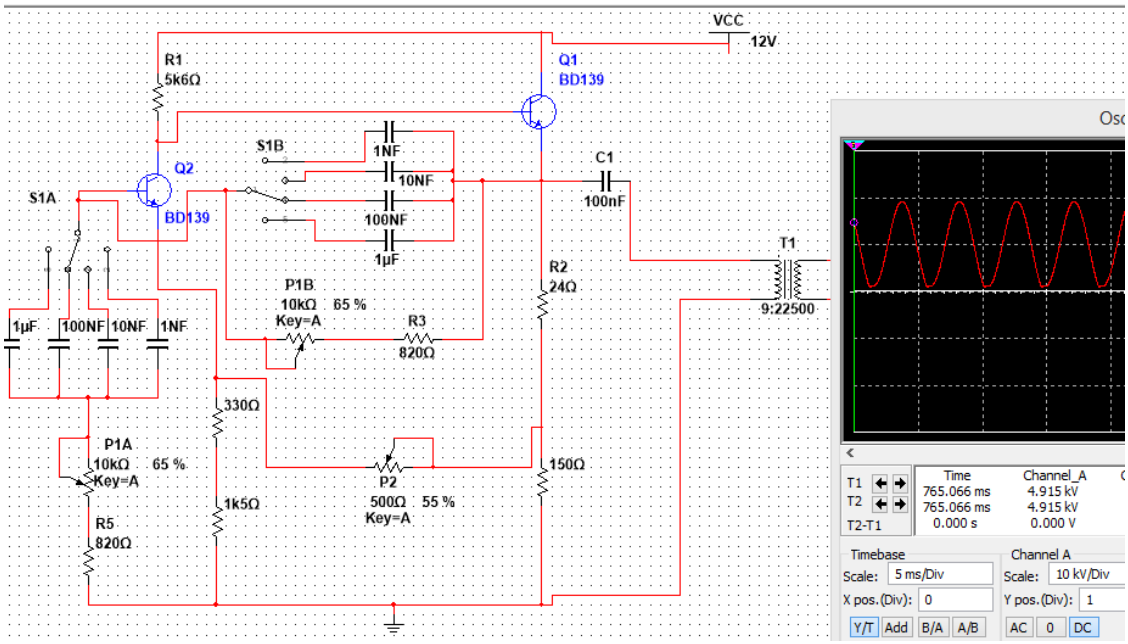

Figure C.8. *Transformer working at 250 Hz*

- Output at the same input frequency 250 Hz
- Voltage at the output 20 kV

- **Module 1 configured for 200 kHz output**

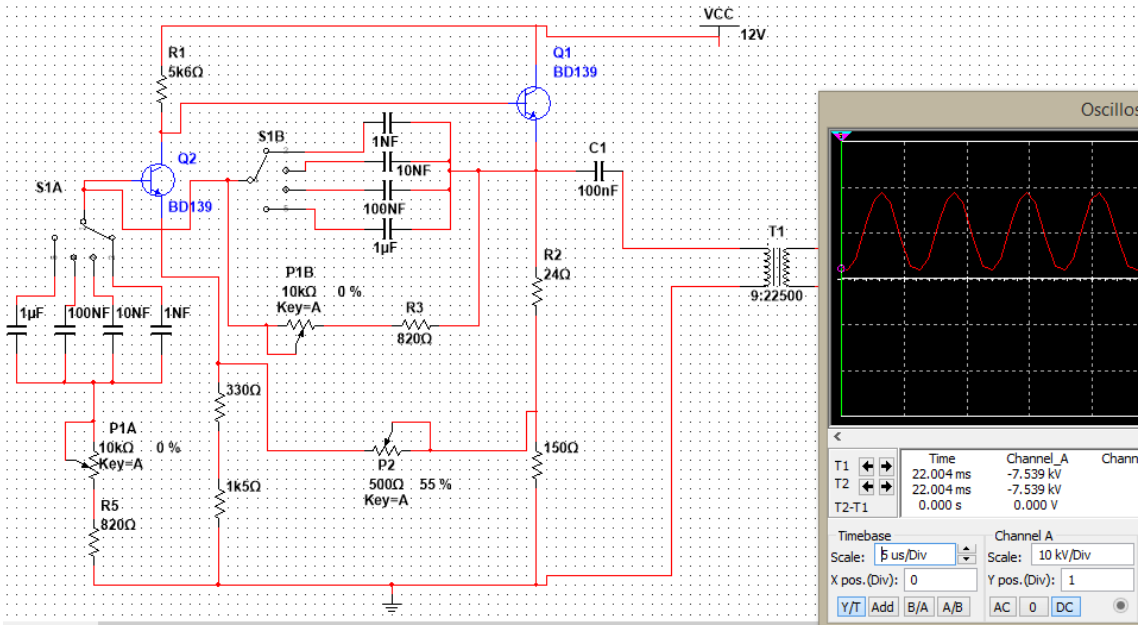

Figure C.9. *Transformer working at 200 kHz*

- Output at the same input frequency 200 kHz
- Voltage at the output 18 kV approximately.

After running this test at both extremes of the workable frequencies it is possible to say that the transformer is working properly along all the range.

C.3 Components datasheet

C.3.1 Transistor BD 139

25C D 8235605 0004332 4 SIEG 7-33-07

NPN Silicon Transistors **BD 135 BD 137 BD 139**

SIEMENS AKTIENGESELLSCHAF

For AF driver and output stages of medium performance

BD 135, BD 137, and BD 139 are epitaxial NPN silicon planar transistors in TO 126 plastic package (12 A 3 DIN 41869, sheet 4). The collector is electrically connected to the metallic mounting area. Together with BD 136, BD 138, and BD 140 as complementary pairs the transistors BD 135, BD 137, and BD 139 are designed for use in driver stages of high performance AF amplifiers.

Type	Ordering code
BD 135	Q62702-D106
BD 135-6	Q62702-D106-V1
BD 135-10	Q62702-D106-V2
BD 135-16	Q62702-D106-V3
BD 135 paired	Q62702-D106-P
BD 137	Q62702-D108
BD 137-6	Q62702-D108-V1
BD 137-10	Q62702-D108-V2
BD 137 paired	Q62702-D108-P
BD 139	Q62702-D110
BD 139-6	Q62702-D110-V1
BD 139-10	Q62702-D110-V2
BD 139 paired	Q62702-D110-P
BD 135/BD 136 compl. pair.	Q62702-D139-S1
BD 137/BD 138 compl. pair.	Q62702-D140-S1
BD 139/BD 140 compl. pair.	Q62702-D141-S1

Type	Ordering code
Mica washer	Q62902-B62
Spring washer A 3 DIN 137	Q62902-B63

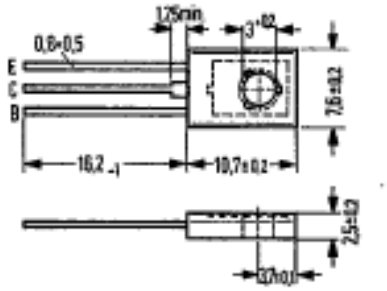

Approx. weight 0.5 g Dimensions in mm

Transistor fixing with M 3 screw. Starting torque < 0.8 Nm; washer or spring washer should be used.

1) If a 50 µ mica washer (ungreased) is used, the thermal resistance increases by 8 K/W and in case of a greased one by 4 K/W.

Maximum ratings		BD 135	BD 137	BD 139	
Collector-emitter voltage ($R_{BE} \leq 1$ kΩ)	V_{CER}	–	–	100	V
Collector-base voltage	V_{CBO}	45	60	–	V
Collector-emitter voltage	V_{CEO}	45	60	80	V
Emitter-base voltage	V_{EBO}	5	5	5	V
Collector peak current	I_{CM}	2,0	2,0	2.0	A
Collector current	I_C	1,5	1,5	1,5	A
Base current	I_B	0,2	0,2	0.2	A
Junction temperature	T_j	150	150	150	°C
Storage temperatur range	T_{stg}	−55 to +125			°C
Total power dissipation ($T_{case} \leq 25$°C)	P_{tot}	12,5	12,5	12.5	W
Thermal resistance					
Junction to ambient air	R_{thJA}	≤110	≤110	≤110	K/W
Junction to case bottom	R_{thJC} [1])	≤10	≤10	≤10	K/W

BD 135
BD 137
BD 139

Static characteristics (T_{amb} = 25 °C)

The transistors BD 135, BD 137, and BD 139 are grouped in accordance with the DC current gain h_{FE}, and marked by numerals of the German DIN standard.

h_{FE} group	6	10	16	
Type	**BD 135** **BD 137** **BD 139**	**BD 135** **BD 137** **BD 139**	**BD 135** – –	**BD 135** **BD 137** **BD 139**
I_C (mA)	h_{FE} I_C/I_B	h_{FE} I_C/I_B	h_{FE} I_C/I_B	V_{BE} (V)
5	>25	>25	>25	–
150	63 (40 to 100)	100 (63 to 160)	160 (100 to 250)	–
500	>25	>25	>25	1.2

Static characteristics (T_{amb} = 25 °C)		**BD 135**	**BD 137**	**BD 139**	
Collector-emitter saturation voltage (I_C = 500 mA; I_B = 50 mA)	V_{CEsat}	<0.5	<0.5	<0.5	V
Collector cutoff current (V_{CB} = 30 V)	I_{CBO}	<100	<100	<100	nA
Collector cutoff current (V_{CB} = 30 V; T_{amb} = 125 °C)	I_{CBO}	≤10	≤10	≤10	µA
Emitter cutoff current (V_{EB} = 5 V)	I_{EBO}	≤10	≤10	≤10	µA
Collector-emitter breakdown voltage (I_{CEO} = 50 mA)	$V_{(BR)CEO}$	>45	>60	>80	V
Condition for matching pairs (I_C = 150 mA; V_{CE} = 2 V)	$\frac{h_{FE1}}{h_{FE2}}$	≤1.41	≤1.41	≤1.41	–
Dynamic characteristics (T_{amb} = 25 °C)					
Transition frequency (I_C = 50 mA; V_{CE} = 10 V; f = 100 MHz)	f_T	>50	>50	>50	MHz

25C D ■ 8235605 0004334 8 ■SIEG D T-33-07

SIEMENS AKTIENGESELLSCHAF

BD 135
BD 137
BD 139

Total perm. power dissipation versus temperature
$P_{tot} = f(T)$; R_{th} = parameter
BD 135, BD 137, BD 139

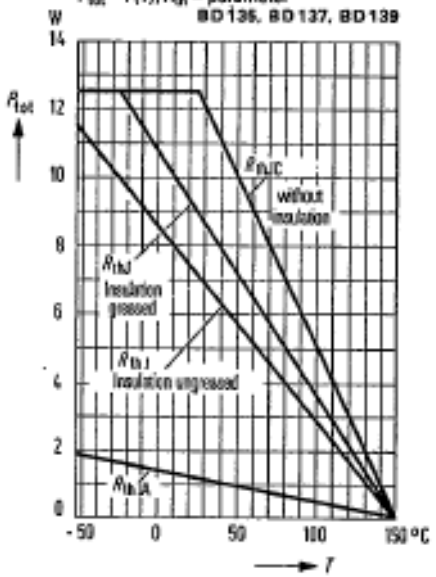

Permissible pulse load
$r_{thJC} = f(t)$; v = parameter
BD 135, BD 137, BD 139

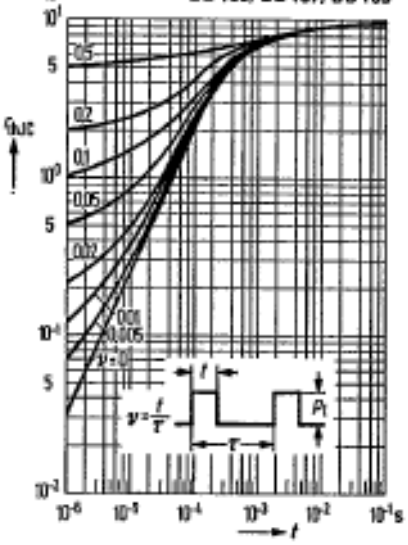

Permissible operating range
$I_C = f(V_{CE})$; $T_{case} = 60$ °C; v = 0
BD 135, BD 137, BD 139

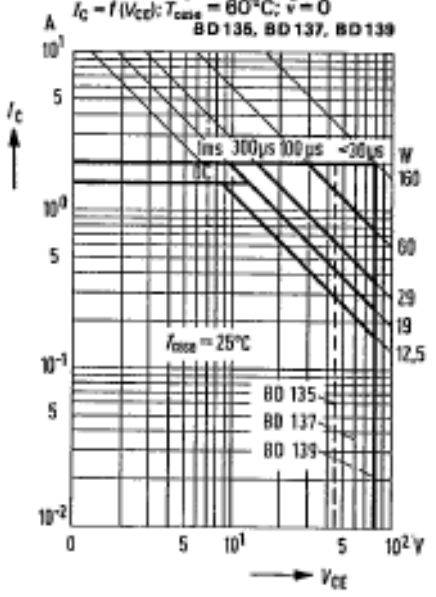

Collector current $I_C = f(V_{BE})$
V_{CE} = 2 V; T_{amb} = parameter
(common emitter configuration)
BD 135, BD 137, BD 139

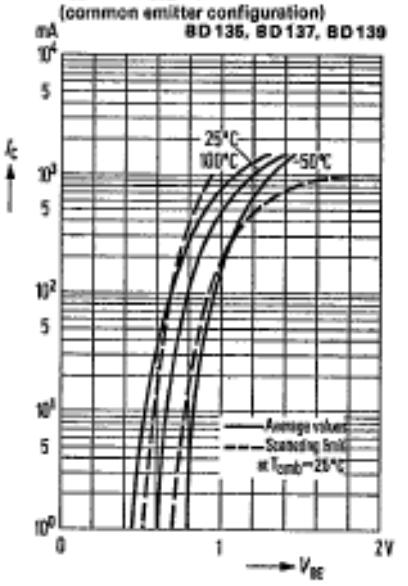

C.3.2 Transformer ferrite core sectional area table

NÚCLEO	POTENCIA MÁXIMA	VUELTAS POR VOLTIO	ÁREA Cm ²
1.6 x 1.9	9W	14	3.04
2.2 x 2.8	37W	7	6.16
2.5 x 1.8	20W	9.3	4.5
2.5 x 2.8	49W	6	7
2.8 x 1.5	17W	10	4.2
2.8 x 2.5	49W	6	7
2.8 x 3.5	96W	4.3	9.8
2.8 x 5	196W	3	14
3.2 x 3.5	125W	3.75	11.2
3.2 x 4	163W	3.3	12.8
3.2 x 5	256W	2.625	16
3.8 x 4	231W	2.76	15.2
3.8 x 5	361W	2.21	19
3.8 x 6	519W	1.85	22.8
3.8 x 7	707W	1.58	26.6
3.8 x 8	924W	1.38	30.4
3.8 x 9	1170W	1.22	34.2
3.8 x 10	1444W	1.1	38

Figure C.10. *Table for communized core dimensions.*

C.3.3 AWG Transformer coil cables table

Calibre	Mils circulares	Diámetro mm	Amperaje
7	20,818	3.67	44.2
8	16,509	3.26	33.3
9	13,090	2.91	26.5
10	10,383	2.59	21.2
11	8,234	2.30	16.6
12	6,530	2.05	13.5
13	5,178	1.83	10.5
14	4,107	1.63	8.3
15	3,257	1.45	6.6
16	2,583	1.29	5.2
17	2,048	1.15	4.1
18	1.624	1.02	3.2
19	1.288	0.91	2.6
20	1,022	0.81	2.0
21	810.1	0.72	1.6
22	642.4	0.65	1.2
23	0.509	0.57	1.0
24	0.404	0.51	0.8
25	0.320	0.45	0.6
26	0.254	0.40	0.5
27	0.202	0.36	0.4
28	0.160	0.32	0.3
29	0.126	0.28	0.26
30	0.100	0.25	0.20

Figure C.11. *AWG table for cable calibre*